Vulnérabilité sismique des ouvrages : évaluation des réponses et des dommages structuraux

Sandra Jerez Barbosa

UNIVERSITÉ PARIS-EST

THÈSE

pour l'obtention du grade de

DOCTEUR

de

L'UNIVERSITÉ PARIS-EST

Discipline : Génie civil

présentée par

Sandra R. JEREZ BARBOSA

Seismic vulnerability of buildings: Response and damage assessment

Vulnérabilité sismique des bâtiments: évaluation des réponses et des dommages structuraux

---

Soutenue le 10 mars 2011

Devant le jury composé de

PR. DJILLALI BENOUAR	RAPPORTEUR
PR. CHRISTIAN LA BORDERIE	RAPPORTEUR
DR. MÉNAD CHÉNAF	EXAMINATEUR
DR. FRÉDÉRIC MERCIER	EXAMINATEUR
PR. AHMED MEBARKI	DIRECTEUR DE THESE

To Gilma and Cecilia (RIP)

For their unconditional love,
for their prayers, for the time
we left them for being here

ACKNOWLEDGMENTS

First of all, I would like to express my gratitude to Professor Ahmed Mebarki, for his guidance, academic support and encouragement during these years of my stay at MSME laboratory. I would like also to thank the members of the dissertation committee: To Professors Djillali Benouar and Christian La Borderie for reading and commenting the main document and with Dr. Ménad Chénaf and Dr. Fréderic Mercier for their invaluable comments and suggestions to improve my research.

Part of this work was supported by the research funds of the Escuela Colombiana de Ingeniería (ECI). This support is gratefully acknowledged. Also in my country, I owe my deepest gratitude to Professors Jairo Uribe, Carlos A. Rodríguez, Gabriel Gomez and Pedro N. Quiroga for inspiring me to pursuit my studies and with my colleagues Nancy Torres, Sandra Aguilar and Adriana Montaño for their friendship, care and support since I left the Materials and Structures laboratory.

I am grateful to the MSME laboratory members for their significant support on several matters: To Professors Christian Soize and Guy Bonnet for accepting me at the laboratory; to Marine Daniel (at the SIE Doctoral School) for providing me with invaluable advice, to Chantal and Isabelle for their always opportune help; and to my dear friends and colleagues: Jeremy (and his family), Eric, Bao, Morad, Thiago, Charles, Mei, Tan, Monsef, Laribi, Carmelo, Camille, Elie, Evangeline…, and so many others, for their friendship and support from the very beginning, for our discussions on so many matters, for their continuous encouragement and advice and for the unforgettable moments at the MSME laboratory.

Now I would like to express my deepest gratitude to my friends here and there: To Natalia, Sulpicio, Francisco, Mona, Nancy, Andrea, Laura, Anita for his friendship, comprehension, help and encouragement all this time, for the good moments we shared and surely we are continuing to share.

Close to the end, I would have never got this far without my family support, to all of them many thanks. And lastly, it is time for me to thank Hernando, even if I can’t find enough words to do it, for his continuous care and encouragement, for reading and hearing me on this subject and for being always by my side even in the most difficult days.

RÉSUMÉ

L’estimation de la réponse sismique ainsi que l’évaluation post-sismique des dommages constituent deux étapes essentielles dans le cadre de l'analyse et de la gestion intégrée des risques sismiques. Les méthodes existantes produisent des résultats acceptables mais des progrès restent encore requis. A cet effet, ce travail développe deux approches visant à améliorer les techniques existantes.

La première consiste en une analyse pseudo-adaptative de réponse modale (PSA) qui estime la réponse sismique des bâtiments à portiques, avec une précision acceptable et un temps de calcul et d’analyse réduit. En effet, dans le cadre de l’analyse de pushover multimodale (MPA), la courbe de capacité se construit sur la base d’un déplacement équivalent calculé par une approche énergétique et le changement des propriétés modales après plastification est évalué à partir des vecteurs de déplacement pendant l’analyse de pushover. Cette technique est une alternative aux méthodes totalement adaptatives car elle permet d’éviter la mise à jour des profils de chargement pendant l’analyse. En plus, les caractéristiques dynamiques des signaux sismiques sont considérées, sans engendrer d’augmentation significative du temps de calcul par rapport aux méthodes statiques. La méthode est testée sur des bâtiments en béton armé de faible et moyenne hauteur et est comparée avec d’autres méthodes existantes ainsi qu’avec des mesures expérimentales. L’estimation des réponses en termes de déplacements absolus et relatifs, forces de cisaillement et rotations est satisfaisante comparativement aux résultats d’analyses non linéaires complètes.

La seconde approche porte sur l’évaluation post-sismique des dommages structuraux à partir de dommages locaux observés. Elle est fondée sur une relation postulée entre le dommage et la probabilité résiduelle de ruine. Deux échelles sont abordées : l’étage et le bâtiment complet. Trois coefficients de calibration sont aussi proposés afin de considérer l’influence du dommage de chaque élément à chaque échelle. Quatre portiques sont analysés et les résultats sont comparés à une approche mécanique qui estime l’endommagement du système à partir de la perte de raideur de la courbe de capacité. Les résultats obtenus montrent de bonnes estimations du niveau de dommage global. Ainsi, cette approche pourrait bien faire partie d’un outil d’aide à la décision dans le cadre des programmes d’évaluation urbaine des dommages qui requièrent des estimations simultanément rapides et précises.

ABSTRACT

Seismic response assessment and post-seismic damage evaluation are both essential stages within the overall framework of seismic risk analysis and management. Several existing methods produce sometimes acceptable results but their improvement is still required. Thus, this study presents two approaches aiming to enhance the existing methods.

Firstly, the Pseudo-Adaptive Uncoupled Modal Response Analysis (PSA) aims to provide improved estimates of seismic response for framed buildings, with an acceptable accuracy and a reduced computational demand. It relies on an energy-based equivalent displacement to develop the capacity curve and a pseudo-adaptive feature that considers changes in modal shapes after yielding, within the framework of the widely used Modal Pushover Analysis. Actually, PSA method is an alternative to fully adaptive methods since it is suitable to be applied without requiring force vector updates during the pushover analysis. Furthermore, the dynamic characteristics of the ground motion are accounted for without causing an appreciable increasing in the analysis duration time in comparison to fully static procedures. Low and medium-rise reinforced concrete buildings are tested. According to the results, PSA is able to provide good estimates of structural responses such as displacements, storey drifts, shear forces and rotations, in comparison to a complete Nonlinear Time History Analysis. These results are also compared to other existing methods and to available experimental measures. Thus, PSA is attractive for current engineering practice and for reliability and vulnerability studies as well as post-quake damage evaluations at large scale.

Secondly, a strategy for post-seismic evaluation of structural global damage is proposed on the basis of observed local damages and the postulation of adequate relationships between damage and residual probability of failure. Actually, global damage is obtained from a two-level analysis: a storey level prior to a building level. Three factors are proposed to reflect the influence of components damage at each of those levels. In order to calibrate and evaluate the efficiency of these factors and with validation purposes, this strategy is applied in the case of four reinforced concrete frames and then compared with a mechanical approach. The obtained results appear as good predictions of the global damage. Accordingly, this strategy has the potential for being a first step within the implementation framework of a decision-making tool for rapid and accurate estimates of structural damages at either individual or large scales: evaluation at urban scale for instance.

TABLE OF CONTENTS

LIST OF FIGURES

LIST OF TABLES

LIST OF NOTATIONS

Acronyms

ATC	: Applied Technology Council
CP	: Collapse Prevention
CQC	: Complete quadratic combination
CSM	: Capacity Spectrum Method
DAP	: Displacement Adaptive Pushover
DCM	: Displacement Coefficient Method
GPA	: Generalized Pushover Analysis
GLD	: Gravity load designed, meaning no seismic design is performed
IDA	: Incremental Dynamic Analysis
IO	: Immediate Occupancy
LM	: Low-Medium level of damage
LS	: Life Safety
MDOF	: Multiple Degrees of Freedom
MH	: Medium-High level of damage
MID	: Maximum Inter storey Drift
MPA	: Modal Pushover Analysis
NLTHA	: Nonlinear Time History Analysis
PBE	: Performance Based Engineering
PEER	: Pacific Earthquake Engineering Research Center
PGA	: Peak Ground Acceleration
PSA	: Pseudo-Adaptive Response History Analysis
RC	: Reinforced Concrete
RC-MRF	: Reinforced Concrete Moment Resisting Frames
SDOF	: Single Degree of Freedom
SRSS	: Square Root of the Sum of Squares
THA	: Time History Analysis
UMRHA	: Uncoupled Modal Response History Analysis

INTRODUCTION

Problem statement

In the past as well as in recent decades, the urban facilities and constructions have suffered important losses due to strong earthquakes and/or their high vulnerability. These disasters have revealed on the one hand that buildings which were not designed to stand earthquakes were extremely vulnerable, as it might be expected, but on the other, that not all the buildings built after the implementation of code provisions resist earthquakes as supposed. In fact, earthquake resistant design is recommended for the engineering practice in recent decades. However, the vulnerability of most of the earthquake-prone big cities is still important, particularly in the developing countries due to the accelerated expansion of urban settlements and the consequent construction of lots of dwellings, having sometimes poor building practices [Bilham, 2009].

Therefore, numerous efforts have been made to develop improved approaches for the design of new buildings and the assessment of existing ones. That is the case of the performance based engineering (PBE) framework, which started being developed after Northridge (1994) and Kobe (1995) earthquakes [Porter, 2003]. In general, a complete risk study includes four stages: i) hazard analysis, ii) structural analysis, iii) vulnerability analysis and damage prediction and iv) risk assessment (sometimes followed by a loss estimation stage) see Figure I.1. The risk evaluation is usually presented in terms of the probability that the structure reaches or exceeds a given limit under a specified hazard level. Depending on the final objective of the evaluation, each stage may have different levels of detailing: very detailed, accurate approaches as the PEER's PBE framework [Porter, 2003; Lee and Mosalam, 2006] or approaches based on simplified global methods such as the probabilistic integrated assessment methodology [Valencia, 2006; Mebarki and Valencia, 2008].

In this context, each stage has also its own methods to be achieved. Having in mind the improvement of strategies like the probabilistic integrated assessment methodology, mentioned above, the first part of this thesis puts the emphasis on the structural analysis stage. In fact, elaborate methods like the nonlinear Time History Analysis (NLTHA) have been

developed to estimate seismic response, taking into account the earthquake characteristics as well as the structural properties in the most accurate way. Nevertheless, when the resources are limited or when evaluations at large scale are required (e.g. urban scale), simplified methods become compulsory, mainly to avoid the inherent high computational cost of NLTHA. Existing approaches for seismic response assessment have succeeded in reducing the time required for its implementation retaining at the same time acceptable levels of accuracy, but some improvements are still required.

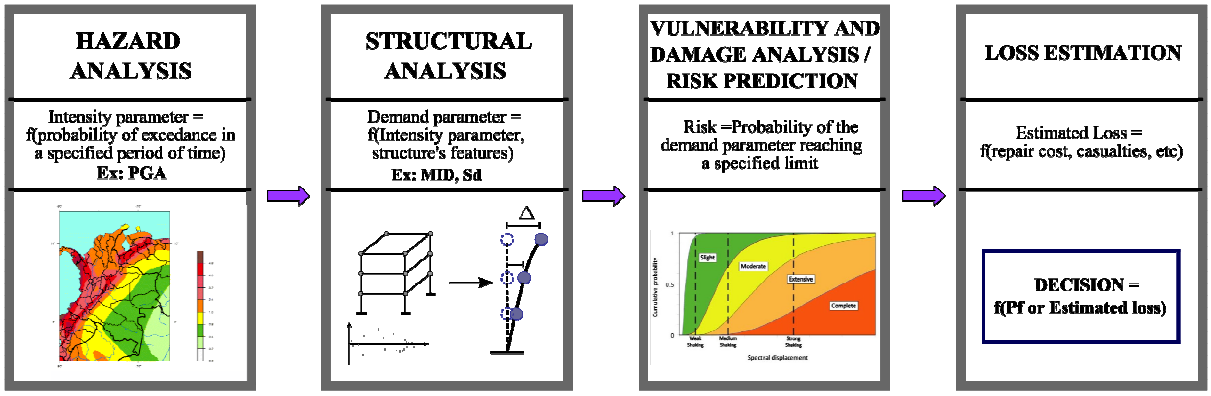

Figure I.1 Overall strategy of risk assessment

Furthermore, once the earthquake has occurred, damage assessment becomes an essential issue. Unlike seismic response, which is characterized and evaluated by means of clearly defined parameters such as displacements, rotations or internal forces, damage is a very complex phenomenon and is not easy to be characterized, since there is a current lack of unified evaluation criteria and clearly defined damage indicators. A number of damage measures, damage indicators and damage states have been already proposed with different objectives: for seismic design purposes as a stage within the framework of the Performance Based Design philosophy; for risk reduction studies, by means of fragility curves as seen before; or for post-earthquake evaluation, aiming to produce habitability decisions.

The latter case requires efficient techniques able to evaluate a large quantity of buildings in very short time as it is the case during a post-quake or post-disaster evaluation process. Of course, several strategies have been proposed and have already been tested. Nonetheless some of them lack of rigorous theoretical basis as they rely on empirical criteria. The necessity of accurate, efficient and straightforward methods is then undeniable; hence, the second part of

this work deals with such methods development.

Objectives and scope

For contributing to the development of simplified methods for the assessment of seismic response and damage, this work aims to accomplish two overall objectives. The first one is the development of a simplified methodology for the evaluation of structural response. For this purpose, several tasks have to be performed in order to:

- Make a critical study of the existing methods for the evaluation of seismic responses with the purpose of identifying features which may produce good results as well as shortcomings which may be overcome.
- Develop a methodology able to estimate seismic responses of frame buildings with acceptable accuracy, easy to put into practice and easy to run in case of reliability and vulnerability studies.
- Validate the proposed methodology with a reasonable number of buildings. Low- and medium-rise buildings.

The second main objective consists in proposing a probability-based methodology for post-earthquake damage assessment of buildings, on the basis of observed damage. The associated tasks to perform are:

- The development of the global failure probability derived from the failure probability of each component.
- The development of a relationship between the failure probability and the structural damage.
- The development of a strategy able to express the global damage as a function of the local damages of the constitutive components.
- The calibration and validation of the proposed methodology. For this task, various reinforced concrete frames are studied under a set of real ground motion records.

Limitations

The proposed methods are limited to two-dimensional models. The extension to three-dimensional models requires essentially the consideration of torsion effects and biaxial bending models, for the column behaviour, for instance. Furthermore, only bare reinforced concrete frames buildings have been considered for validation purposes. The application of the proposed strategies in the case of other materials (e.g. steel or wood frames) or structural types (e.g. infilled frames, masonry buildings) was not studied and is proposed for further development.

Outline of dissertation

This work is divided into two parts:

PART I: This section deals with the seismic response evaluation of existing buildings. It contains three chapters.

Chapter one: Two brief reviews are made. On the one hand, some fundamental concepts inherent to seismic behaviour and modelling of buildings are revised, given the necessity of their suitable understanding for the development of the proposed methods. On the other, the existing nonlinear methods for the analysis of buildings under earthquake actions are studied. An evaluation is made about the advantages and limitations of these methods and the requirements for their performance improvement.

Chapter two: Following the first chapter's conclusions, a proposal of an approximate method for the assessment of building responses is presented: the Pseudo-Adaptive Uncoupled Modal Response Analysis (PSA). The implementation of an energy-based approach for the development of the capacity curve is presented first. Then, a pseudo-adaptive technique for considering the changes in modal shapes is proposed. The complete procedure as well as an application example is provided.

Chapter three: Results of the implementation of the PSA method on six different reinforced concrete moment resisting frames are provided. The study is performed under a set of six real ground motion records. The efficiency and accuracy of the proposed method is studied by a comparison with a reference method as well as other current simplified

approaches. Responses in terms of storey displacements, drifts, shear forces and beam and column rotations are considered for comparison purposes.

PART II: This part deals with global damage assessment and contains two chapters.

Chapter four: A brief review is made about the definition and representation of buildings damage suffered after the occurrence of a strong seismic event. Existing methods for local as well as global evaluation of damage are revised.

Chapter five: A probabilistic based approach to evaluate buildings damage on the basis of given local damage on components is presented. An example is made for illustration purposes. The efficiency of the importance factors, proposed to reflect the relative importance of each component on the overall result, is evaluated. Further results of the implementation are presented in order to evaluate the efficiency and accuracy of the proposed strategy. The validation is performed on four reinforced concrete frames.

The dissertation concludes with a summary of the major findings, the development of the two proposed methods and main purposes for further research and development.

PART I
SEISMIC RESPONSE ASSESSMENT

CHAPTER 1
SEISMIC RESPONSE ASSESSMENT: STATE OF THE ART

1.1. INTRODUCTION

Since the nature of the seismic phenomenon itself and the response of buildings facing it are extremely complex, a number of hypothesis and simplifications has been required for developing models which permit to represent both components of the event, as well as for developing methods for the response evaluation. In this context, this chapter aims to provide first, a brief revision of the fundamental concepts required for the understanding of frame buildings seismic response; and, second, it is intended to establish a brief state of the art of the existing methods for the analysis of buildings under seismic loads.

1.2. BASIC CONCEPTS OF BUILDING SEISMIC RESPONSE

1.2.1. Frame buildings: the seismic action

An earthquake may be defined as a sudden shaking of the earth's crust caused by different phenomena: natural or human-induced. Tectonic events, meaning sudden displacements of tectonic plates, are among the most severe of these phenomena which may cause strong earthquakes. Regardless of the earthquake source, important quantities of seismic energy are radiated by means of vibration waves travelling through the earth's crust.

Concerning a given structure, when such waves reach its foundation, the vibration movement is transmitted to the whole structural components. The movement of the structural masses generates inertial forces and damping effects. As a result, for resisting those forces, significant stresses are developed on each component and each joint, leading to variable levels of damage or eventually the complete failure [Bazán and Meli, 2002]. A sketch of the transmission of these forces is depicted in Figure 1.1.

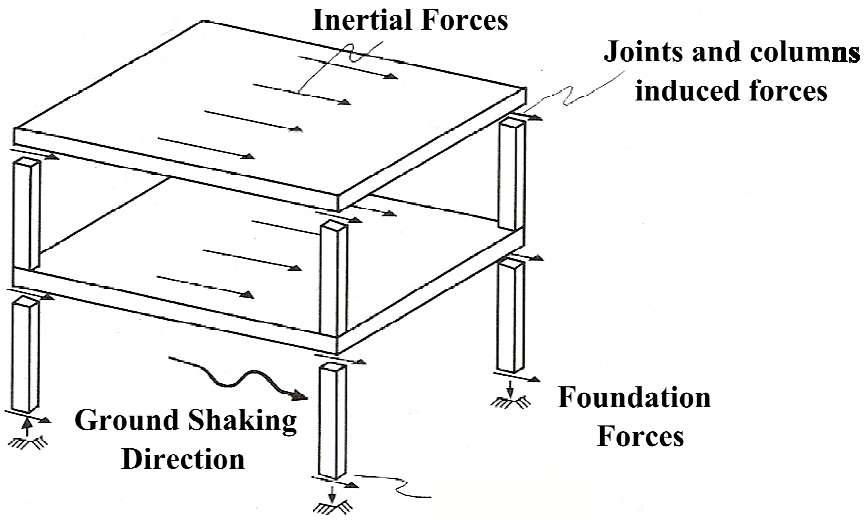

Figure 1.1 Transmission path of inertial forces to other components of the structure in a frame building [Bazán and Meli, 2002]

As illustrated above, the components and their masses resist the displacements imposed by the ground motion, giving place to inertial forces. These induced forces depend on the characteristics of the earthquake itself (e.g. magnitude, fault distance), on the modifications of the seismic signal while travelling from the source to the building base ground (the attenuation process) and of course on the mass and damping properties of the building. This dependence is expressed in the dynamic equilibrium equation (1.1) that rules the response of elastic single degree of freedom (SDOF) systems, where the acting inertial force $m\left(\ddot{u}+\ddot{u}_g(t)\right)$ is present, as well as the damping and resisting forces: $c\dot{u}$ and ku [Clough and Penzien, 1993].

$$m\ddot{u}+c\dot{u}+ku=-m\ddot{u}_g(t) \tag{1.1}$$

The base ground movement is represented by an acceleration record $\ddot{u}_g(t)$, having its own magnitude, duration and frequency content specific to the particular seismic event. The structure properties (*m, c* and *k*) are the mass, damping and stiffness respectively, and *u*, $\dot{u}$ and $\ddot{u}$ represent the system's response: displacement, velocity and acceleration respectively.

1.2.2. Frame Buildings: the seismic response

For getting a first insight into seismic response, the latter equation (1.1) of a SDOF system is considered. When divided by the mass *m*, it generates an equation in terms of ω, the structure's natural angular vibration frequency –computed as $\sqrt{k/m}$– and ξ, the damping

ratio [Clough and Penzien, 1993]:

$$\ddot{u} + 2\xi\omega\dot{u} + \omega^2 u = -\ddot{u}_g(t) \tag{1.2}$$

From Equation (1.2) it is evident that the ground motion signal $\ddot{u}_g(t)$ will be filtered and therefore modified by the structure properties ω and ξ, so that the structural response u, $\dot{u}$ and $\ddot{u}$, will deeply depend on the relative relation between ω, ξ and $\ddot{u}_g(t)$. This dependence may be well understood by means of the response spectrum shown in Figure 1.2 a). Actually, a response spectrum expresses the variation of peak responses (either displacement or velocity or acceleration) with the vibration period –or frequency–, for a specific ground motion, under a given damping level [Paulay and Priestley, 1992]. These responses are obtained from a large number of dynamic elastic analyses on SDOF systems for a specific damping level, i.e. solving the Equation (1.2). Thereby, response spectra are an essential tool for the estimation of structural responses since they provide directly peak values of response for a given vibration period.

However, for design purposes, design spectra are required in order to obtain expected demands consistent with a defined hazard level, instead of particular demands for a single motion. Thus, design spectra are smoothed curves, based on response spectra of past earthquakes, intended to represent the expected demand for a given vibration period, see Figure 1.2 b).

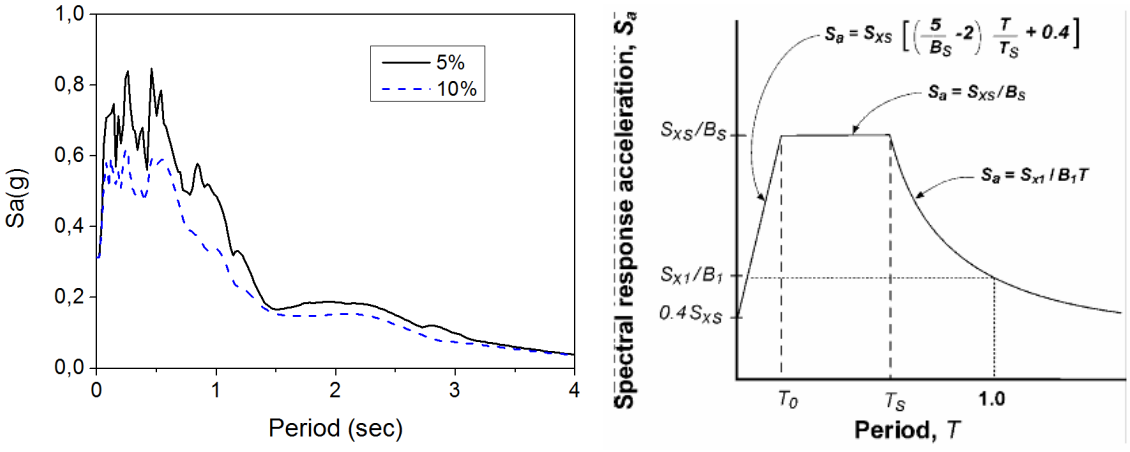

a) **b)**

Figure 1.2 a) Response spectra of "El Centro" record, for damping values of 5% and 10%, b) Example of a design spectrum [ASCE, 2000]

Furthermore, as a general rule, response decrease with damping as it is observed in Figure 1.2a). Hence the importance of adequate handling of hysteretic damping in modern seismic design philosophy. Actually, in the search for additional sources of damping, numerous efforts have been devoted for implementing damping devices on some structures like bridges and high-rise buildings. Concerning the relationship between the dominant frequencies of the seismic signal and ω, the closer this relationship is to one, the larger the response will be.

These rules remain valid when dealing with Multiple Degree of Freedom (MDOF) systems. In fact, the structural response may be decomposed according to the structure's vibration modes, each one having a well defined frequency and damping. In this case, despite the existence of several frequencies, the most important relations to care about are those with the frequencies of the first modes, which have proven to be the most influential on response. Actually, they may completely modify the expected response and cause important damage if neglected. Furthermore, a particular difficulty to be tackled arises when going beyond the elastic limit since the frequencies may change during the seismic movement.

Regarding the estimation of responses, small earthquakes generate structural responses which usually remain within the elastic domain so that even simplified elastic procedures based on equivalent first-mode SDOF systems are sufficient to predict response with an acceptable accuracy. For larger magnitudes, except for the mass properties in general, the structural properties do change: damping increases as hysteretic sources of energy dissipation appear and stiffness decreases since materials reach or exceed their elastic strength causing cracking or yielding phenomena. Also, additional properties start playing a significant role: ductility of sections and components, joint detailing and sequence of failure mechanism development will also determine the response characteristics and whether a failure is likely or not to happen. Accordingly, the consideration of nonlinear behaviour of materials, components and the whole structure is compulsory.

1.2.3. Frame buildings: Failure mechanisms

Global behaviour of current structures depends on the distribution of components, on the connections between them, on the number of sections exceeding their elastic limit and how these sections resist inelastic deformations. For representation purposes at the structure level, an overall force-displacement relationship is considered to provide the lateral-resisting capabilities of the whole building [Bazán and Meli, 2002]. This curve represents usually the

base shear *vs.* the roof displacement as illustrated in Figure 1.3.

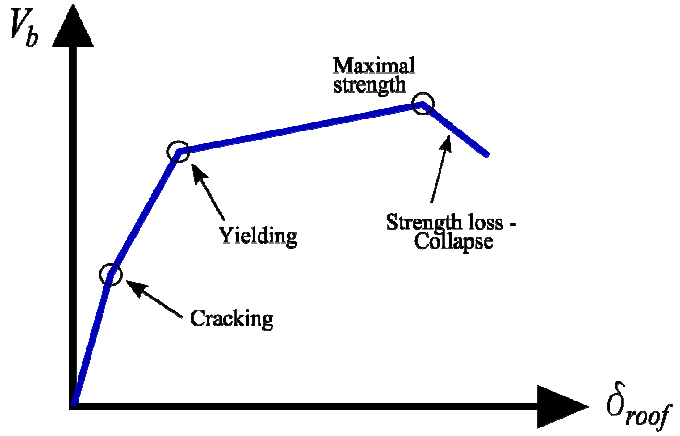

Figure 1.3 Usual representation of building lateral global behaviour

Four main stages may be observed: firstly, a fully elastic section between the undeformed state and the first cracking, secondly the yielding point from which more sections of the structure exceed their elastic limit until reaching the third stage, the maximal strength (bearing capacity) and then finally a mechanism is formed causing strength loss and/or instability, leading eventually to collapse. For modelling purposes, the first stage is often neglected and replaced with a straight line up to the second stage.

Relying on this curve, the building response may be classified into ductile and brittle type, according to the behaviour after the yielding point, as it may be observed in Figure 1.4, where these two possible types of response are compared. A ductile behaviour is obtained when the distribution of components, their relative strengths and the detailing of cross sections allow the development of extensive inelastic deformations in a sufficient number of sections without strength loss. Of course a considerable quantity of damage is expected to develop. Hence an important amount of seismic energy may be dissipated, reducing the quantity of kinetic energy and the inertial forces as well [García, 1998]. For example, the configurations *D1* and *D2* in Figure 1.4 represent this kind of behaviour by a weak-beam strong-column mechanism.

On the contrary, brittle behaviour is characterized by limited inelastic deformations, low amounts of dissipated energy and sudden, brittle collapse mechanisms like the storey-mechanism illustrated in the weak-column configuration *F1*.

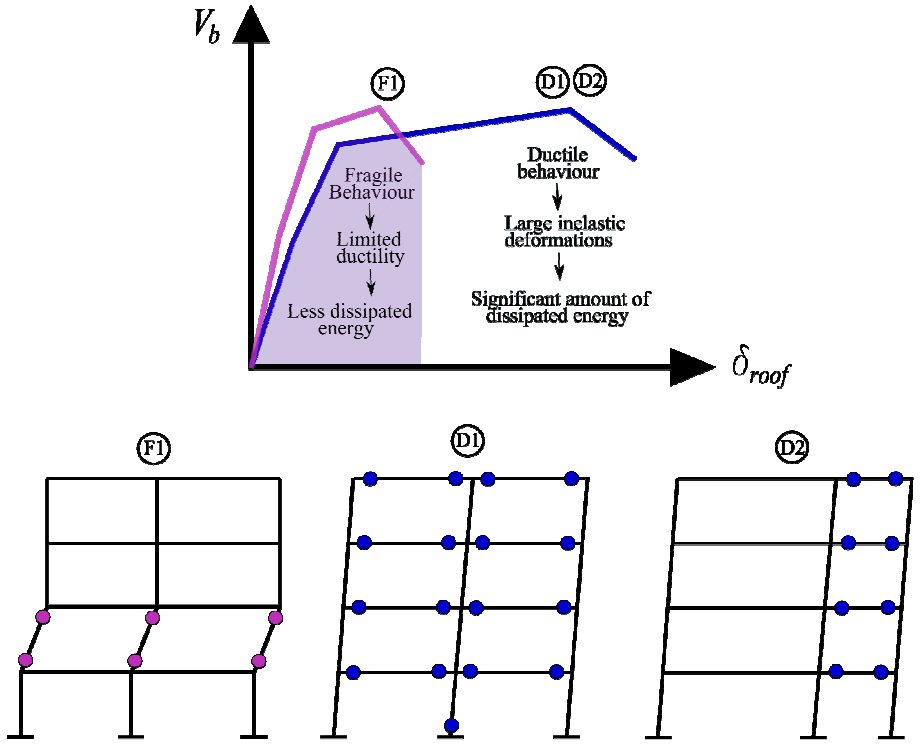

Figure 1.4 Ductile and brittle typical mechanisms and their associated force-displacement curves

1.2.4. Components behaviour

At the component level, nonlinear behaviour is also represented by force-deformation relationships, e.g. Moment-curvature, shear-distortion or force-displacement in the case of flexion, shear or axial stresses respectively. Since earthquake events are time-variant, the hysteretic properties play a major role in the representation of the component behaviour. Therefore, the response of components under cyclic loading must be well understood. Numerous models, from the bilinear to the strength and stiffness deteriorating model, have been proposed and calibrated by means of experimental studies [Takeda *et al.*, 1970; Ibarra *et al.*, 2005]. They are usually characterized by envelopes of the dynamic behaviour (see Figure 1.5), intended to represent the actual behaviour by means of a backbone curve and some hysteretic rules.

Figure 1.6 presents three typical hysteretic behaviours, ranging from one which dissipates the most quantity of energy (case a)), represented by the area enclosed within the loop, to a strength deteriorating behaviour (case c)) [Bazán and Meli, 2002]. All of them are typical of some components according to their respective function, as follows.

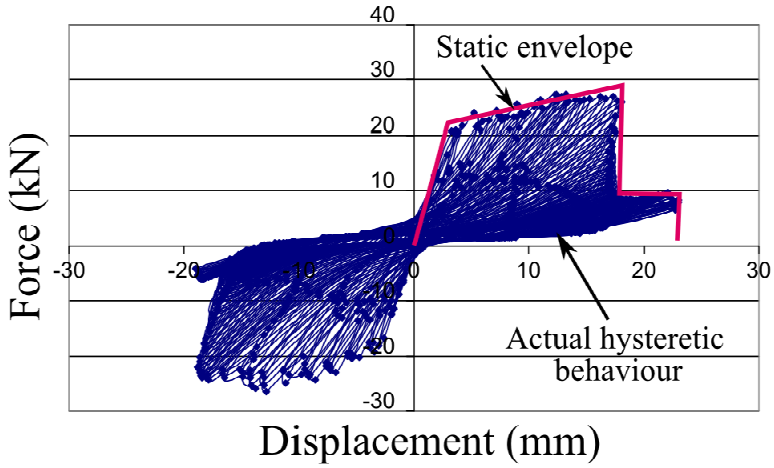

Figure 1.5 Force-displacement experimental curve of a reinforced concrete column and its envelope

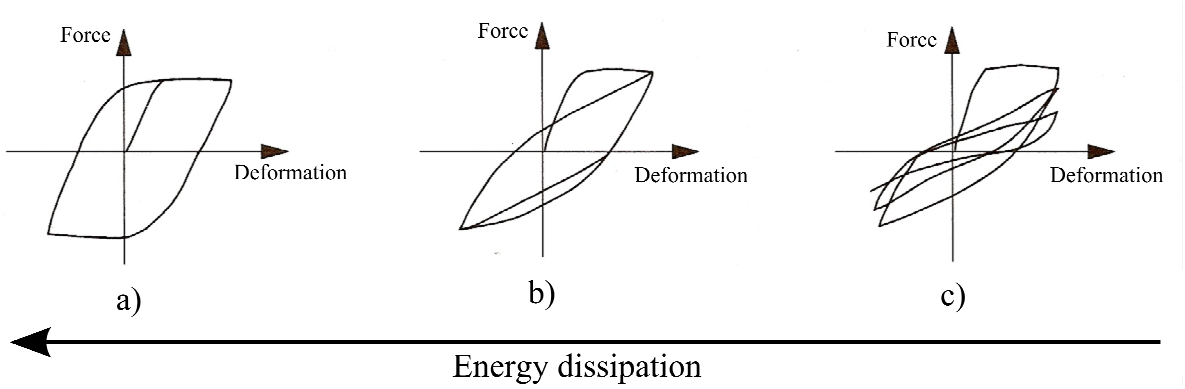

Figure 1.6 Examples of different hysteretic behaviours [Bazán and Meli, 2002]

1.2.4.1. Beams

Beam-type components must usually bear considerable bending and shear stresses. Axial forces, although present, are usually neglected for analysis purposes due to their low magnitude. Between bending and shear stresses, the former is preferred to be the predominant stress as bending behaviour may be an important source of ductility, providing therefore a ductile behaviour of the structure. In fact, well detailed, under-reinforced beams, with low shear stresses, may have hysteretic loops as that of Figure 1.6a. Shear behaviour, on the contrary, restricts the capacity of developing inelastic deformations and may lead to brittle mechanisms which must be avoided since they produce loops with strength and stiffness loss, as shown in Figure 1.6c [Bazán and Meli, 2002]. In the case of reinforced concrete beams,

ductility is a function of tension and compression reinforcement as well as critical section detailing, requiring enough stirrups in order to avoid buckling of bars and guarantee the core integrity.

1.2.4.2. Columns

Unlike beam elements, column-type elements do bear large axial loads, combined with shear and bending forces. Therefore it is difficult to predict their behaviour when dealing with seismic forces since the existing axial forces change a lot during the earthquake: the columns may be subjected to tension stresses or excessive compression stresses. The magnitude of axial forces determines partly the hysteretic behaviour. Thereby, the more axial load is sustained by the column, the less wide the cyclic loops are and the less energy is dissipated. Figure 1.6b is an example of the hysteretic behaviour of a column with low to moderate axial loads.

1.2.5. Modelling of components

When dealing with the representation of the nonlinear behaviour of frame elements two basic options are available: i) lumped plasticity (see Figure 1.7a) and ii) distributed plasticity models (see Figure 1.7b). Generally speaking, they are global models built on the basis of the component behaviour determined usually by experimental tests and represented by force-deformation relationships like those already mentioned in the above section.

First option consists in separating the different behaviours that may be present in the element –linear elastic and inelastic– in several elements connected in series [D'Ambrisi and Filippou, 1999]. Thereby, it concentrates the nonlinear behaviour on finite-length, critical sections where the development of plastic hinges is expected, while considering the remaining element as elastic. Usually plastic hinges are represented by nonlinear springs characterized in the bending direction by moment-rotation relationships. Strains and stresses are thus determined at only two points per element, i.e. at the plastic hinges. Limiting inelastic response to occur in these critical sections becomes its main disadvantage since it is very hard to predict the exact localization of those sections given the highly variable nature of earthquake forces. On the other hand this is the most common way of modelling since the computational cost is very attractive when multiple (requiring Monte Carlo simulations for

instance) or extensive dynamic analysis must be done.

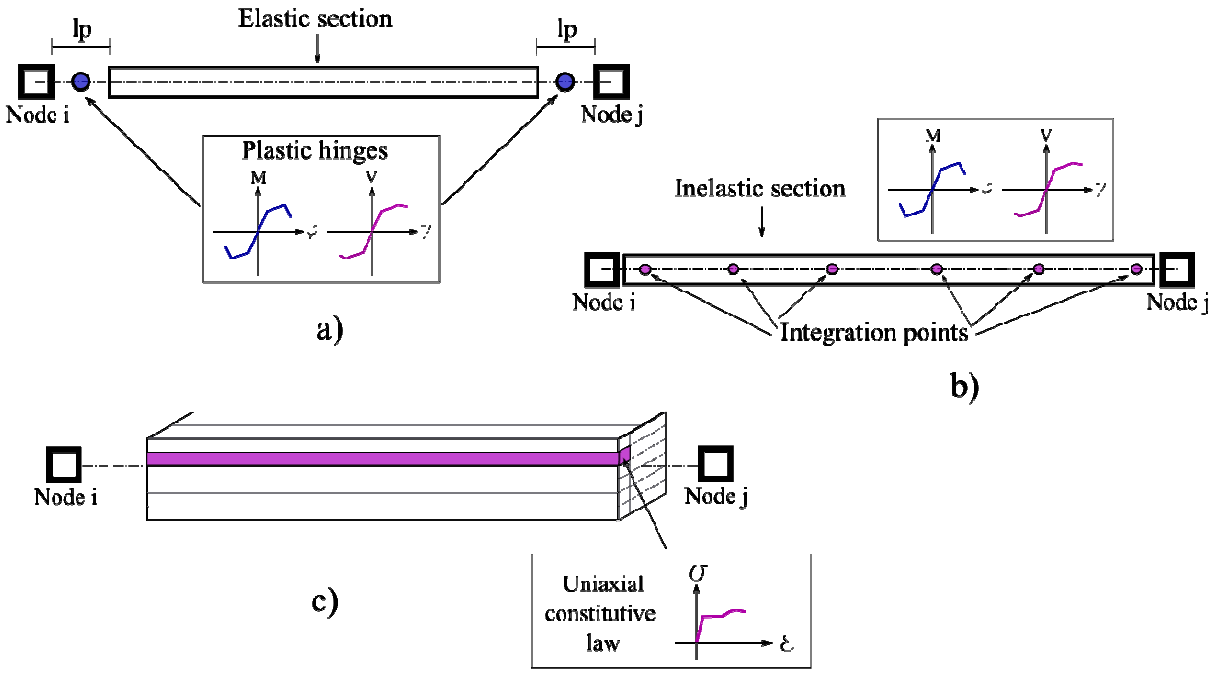

Figure 1.7 Different ways of modelling frame elements: a) Concentrated plasticity, b) Distributed Plasticity and c) Fibre modelling

The second option represents distributed plasticity models which account for inelasticity all along the element, computing response quantities on specified integration points, usually five or six [Spacone *et al.*, 1996]. This model has the advantage of identifying inelastic response at any location in the element, requiring of course more analysis duration time.

The characterization of sections may be done by a global or a local approach. Global approach consists in representing the global behaviour by means of force-deformation relationships as shown in Figure 1.7 a) and b).

Local approach is a fibre modelling, intended to take into account the behaviour and the distribution of each component material (e.g. steel and concrete in reinforced concrete elements) see Figure 1.7c). In this model, the cross section is represented by a finite element mesh of one-dimensional elements composed of a constitutive material, usually characterized by its axial constitutive law [Taucer *et al.*, 1991]. Fibre modelling allows considering the interaction between axial loads and bending moments in column-type elements and provides more accurate representations of inelasticity. Nevertheless, it is not of current use because of

its high computational cost.

1.2.6. Performance Based Engineering

PBE or Performance Based Engineering may be defined as a set of techniques that permits seismic behaviour analysis of structures by means of what is called *performance*, for design or evaluation purposes. In fact, performance means the ability of something to meet a specified requirement under specific conditions. Therefore it has to be defined on the basis of a required *performance level* and a *performance ground motion*. They are in fact related but their relationship depends on the structural use (residential, essential, etc), or on the structure's importance.

The most common structural performance levels have been stated in the FEMA356 guidelines [ASCE, 2000]. They are: Immediate Occupancy (IO), Life Safety (LS) and Collapse Prevention (CP).

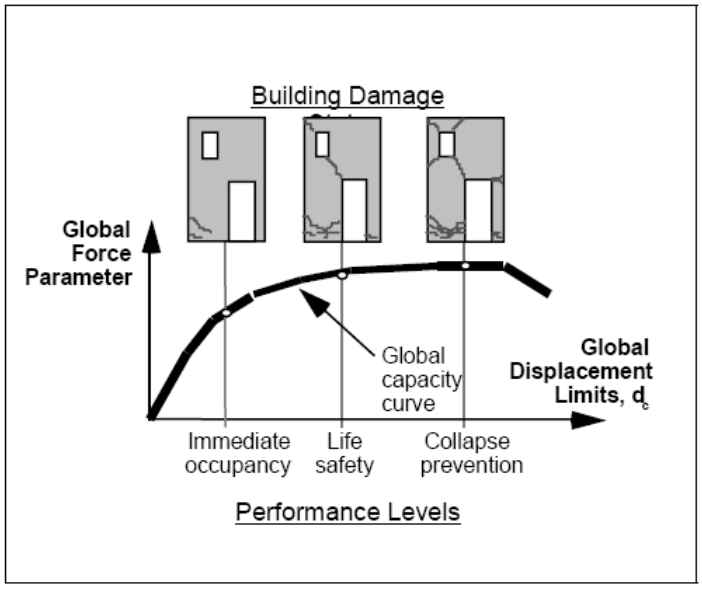

Figure 1.8 Structural performance levels and building damage, FEMA 308 [ATC, 1998b]

Figure 1.8 illustrates these levels on the capacity curve. In general terms, it may be said that IO stands for slightly inelastic responses with very limited damage: it does not require immediate repair so that reoccupation after the shaking is allowed. Under LS level, significant structural damage is expected; possible reoccupation requires temporary repairs and the

definite repair of the structure should be possible but not always feasible due to economical considerations. However, important residual security in order to face possible collapse must exist and the risk of injuries threatening life should be low. Finally, under CP level the structure is about to collapse partially or totally. Large structural damage is present and the risk of injuries is important. Usually, structural repair is not possible. Nevertheless, the main elements of the gravity-load resisting system still bear vertical loads although aftershocks may lead to collapse [ASCE, 2000].

1.2.7. Code provisions

Current code provisions rely on the assumption that an ordinary structure must support frequent, low magnitude earthquakes without damage, moderate earthquakes with some damage and rare, severe ground motions with extensive damage, preventing collapse. This hypothesis leads to the necessity of providing the structure with the required ductility according to the expected seismic demand so that it is able to bear the associated cyclic, inelastic deformations, retaining at the same time its safety and vertical loads bearing capacity. For important structures on the contrary, an almost elastic behaviour is requested.

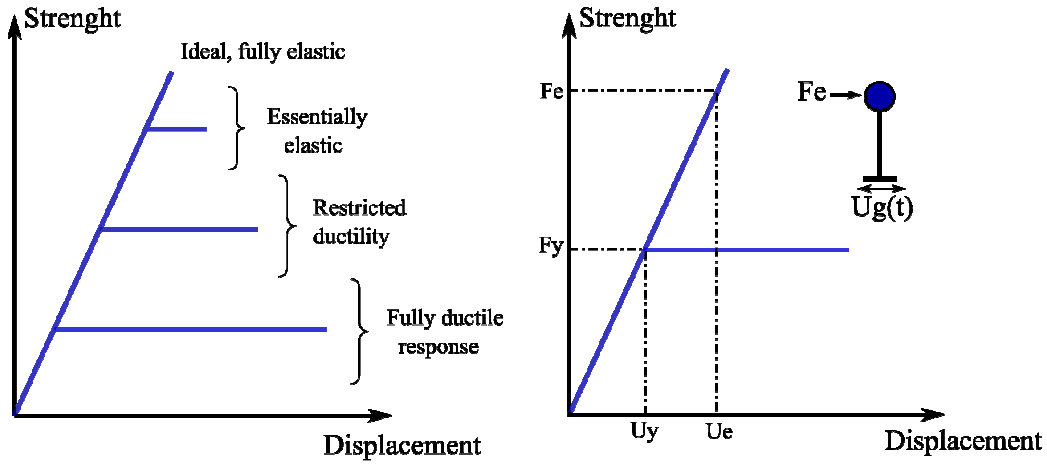

a) **b)**

Figure 1.9 a) Relationship between strength and ductility [Paulay and Priestley, 1992], b) Definition of the energy dissipation capacity [García, 1998]

Thus, it is possible to support seismic forces caused by strong earthquakes with a wide range of systems. Hence, the response of buildings will range between high-strength, essentially elastic systems to highly inelastic systems with reduced strength and high levels of

ductility, as illustrated in Figure 1.9a [Paulay and Priestley, 1992].

The relation between strength and ductility is also apparent in this figure. In fact, modern codes establish a basic coefficient R intended to reduce the required elastic seismic strength F_e (see Figure 1.9b) and to constrain the structure to respond in the inelastic domain. Thus, the yielding strength F_y (i.e. the required strength for which the system will be designed) may be computed with Equation (1.3) [García, 1998].

$$R_0 = \frac{F_e}{F_y} = \frac{U_e}{U_y} \quad \rightarrow \quad F_y = \frac{F_e}{R} \tag{1.3}$$

The coefficient R depends on the expected seismic hazard but also on the component material (steel or reinforced concrete, for instance) and the structural system (whether it is a bare frame, shear wall, etc) since they determine the capability of the system to dissipate seismic energy. As seen before, there is a clear relationship between strength and ductility. However the required ductility is not exactly equal to R. In fact, for systems fulfilling the *equal displacement principle*[1] it is found that coefficient R is approximately equal to ductility μ [Paulay and Priestley, 1992]:

$$\mu = R \tag{1.4}$$

But for systems with shorter vibration periods, it is found that required ductility is larger and may be estimated from the *equal energy principle*[2] as:

$$\mu = \frac{R^2 + 1}{2} \tag{1.5}$$

In summary, for most ordinary buildings, acting seismic forces are computed on the basis of elastic behaviour (by means of elastic, damped design spectra) and the required strengths are reduced by the R factor. Various methods are allowed by design codes to obtain seismic forces, from equivalent elastic forces and elastic modal analysis to dynamic analyses for a set of accelerograms. Finally, the components are provided with the required ductility by means

[1] For a given ground motion, those are systems with vibration periods larger than that producing the peak elastic spectra response. Once their strengths reduced, they will develop displacements approximately equal to those produced by their elastic counterparts. [Paulay and Priestley, 1992]

[2] The elastic system and the strength-reduced system are supposed to have the same area under the force-displacement curve, so the same energy. [Paulay and Priestley, 1992] It necessarily produces larger displacements of the latter system, unlike the equal displacement principle.

of adequate detailing.

Provided the application of these provisions with judgement a structure is expected to perform adequately when facing a moderate or severe earthquake. However, code provisions have not always been applied or existed everywhere and even now there are still so many places where their current application is not a common practice for the whole of the new building stock. As a result, there are a number of buildings, either designed only for gravity loads or seismic designed but not fulfilling code provisions, placed in moderate or high seismic risk areas. For these cases, seismic evaluation with reinforcing or retrofitting purposes is a way to reach the required safety level against a given seismic hazard.

Concerning the seismic evaluation of existing buildings, various analysis procedures (linear and nonlinear, static and dynamic) are permitted by the concerned codes, mostly according to the structural configuration [ASCE, 2000]. Nonlinear static procedures are usually allowed only for structures responding predominantly in the first mode. For structures where higher mode effects are expected to be significant, the dynamic nonlinear procedure is compulsory. This is perfectly feasible when dealing with a single or a few buildings to be evaluated. But when a large quantity of analyses is requested for probabilistic or reliability studies, simplified nonlinear methods capable of producing acceptable estimations of response are required.

1.3. NONLINEAR METHODS FOR THE ANALYSIS OF BUILDINGS UNDER EARTHQUAKE ACTIONS

For given ranges and contents of the seismic signal generated by an earthquake, the expected response of buildings subjected to these loads can be nonlinear in many cases, as stated before. Furthermore code seismic provisions rely on the assumption of the structure having enough ductility for resisting large inelastic deformations so that buildings are designed to respond in the nonlinear domain during the design earthquake shaking. For those reasons the implementation of accurate nonlinear methods to estimate the seismic response is a significant issue.

Several methods have been proposed so far, detailed nonlinear time history analysis (NLTHA) as well as simplified methods based on a few characteristics of the structure. Many of the existing methods present important drawbacks depending on the adopted assumptions.

In general, they may be classified according to their relative uncertainty, as presented in Figure 1.10 [FEMA440, 2005].

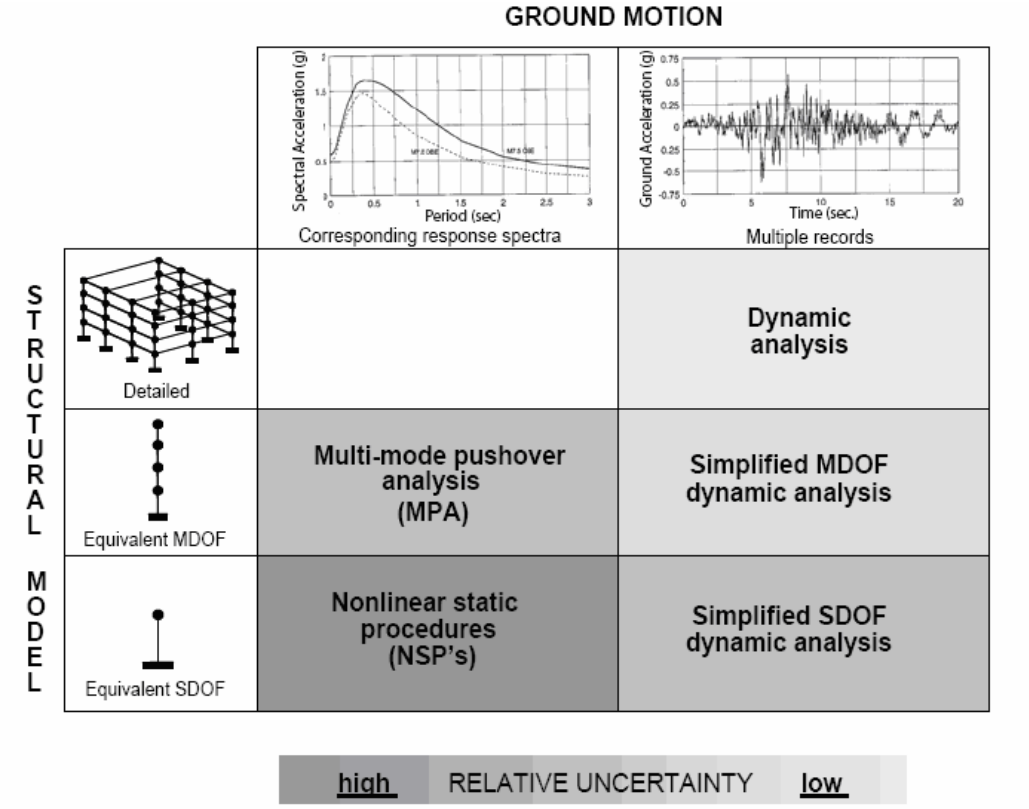

Figure 1.10 Some nonlinear methods classified according to the relative uncertainty for different models and ground motion characterization. From [FEMA440, 2005]

There may be observed that structural model features and the representation of ground motion effects are of major relevance on uncertainty. A brief description of the fundamentals and the application of some of the approximate methods are presented hereafter. The emphasis is put on methods based on multimode pushover analysis and simplified dynamic analysis over equivalent Single Degree of Freedom (SDOF) systems, given our interest on them. The Table 1-1 provides a classification of some of the methods that will be referenced here.

STATIC PROCEDURES	DYNAMIC PROCEDURES
First-mode pushover based - Capacity Spectrum Method (CSM) - Displacement Coefficient Method (DCM) - N2 Method	Pure dynamic - Nonlinear time history analysis (NLTHA)
Multi-mode pushover based - Modal Pushover Analysis (MPA) - Adaptive Modal Combination (AMC) - Displacement-based adaptive pushover (DAP) - Actual displacement based pushover (ADAP) - Generalized pushover analysis (GPA)	Multimode pushover based - Incremental Dynamic Analysis IDA - Uncoupled Modal Response History Analysis (UMRHA) - Enhanced UMRHA

Table 1-1 Overview of some nonlinear methods for seismic analysis of buildings

1.4. COMPLETE NONLINEAR TIME HISTORY ANALYSIS (NLTHA)

The most accurate procedure for solving the dynamic problem of a structure subjected to earthquake actions, considering its inherent nonlinear character, is a nonlinear time history analysis. The equation describing such a dynamic problem may be expressed as [Chopra, 2007]:

$$\mathbf{m}\ddot{\mathbf{u}} + \mathbf{c}\dot{\mathbf{u}} + \mathbf{f}_s(\mathbf{u}, sign\,\dot{\mathbf{u}}) = -\mathbf{m}\boldsymbol{\iota}\,\ddot{u}_g(t) \tag{1.6}$$

In this equation, which has the same form of Equation (1.1), **m** and **c** are the mass and damping matrices of the MDOF system; **u**, $\dot{\mathbf{u}}$ and $\ddot{\mathbf{u}}$ are, respectively, the displacement, velocity and acceleration vectors; $\ddot{u}_g(t)$ the seismic signal and $\boldsymbol{\iota}$ the influence vector [Chopra, 2007]. As the excitation $\ddot{u}_g(t)$ may be defined as a discrete time-dependent function, a NLTHA makes a numerical evaluation of dynamic response through time-stepping methods (e.g. Newmark's method, average acceleration method). For doing so, it solves the dynamic equation (1.6) step by step, with the initial conditions $\mathbf{u}(0) = 0$ and $\dot{\mathbf{u}}(0) = 0$, and produces the vector $\mathbf{u}(t)$ as immediate result.

Naturally the results accuracy depends deeply on the quality of the input information, on the models used to represent the nonlinear behaviour as well as on the judgment and

experience of the designer. Given the detailed level of the required information about the structure, most of cases in which NLTHA is employed are special structures (e.g. very important or strategic because of its function or highly irregular structures) or those with an important participation of higher modes in response. Besides that, analysis and post-processing duration time still remain the main drawbacks for this method regarding its current use in practical applications.

1.5. PUSHOVER-BASED METHODS

In order to reduce the computational cost associated to complete dynamic analysis several approximate methods have been proposed with variable levels of simplification. A special nonlinear static analysis, called henceforth “pushover analysis”, has been used as the basis of most of the simplified methods. It uses a specific load profile which is applied on a detailed nonlinear model of the structure. This procedure is performed step by step until the structure reaches a predefined limit or until it becomes unstable [ATC, 1996].

The load profile may be uniform, triangular, in accordance with a code distribution or proportional to the first (or a higher) modal shape. Then by tracking the base shear (V_b) and the roof displacement (U_r), a special nonlinear force-displacement curve called “the capacity curve” may be developed taking U_r as abscissa and V_b as ordinate. This curve is assumed to represent the whole building as if it were a SDOF system, which is one of the fundamental assumptions of pushover analysis.

On the basis of first–mode pushover analysis, three methods have become currently used in engineering practice: the Capacity Spectrum Method (CSM), the Displacement Coefficient Method (DCM) and the N2 Method.

1.5.1. The Capacity Spectrum Method

The CSM was originally presented by Freeman *et al.* [1975] as a graphical method permitting the comparison between capacity and demand on the same format. Now, it is one of the procedures suggested in the ATC-40 guidelines [ATC, 1996] to estimate the maximum displacement of a structure under earthquake actions by using a performance based approach.

It is essentially an equivalent linearization technique which approximates the maximum inelastic deformation through an iterative process. In fact, it modifies the elastic demand

spectrum by an equivalent damping which is proportional to the relationship between the area enclosed within the capacity curve loop and the maximum strain energy, as shown in Figure 1.11b). The structural performance is represented by the performance point, found as the intersection of the so called capacity spectrum and a reduced demand spectrum, in a S_a-S_d format, as shown in Figure 1.11a).

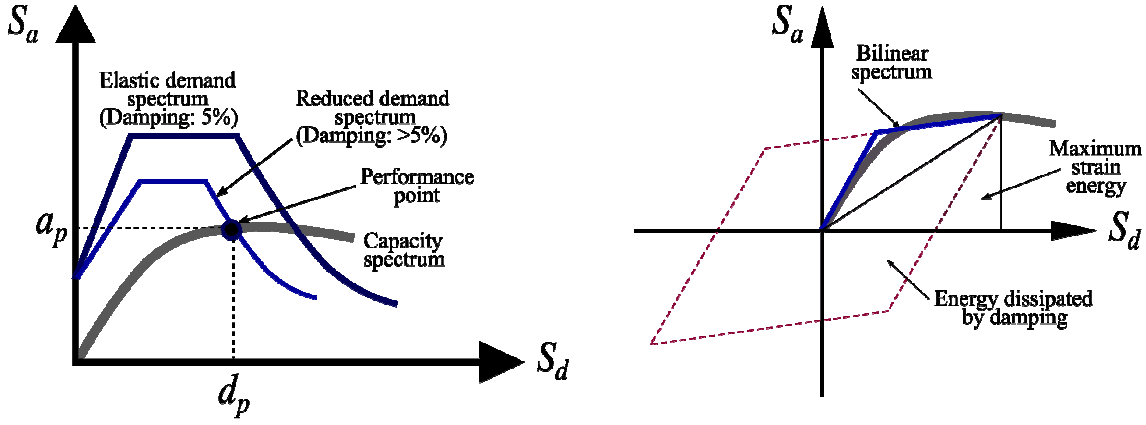

a) **b)**

Figure 1.11 CSM method: a) Getting the performance point (d_p, a_p), b) Areas for computing the equivalent damping

The capacity spectrum is obtained from the capacity curve developed from a pushover analysis. For having the capacity curve in an ADRS (Acceleration displacement response spectrum) format, the following expressions are to be used [ATC, 1996]:

$$S_a = \frac{V_b / W}{m_{ef}^1} \qquad S_d = \frac{\Delta_{ROOF}}{\alpha_1 \phi_{ROOF}^1} \tag{1.7}$$

Where S_a and S_d are the spectral acceleration and the spectral displacement respectively; V_b and W are the base shear and the total weight; m_{ef}^1 is the effective modal mass ratio; Δ_{ROOF} and ϕ_{ROOF}^1 are the lateral displacement and the first modal shape amplitude at the roof level; and α_1 is the modal participation factor for the first mode.

At the same time it is necessary to convert the response or design spectrum to the ADRS format. As this spectrum is already on a S_a - T format, it is only necessary to find S_d by means of Equation (1.8), T being each vibration period in the spectrum:

$$S_d = \frac{S_a}{\omega^2} = \frac{S_a T^2}{4\pi^2} \tag{1.8}$$

The location of the performance point must satisfy two relationships: First, the point must rely on the capacity spectrum in order to represent the structure at a given displacement, and, second, it must rely also on a demand spectrum, reduced from the elastic, 5% spectrum, so that it represents the nonlinear demand at the same structural displacement. To achieve this two criteria, a trial and error search must be performed [ATC, 1996].

1.5.2. The Displacement Coefficient Method

This method relies also on the capacity curve but it modifies the elastic response of the equivalent SDOF system in order to estimate the so-called target displacement (δ_t). So, based on a specific bilinear representation of the capacity curve, an effective fundamental period T_e is obtained from [ASCE, 2000]:

$$T_e = T_i \sqrt{\frac{K_i}{K_e}} \tag{1.9}$$

T_i being the elastic period, K_i is the elastic lateral stiffness and K_e is the effective lateral stiffness, as shown in Figure 1.12.

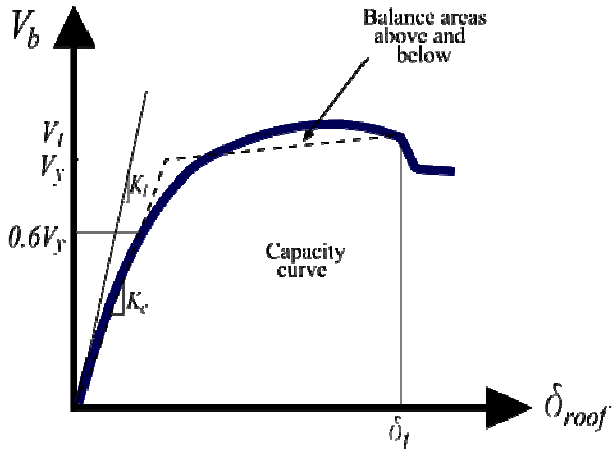

Figure 1.12 Displacement Coefficient Method: Estimating the target displacement, δ_t

Once T_e is known, the elastic demand of the equivalent SDOF system may be computed by means of Equation (1.8). This displacement is then modified by four coefficients in order to estimate the target displacement (δt) as:

$$\delta_t = C_0 C_1 C_2 C_3 S_a \frac{T_e^2}{4\pi^2} \quad (1.10)$$

C_0 relates the spectral displacement of the equivalent SDOF system with the buildings' roof displacement; C_1 relates the expected maximum inelastic response with the elastic one; C_2 takes into account the effect of hysteretic pinched shape, stiffness degradation and strength deterioration on inelastic displacement; and C_3 accounts for dynamic P-Delta effects on the response displacement [ASCE, 2000].

1.5.3. The N2 Method

The development of the N2 method arises from the need of fixing some identified flaws present in the CSM method. In fact, estimating inelastic demands on the basis of elastic spectra, modified by the equivalent damping, lacks of theoretical foundation since there is no evidence of a clear relationship between these two parameters [Fajfar, 1999].

Thereby, the N2 method proposes a more rational strategy: it uses the CSM framework for the graphical representation of capacity and demand but instead of using equivalent damped spectra it estimates the demand by means of inelastic demand spectra. These latter spectra are obtained from elastic spectra and reduction factors based on ductility [Fajfar and Gašperšič, 1996; Fajfar, 1999; Fajfar, 2007]. This method was also intended to be an efficient tool for practical design purposes. In fact, it was implemented in the Eurocode 8 standard [CEN, 2003].

Due to some identified problems, the CSM and the Displacement Coefficient Method, were improved in FEMA440 report [ATC, 2005]. However, despite the useful insight on the expected inelastic response provided by these procedures, their application remains limited to systems responding predominantly in the first mode (which means buildings with a period of vibration up to about 1 second). Thus, pushover based multimodal procedures have arisen as an alternative in order to take into account higher mode effects on the structural response.

1.6. MULTIMODAL PUSHOVER BASED METHODS

One of the first attempts to consider higher modes on the seismic response, on the basis of standard pushover analysis was that of Paret *et al*. [1996] which used the CSM framework to identify failure mechanisms caused by higher mode effects. Several improvements as well as

new approaches have been presented ever since, e.g. the Adaptive Spectra-Based Pushover [Gupta and Kunnath, 2000] and the modal pushover analysis (MPA) [Chopra and Goel, 2002] among an extensive list, since it was reported that such a procedure results in important improvements of the responses accuracy in comparison to classic first-mode based methods. Some of these methods are described later.

Most multi-modal pushover based methods rely on the same basic assumptions. Based on the capacity curve, an equivalent SDOF system is used to represent the lateral behaviour of the whole structure which is usually a Multi-Degree of Freedom (MDOF) system. The capacity curve development requires a pushover analysis for a detailed model under a specific load profile. Depending on the required responses and the available information, the SDOF system can therefore be submitted to a ground motion record or to a response (or design) spectrum. The resulting displacement D_n or history of displacements $D_n(t)$ becomes the basis to estimate global demand parameters such as storey displacements and drifts directly and other response quantities such storey shears, internal forces or element rotations, indirectly. An overall view of this kind of strategy is illustrated in Figure 1.13 where R^i_{nj} represents any response parameter to be studied: displacement, storey drift, internal force or rotation, for instance.

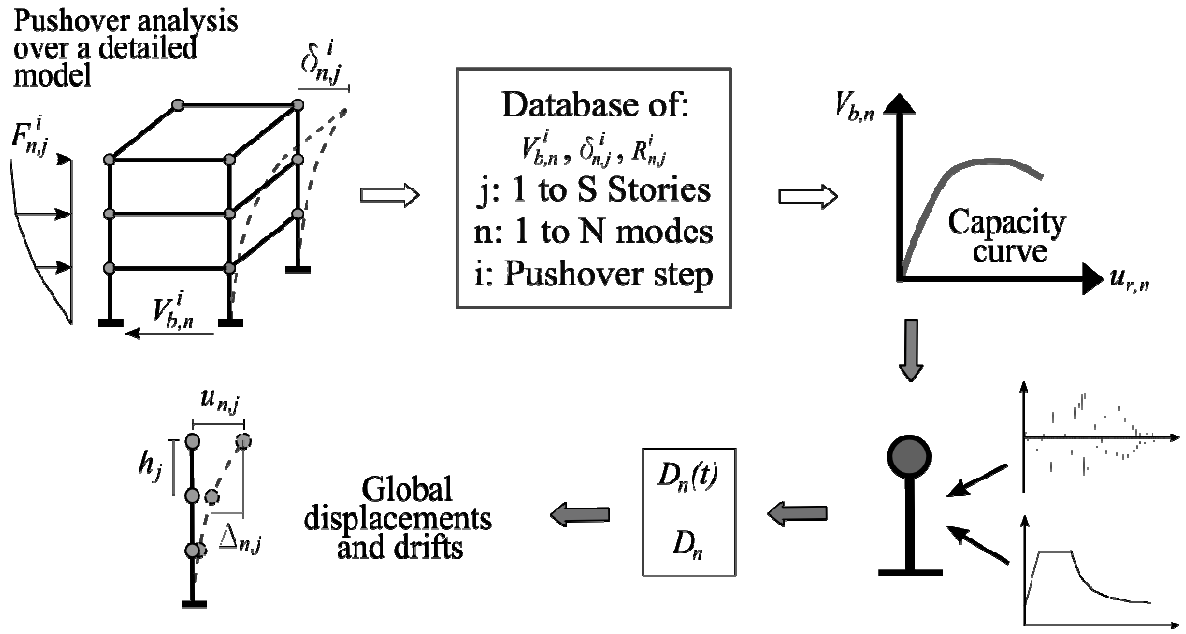

Figure 1.13 General scheme of a multimodal pushover based method [Jerez and Mebarki, In press]

This procedure is to be performed for each mode until obtaining an adequate accuracy. Usually considering a few modes is enough to obtain a good accuracy. Finally the peak responses are obtained from superposition of modal responses or from modal combination rules such as the square root of the sum of squares (SRSS) or the complete quadratic combination (CQC).

1.6.1. Uncoupled Modal Response History Analysis (UMRHA)

The UMRHA was introduced as an approximate method with the only aim of being the base of a simpler method, the Modal Pushover Analysis (MPA) [Chopra and Goel, 2002]. Both methods have become important references for the estimation of responses under earthquake loads when higher modes need to be considered. In fact their theoretical basis lies on structural dynamics, particularly in the classic elastic modal analysis developed in a convenient way. The main assumptions in their development are i) the modal coupling after yielding is neglected, ii) the superposition of responses is still valid for nonlinear systems and iii) the capacity curve is approximated as a bilinear curve. The development for elastic as well as the extension for inelastic systems is presented hereafter.

1.6.1.1. Elastic systems

The development of the classic modal response history analysis for elastic systems is based on the differential equations (1.11) of a MDOF system, under earthquake induced forces in this particular case [Chopra, 2007]:

$$\mathbf{m}\ddot{\mathbf{u}} + \mathbf{c}\dot{\mathbf{u}} + \mathbf{k}\mathbf{u} = -\mathbf{m}\boldsymbol{\iota}\ddot{u}_g(t) \tag{1.11}$$

In this equation **k** represents the elastic stiffness matrix of the structure. Direct solution of this set of equations leads to the standard and so considered ‘exact’ approach, the time history analysis (THA). Thus, for finding a modal solution, the right side of the equation (1.11) may be seen as the effective earthquake forces, $P_{eff}(t)$ [Chopra, 2007]:

$$\mathbf{p}_{eff}(t) = -\mathbf{m}\boldsymbol{\iota}\ddot{u}_g(t) \tag{1.12}$$

Spatial distribution and modal expansion of these forces could be defined by the following expressions:

$$\mathbf{m\iota} = \sum_{n=1}^{N} \mathbf{S}_n \qquad \mathbf{S}_n = \Gamma_n \mathbf{m}\boldsymbol{\phi}_n$$
$$\Gamma_n = \frac{L_n}{M_n} \qquad L_n = \boldsymbol{\phi}_n^T \mathbf{m\iota} \qquad M_n = \boldsymbol{\phi}_n^T \mathbf{m}\boldsymbol{\phi}_n \tag{1.13}$$

Γ_n represents the modal participation factor, $\boldsymbol{\phi}_n$ the n*th* modal shape and M_n the generalized mass for each mode *n*. Then, for each mode, the equation (1.11) becomes:

$$\mathbf{m}\ddot{\mathbf{u}} + \mathbf{c}\dot{\mathbf{u}} + \mathbf{k}\mathbf{u} = -\mathbf{s}_n \ddot{u}_g(t) \tag{1.14}$$

Developed in this way, the response of the MDOF system to the modal effective forces $\mathbf{s}_n$ depends only on the n*th* mode, regardless of the other modes. Accordingly, a solution for the equation (1.14) in terms of the n*th* modal coordinate q_n is found as:

$$\mathbf{u}_n(t) = \boldsymbol{\phi}_n q_n(t) \tag{1.15}$$

When substituting this last relationship into the equation (1.14) an equation with the vibration and damping properties of the n*th* mode is found:

$$\ddot{q}_n + 2\zeta_n \omega_n \dot{q}_n + \omega_n^2 q_n = -\Gamma_n \ddot{u}_g(t) \tag{1.16}$$

This equation can be compared with the governing equation of a SDOF system (1.17), leading to the relationship (1.18).

$$\ddot{D}_n + 2\zeta_n \omega_n \dot{D}_n + \omega_n^2 D_n = -\ddot{u}_g(t) \tag{1.17}$$

$$q_n(t) = \Gamma_n D_n(t) \tag{1.18}$$

Consequently, the solution turns into *N* uncoupled single equations which could be solved easily for D_n by classic time-stepping methods.

1.6.1.2. Extension to inelastic systems

Once the elastic limit is exceeded, the relationship between lateral forces and lateral displacements depends on the complete history of displacements. It means that the restoring force (the term **ku** of the equation (1.14)) becomes $\mathbf{f}_s(\mathbf{u}, sign\,\dot{\mathbf{u}})$, leading to the equation (1.6) repeated here for convenience:

$$\mathbf{m}\ddot{\mathbf{u}} + \mathbf{c}\dot{\mathbf{u}} + \mathbf{f}_s(\mathbf{u}, sign\,\dot{\mathbf{u}}) = -\mathbf{m\iota}\,\ddot{u}_g(t) \tag{1.6}$$

Developing a modal solution, in this case, will lead to a coupled system of equations which would not have any advantage over the classic solution. However, if the response of elastic systems to the effective forces is entirely in the n*th* mode, for nonlinear systems it is expected that the n*th* mode is predominant in the response. Concerning this assumption, research works have confirmed weak coupling between modes in nonlinear systems, even for unsymmetrical-plan buildings [Chopra and Goel, 2002; 2004]. Therefore, it seems acceptable to neglect modal coupling and a system of uncoupled equations is possible through the approximation of the restoring forces in modal coordinates **q**, depending on one modal coordinate, q_n, instead of all of them, **q** (coupled system) [Chopra and Goel, 2002]:

$$F_{sn} = \boldsymbol{\phi}_n^T \mathbf{f}_s(q_n, sign\,\dot{q}_n) \tag{1.19}$$

The term F_{sn} represents a 'nonlinear hysteretic function of the nth modal coordinate q_n' according to Chopra [2007], which depends on the displacement and the direction of velocity beyond the elastic limit. Next, by means of Equation (1.18) an expression similar to (1.17) is derived:

$$\ddot{D}_n + 2\zeta_n \omega_n \dot{D}_n + \frac{F_{sn}}{L_n} = -\ddot{u}_g(t) \tag{1.20}$$

As before, the equation (1.20) may be solved by any classic nonlinear method provided the "$F_{sn}/L_n - D_n$" curve. This curve is analogous to the capacity spectrum of the CSM method since it represents the lateral behaviour of the equivalent SDOF system and it is generated in the same way from the capacity curve, through the following equivalent equations [Chopra and Goel, 2002]:

$$\frac{F_{sn}}{L_n} = \frac{V_{bn}}{M_n^*} \qquad D_n = \frac{u_{rn}}{\Gamma_n \phi_{rn}} \tag{1.21}$$

V_{bn} is the base shear, M_n^* is the effective modal mass and u_{rn} and ϕ_{rn} are the displacement and modal shape amplitude at the roof level, all for the n*th* mode. In the case of UMRHA and MPA the chosen profile to develop the capacity curve is $\mathbf{s}_n = \mathbf{m}\boldsymbol{\phi}_n$, regarded as the most adequate due to the lack of an invariant profile which produces displacements proportional to modal shapes with increasing D_n ($\mathbf{u} = \boldsymbol{\phi}_n D_n$) even after yielding [Chopra and Goel, 2002].

Once made this extension to nonlinear systems, the substitution of the equation (1.18) into the equation (1.15) gives storey displacements and storey drifts:

$$\mathbf{u}_n(t) = \Gamma_n \boldsymbol{\phi}_n D_n(t) \tag{1.22}$$

$$\Delta_{jn}(t) = \Gamma_n (\phi_{jn} - \phi_{j-1,n}) D_n(t) \tag{1.23}$$

Then, under the assumption that superposition principle is still valid, the general framework of classic modal analysis remains applicable even for inelastic systems [Chopra and Goel, 2002]. Thereby, the total response is computed from:

$$\mathbf{u}(t) = \sum_{n=1}^{N} \mathbf{u}_n(t) = \sum_{n=1}^{N} \Gamma_n \boldsymbol{\phi}_n D_n(t) \tag{1.24}$$

$$\Delta_j(t) = \sum_{n=1}^{N} \Delta_{jn}(t) = \sum_{n=1}^{N} \Gamma_n (\phi_{jn} - \phi_{j-1,n}) D_n(t) \tag{1.25}$$

Peak responses are easily computed from maximum values of total responses.

1.6.2. Modal Pushover Analysis

Derived from the UMRHA, the MPA is itself an improved multi-mode pushover analysis which aims to take into account, in a simpler way, higher mode effects in the response of MDOF systems. It adopts the main starting steps of the UMRHA but it estimates peak responses directly from the pushover analysis. In fact, the peak modal equivalent displacement D_{no} may be obtained either by solving the equation (1.20) and computing the peak of $D_n(t)$ or directly from a response or design spectrum. Subsequently the peak modal roof displacement is computed as [Chopra and Goel, 2002]:

$$u_{rn} = \Gamma_n \phi_{rn} D_{no} \tag{1.26}$$

Therefore, any peak modal response quantity r_{no} may be estimated by relating the peak roof displacement u_{rn} and the pushover database (displacements, drifts or any other response quantity) for each mode. Finally, to compute peak responses, the modal responses are combined by any suitable rule (e.g. SRSS).

Since its publication, the MPA is considered as an effective tool for estimating global peak responses of the structure, such as floor displacements and storey drifts, as it accounts for higher mode effects while requiring a reasonable computational cost. Nevertheless, there are some points, related with its main assumptions, which still require improvements: lateral load profiles are invariant, modal properties are considered constant during the whole range of

behaviour and roof displacement is still used as an indicator of the whole lateral deformation properties. Consequently, this method may suffer lack of accuracy when extensive damage is developed in the nonlinear domain.

1.6.3. Improvements to the MPA or UMRHA

Several modifications to MPA or UMRHA have been proposed so far, aiming to improve one or more of their basic assumptions. Some of these proposals are referenced below.

1.6.3.1. The energy-based approach

Most classic pushover methods use the roof displacement as an indicator for representing the whole lateral behaviour of a structure through its capacity curve. This choice is made mainly for convenience but it could not be valid when applied to other modes than the first. In fact, some problems developing higher mode capacity curves, like reversals or stiffening in the post yield response have been already identified [Hernández-Montes *et al.*, 2004; ATC, 2005; Tjhin *et al.*, 2006]. As a result, Hernandez-Montes *et al*. [2004] proposed an alternative capacity curve expressed in terms of shear force and an equivalent displacement, computed from the absorbed energy during pushover analysis.

In summary, the basis of this approach relies on the basic equation of motion expressed in terms of energy [Hernández-Montes, *et al.*, 2004]. The integration of this equation with respect to displacement, results in:

$$\frac{1}{2}\dot{\mathbf{u}}_t^T \cdot \mathbf{m} \cdot \dot{\mathbf{u}}_t + \int \dot{\mathbf{u}}^T \cdot \mathbf{c} \cdot d\mathbf{u} + \int \mathbf{f}_s^T d\mathbf{u} = \int (\sum_{i=1}^{N} m_i \ddot{u}_{ti}) du_g \tag{1.27}$$

Then, the absorbed energy may be expressed as:

$$E_a = \int \mathbf{f}_s^T \cdot d\mathbf{u} \tag{1.28}$$

The static force associated to each mode is $\mathbf{f}_n(t)$ and the restoring force $\mathbf{f}_s$ is assumed to be the summation of the modal components $f_n(t)$, which may be expressed in terms of its modal properties as:

$$\mathbf{f}_s(t) = \sum_n f_n(t) = \sum_n \omega_n^2 \mathbf{m} \phi_n \Gamma_n D_n(t) \tag{1.29}$$

Moreover, absorbed energy in the elastic domain may be computed as:

$$E_n = \frac{1}{2}\mathbf{f}_n^T \cdot \mathbf{u}_n = \frac{1}{2}\omega_n^2 \boldsymbol{\phi}_n^{\mathrm{T}} \mathbf{m} \boldsymbol{\phi}_n \Gamma_n^2 D_n^2(t) = \frac{1}{2}\omega_n^2 \Gamma_n^2 \mathrm{M}_n D_n^2(t) \tag{1.30}$$

And the corresponding base shear for the n*th* mode is:

$$V_{bn} = \mathbf{f}_n^T \cdot \mathbf{1} = \omega_n^2 \Gamma_n^2 \mathrm{M}_n D_n(t) \tag{1.31}$$

Thereby the equation (1.30) turns into:

$$E_n = \frac{1}{2} V_{bn} D_n(t) \tag{1.32}$$

The equation (1.32) may be considered as expressing the area beneath the curve V_{bn} - D_n in the elastic domain. Now, an energy-based displacement $D_{eq,n}$ is defined from the latter equation, it would be equal to $2E_n/ V_{bn}$ for being certain that $D_{eq,n}$ is equal to D_n in the elastic domain. Extending this approach for both the elastic and the inelastic response, the absorbed energy dE_n, may be expressed as the work done by V_{bn} in a differential displacement $dD_{eq,n}$:

$$dE_n = V_{bn} \cdot dD_{eq,n} \tag{1.33}$$

When expressing the latter equation in an incremental formulation, it is possible to obtain the displacement increment $\Delta D_{eq,n}$ at each step *i* from:

$$\Delta D_{eq,n}^i = \frac{\Delta E_n^i}{V_{bn}^i} \tag{1.34}$$

Where ΔE_n^i and V_{bn}^i are the energy increment and the shear force computed for each step *i* in the pushover analysis. ΔE_n^i is obtained as the sum of the work done by each applied force $F_{n,j}^i$ at each storey *j*, going through each storey displacement increment $\Delta u_{n,j}^i$ up to the *S* total storeys, as seen in Figure 1.14 which shows a scheme of the energy based capacity curve construction.

$$\Delta E_n^i = \sum_{j=1}^{S} F_{n,j}^i \Delta u_{n,j}^i \tag{1.35}$$

Finally, the total displacement $D_{eq,n}$ is obtained from:

$$D_{eq,n}^i = D_{eq,n}^{i-1} + \Delta D_{eq,n}^i \tag{1.36}$$

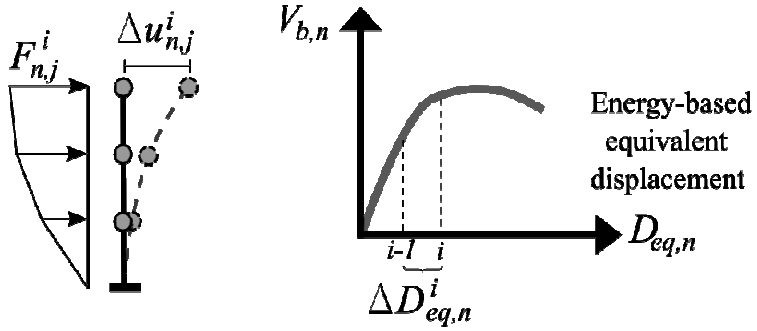

Figure 1.14 Overview of the energy-based capacity curve, adapted from [Hernández-Montes, *et al.*, 2004].

As a result, instead of considering just the roof displacement, the whole displacement pattern of the building is taken into account by the equivalent displacement. This achievement results in a better representation of the lateral behaviour of the MDOF system, which produces smoother and more stable capacity curves [Tjhin *et al.*, 2005; Kalkan and Kunnath, 2006]. Nevertheless, despite the important contribution in building more appropriate capacity curves, this approach lacks of accuracy since it still considers the modal properties as constant during the nonlinear incursion. In fact, its authors suggest an adaptive modification to tackle this drawback.

1.6.3.2. Enhanced Uncoupled Modal Response History Analysis

With the aim of estimating damage in welded connections of moment resisting steel frames, the Enhanced uncoupled modal response history analysis (EUMRHA) is proposed as a modification to the UMRHA [Li and Ellingwood, 2005; 2007]. Briefly, it consists in taking into account the abrupt changes in modal properties produced by extensive damage in beam-column connections, by means of modified modal properties determined from the displaced-shape of the structure during the very pushover analysis. Also a moment–rotation relationship is proposed for modelling this kind of connections. In practice, the main differences with the UMRHA are:

- The development of the base shear – roof displacement pushover curve is made through a variable, instead of constant, load profile $\mathbf{s}_n^* = \mathbf{m}\boldsymbol{\phi}_n$, with changing $\boldsymbol{\phi}_n$, so it is essentially an adaptive approach.
- The transformation between the capacity curve and the force - deformation

relationship for the equivalent SDOF system is made differently for elastic and inelastic ranges. In the elastic range (first segment of the pushover curve), conversion is made through equations which are essentially equivalent to equations (1.21):

$$D_{n,(1)} = \frac{\mathbf{u}_{rn,(1)}}{\Gamma_n \phi_{rn}} \qquad F_{sn,(1)} = \omega_n^2 D_{n,(1)} \tag{1.37}$$

For the inelastic range, the restoring force is reduced in proportion to the peak elastic demand and the spectral displacement of a point (i+1) is calculated as:

$$D_{n,(i+1)} = D_{n,(i)} + \frac{\mathbf{u}_{rn,(i+1)} - \mathbf{u}_{rn,(i)}}{\Gamma_{n,(i)} \phi_{rn,(i)}} \tag{1.38}$$

Where $\mathbf{u}_{rn}$ is the roof displacement from the pushover analysis at the indicated point (i or i+1) and $\Gamma_{n,(i)}$, $\phi_{rn,(i)}$ are the modal properties at point i.

Once the NLTHA is performed for the equivalent n*th*-mode SDOF system, peak roof displacement is determined from:

$$\mathrm{u}_{rno} = \Gamma'_n \phi'_{rn} D_n \tag{1.39}$$

Where D_n is the peak displacement of the n*th*-mode SDOF system and Γ'_n and ϕ'_{rn} are the "assumed" modal properties at this displacement, calculated from the displaced shape of the structure. In fact, for the peak roof displacement u_{rno}, an associated displacement vector, $\mathbf{u}_n$ is taken as the base to obtain the assumed modal shape as:

$$\boldsymbol{\phi}'_n = \frac{\mathbf{u}_n}{\mathbf{u}_n^T \mathbf{m} \mathbf{u}_n} \tag{1.40}$$

Once the modal shape at the maximum displacement is known, the assumed modal participation factor is derived [Li, 2006]:

$$\Gamma'_n = \frac{\Gamma_{n,(0)} D_{n,(1)} + \Gamma_{n,(2)} (D_{n,(3)} - D_{n,(1)}) + \ldots + \Gamma_{n,(2i)} (D_{n0} - D_{n,(2i-1)})}{D_{no}} \tag{1.41}$$

As proposed by the authors, the enhanced UMRHA is able to reflect the abrupt changes in modal properties in the particular case of steel frames with sharp capacity curves that can be idealized as shown in the Figure 1.15. It means that the adaptive proposed procedure is

performed over a few steps following the particular shape of the curve.

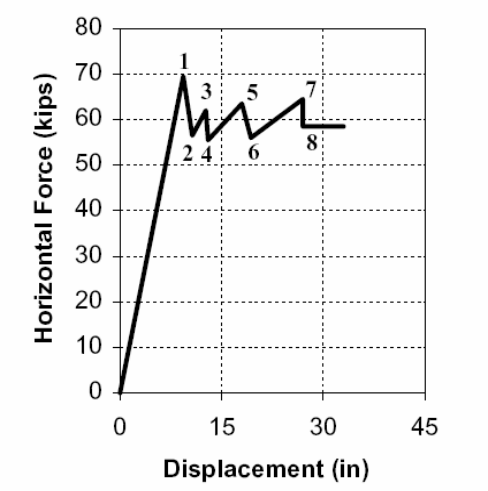

Figure 1.15 Idealized first mode capacity curve of the 9-storey SAC building [Li and Ellingwood, 2005]

This proposal relies on the same assumptions as UMRHA and MPA methods but by means of the "modified" modes it succeeds in reflecting the effects of modal changes in the structural responses for these particular structures. However, its validity in estimating responses of other building types characterized by smoother capacity curves is to be verified. A similar scheme is presented as the actual displacement based pushover (ADAP) but limited to the first mode [Galasco *et al.*, 2006].

1.6.3.3. MPA for Seismic Evaluation of Reinforced Concrete Special Moment Resisting Frame Buildings

An enhancement to the MPA intended to overcome some drawbacks and for improving its accuracy is presented by Bobadilla and Chopra [2007]. Actually, a new step in the basic MPA procedure has been added to account for the hysteretic behaviour of the system. In fact, the peak – oriented model developed by Ibarra *et al*. [2005] was chosen to represent the global monotonic and cyclic behaviour of buildings through their pushover curves. Of course, this model being more complex than the classic bilinear one, a cyclic procedure is required for finding its properties. The procedure consists in performing consecutive pushover analyses for increasing values of roof displacement (see Figure 1.16). Then the parameters for the peak – oriented model may be defined and the MPA method is applied as explained before.

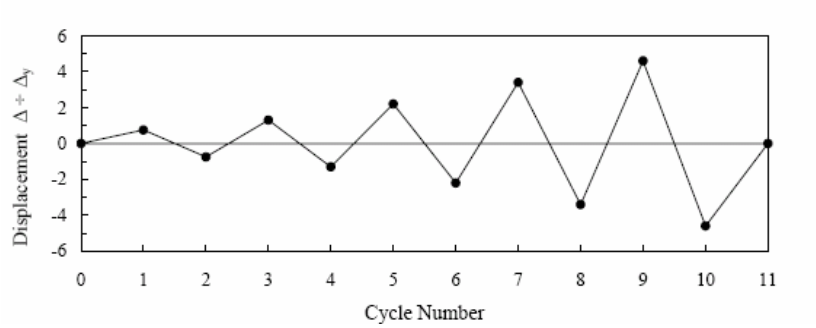

Figure 1.16 Roof displacement cycles for a cyclic pushover analysis [Bobadilla and Chopra, 2007]

Important improvements in the accuracy of MPA are obtained when considering more suitable models to represent the equivalent SDOF system as it is reported by the authors. However, the increasing number of steps makes this approach more difficult to implement. Then in practice, its use is restricted to research works and as for other methods it remains far from current engineering.

1.6.4. Adaptive Modal Combination (AMC)

Another multimodal based method called the Adaptive Modal Combination (AMC) is proposed for evaluating the seismic performance of building structures [Kalkan and Kunnath, 2006]. Its main objective is to retain and enhance the advantages of both adaptive and modal pushover procedures. In fact this method is supposed to eliminate the need of pre-estimating the target displacement (or displacement demand) and uses the already mentioned energy-based scheme to find stable estimates of seismic demand. Figure 1.17 shows an overview of this procedure.

As an adaptive procedure, a set of calculations need to be performed at each step. First of all, an eigenvalue analysis is required to find instantaneous modal properties as well as the lateral load profile ($\mathbf{s}_n^* = \mathbf{m}\boldsymbol{\phi}_n$). After applying this variable load profile to the structure, the capacity spectrum may be derived. For this purpose the spectral displacement is estimated through the energy based approach (see Eq. (1.34) to (1.36)) and the spectral acceleration is computed by the classic expression (see Eq. (1.7)). When yielding appears, the system's ductility is computed as the ratio between the actual and the yield spectral displacement. The post-yield stiffness ratio is also derived approximating the capacity curve as a bilinear one.

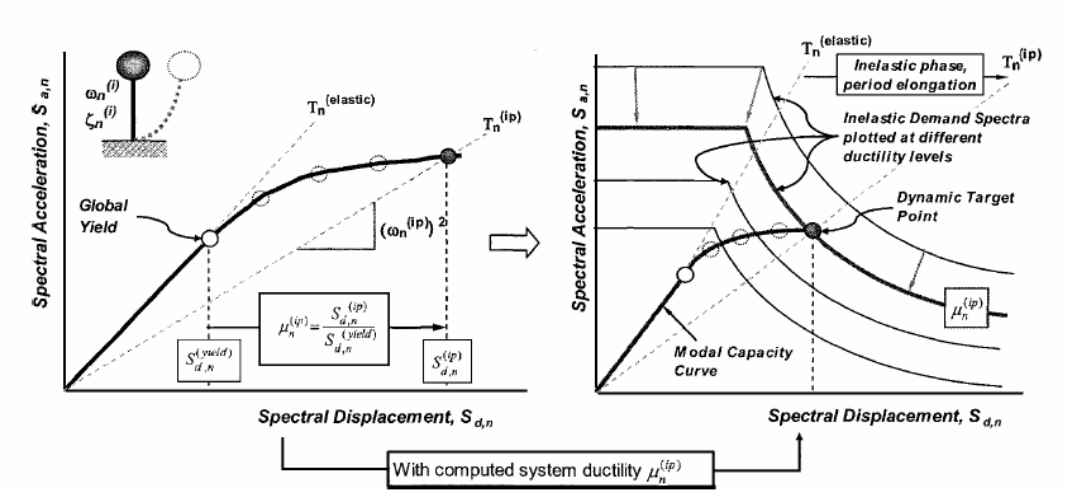

Figure 1.17 Overview of the Adaptive Modal Combination. [Kalkan and Kunnath, 2006]

Earthquake loading is represented by a set of inelastic demand spectra with different levels of ductility. Plotting in the same curve the demand spectra and the capacity spectrum allows for finding the target displacement. In fact, when a point with ductility level μ in the capacity spectrum intersects a demand spectrum with a corresponding ductility (with a reasonable approximation), this point of intersection becomes the target displacement.

Once the target displacement is known, the associated roof displacement u_{rn} is computed (see Eq. (1.26)). At this stage, for the displacement u_{rn}, any response quantity may be extracted from the pushover database. As a multi-mode method these steps are performed for a reasonable number of modes to get enough accuracy. Finally modal responses are combined by the SRSS rule to obtain peak responses.

The AMC method achieves in producing estimates of responses close enough from those of the NLTHA. However there are some remarks to do. This method is intended to find the target displacement without requiring its pre-estimate. Nevertheless, since parameters such as ductility and post-yielding stiffness ratio are not known at first hand in an adaptive framework, an initial adaptive pushover analysis is required to estimate these quantities. Then, the AMC becomes less advantageous as several iterations are necessary as for any other pushover-based method. Furthermore, since eigenvalue analysis must be performed at each step after yielding the AMC method could be computationally demanding in comparison with non-adaptive schemes.

1.6.5. Generalized Pushover Analysis (GPA)

Recently a non-adaptive pushover-based method was presented on the basis of generalized load profiles obtained as a combination of modal components computed from linear response spectrum analysis parameters [Sucuoğlu and Günay, 2010].

This strategy aims to provide peak seismic responses such as displacements as well as internal forces coming from the envelopes of a series of pushover analyses. Each pushover is performed for the purpose of reaching a specified demand parameter such as a storey drift, which is supposed to be maximized by the load profile, for a specific response or design spectrum. Therefore, for this method to be completely applied, (N+1) pushover analyses are required, N being the number of lateral dynamic degrees of freedom.

This procedure has the advantage of not being adaptive, consuming then less computational effort. Also, it may produce further insight into the effect of modal components on the different seismic response parameters since the load profiles may be derived to maximize any response parameter. However, while non adaptive, it requires several steps of different kinds for a single ground motion, e.g. a linear response spectrum analysis, an “a priori” pushover analysis and the set of (N+1) pushover analyses. This may become an inconvenient for large scale studies such as probabilistic approaches for risk and reliability purposes, for instance.

1.6.6. Incremental Dynamic Analysis (IDA)

Finally in this review, the IDA is a parametric analysis which is getting growing interest since it provides accurate estimates of demand and capacity of structures through a wide range of responses, from elastic up to dynamic instability.

In summary, it performs a series of complete nonlinear dynamic analysis under incrementally scaled ground motion records. Each series of analysis –for a single record– provides an IDA curve, see the Figure 1.18a. The IDA curve is characterized by two quantities, a scalable intensity measure IM –e.g. the spectral acceleration, Sa– which is proportional to the ground motion scale factor, and an engineering demand parameter EDP –e.g. the maximum inter storey drift MID– for recording the structural response [Vamvatsikos and Cornell, 2002].

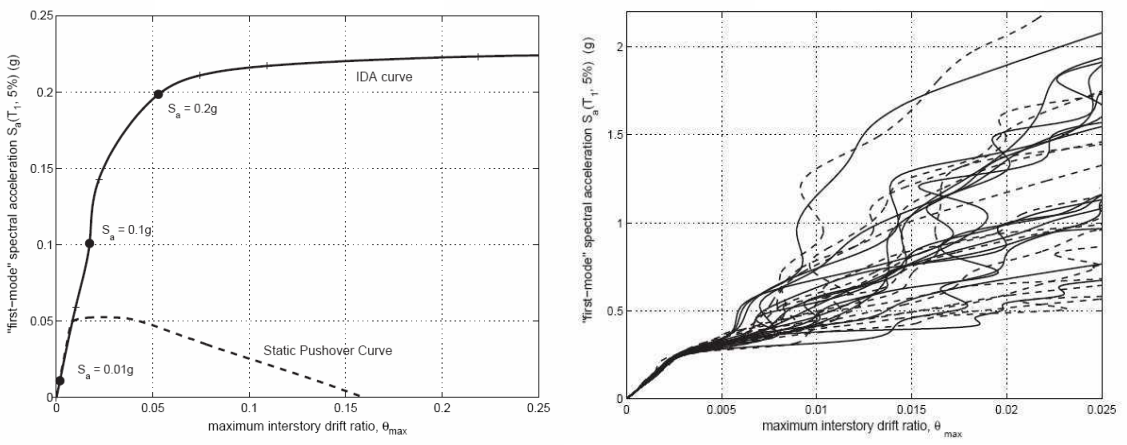

a) Single IDA curve **b) Multi-record IDA curves**

Figure 1.18. Examples of IDA curves. [Vamvatsikos and Cornell, 2002])

As for any other method based on nonlinear dynamic analyses, IDA is highly dependent on the record's features. As a result, for having useful results covering a wide range of responses, a sufficient number of records need to be employed, leading to a set of IDA curves like that of the Figure 1.18b. Then all these outcomes must be statistically treated to obtain meaningful results and to use them for prediction purposes, as it is required in a performance based engineering framework.

With the aim of reducing the computational cost of IDA, a simpler procedure to find the IDA curve of MDOF systems dominated by the first mode is proposed. This scheme relies on observations of the similarities or connection between SPO and IDA curves when the first one is plotted on MID *vs* Sa format (dividing Vs/W) and scaled by an appropriate factor to match the elastic part of the IDA [Vamvatsikos and Cornell, 2005]. This is possible by using a SDOF system pushover curve and some empirical quantitative rules. The main objection is that IDA estimated curves deeply depends on the SPO curves, and SPO curves can be calculated taking into account the first mode or a combination of more modes, thus generating several possible curves. A proposed solution is to choose the worst pushover curve since it is thought that a structure will fail by the weakest link, most damaging, least-energy path.

Another solution for decreasing the computational demands is the use of MPA method to find IDA curves instead of performing complete NLTHA [Han and Chopra, 2006]. This approach results in satisfactory estimations of IDA curves, provided the use of adequate models for representing the hysteretic behaviour of the modal SDOF systems.

Despite the useful insight in the seismic behaviour of structures provided by the IDA scheme, its implementation on current engineering problems is simply unlikely since numerous complete dynamic analyses are required for a single curve. It means that IDA, as initially thought is reserved for special structures or for particular analysis when a deep study on seismic behaviour is needed. Concerning the derived proposals for reducing the analysis duration time, they may produce satisfactory results but they become complicated to run in practice as further steps must be added.

1.7. SUMMARY AND CONCLUSION

A brief state of the art of the existing analysis methods for the seismic evaluation of buildings response has been presented. They have been classified into static and dynamic procedures and into first mode pushover based and multi-mode pushover based methods. A nonlinear time history analysis is thought to be the most complete and accurate method, thus it is usually considered as the reference method when experimental studies are not available, which is a common situation in the domain of seismic evaluation. Consequently, the aim of approximate methods is to produce acceptable estimates of seismic response, as close as possible of the NLTHA results, but reducing the analysis and/or the modelling duration time. A number of assumptions and simplifications are required for fulfilling this objective. This chapter underlines those assumptions and their consequences on the quality of the response estimates.

Firstly, any static procedure is not capable of accounting for the whole characteristics of ground motions, as it has been observed by several authors. However, the difference in the analysis duration when using static instead of dynamic procedures is large enough to let static procedures being an attractive alternative if the difference between the respective results remains under acceptable limits. Pushover based methods belong to this group. First mode pushover based methods, e.g. CSM or N2 method, provide acceptable results when applied to first-mode dominated structures, it means with low fundamental periods.

When higher modes have a significant influence in the lateral behaviour, multi-mode pushover based methods are required e.g. MPA method. Taking account of higher modes increase the accuracy, certainly, but also add uncertainty by relying on more arguable assumptions. Defining the overall lateral behaviour of the structure on the basis of roof

displacement, when it is not proportional to the other floor displacements in the nonlinear domain, is a drawback to consider. Also working with elastic modes and consider uncoupled modes in nonlinear domain are shortcomings to be handled.

Several methods have been presented to improve multi-mode procedures by fixing one or more of the mentioned problems. For instance, adaptive schemes propose to compute modal properties step by step in pushover analyses. However performing eigenvalue analyses and updating lateral load profiles at each step after yielding is possible when open source or special software platforms are used, as it was also pointed out by Sucuoğlu, H. and Günay, M. S. [2010]. It may become an obstacle for current engineers working with non-open software, as is the case of current commercial software. Moreover, as it was stated by Antoniou and Pinho [2004] the advantage of adaptive force-based methods over non-adaptive ones is limited for estimating deformation patterns. Besides, some proposals producing appropriate estimates of response require the addition of several steps of variable difficulty, which turns the evaluation to be a complicated task and becomes an inconvenient for large scale studies such as probabilistic approaches.

Accuracy, simplicity and reduced computational demands should remain the main objectives to be reached by simplified methods when they estimate structural response. Many of the existing approaches fulfil partly these objectives but further improvements are still required. Since all the revised methods present some problems concerning its accuracy, its calculation time or its suitability in practical applications, the main conclusion of this chapter is the necessity of a proposal which improves the existing methods, retaining their advantages and aiming to produce a simple but accurate scheme for the evaluation of seismic response of buildings.

CHAPTER 2
PSEUDO-ADAPTIVE UNCOUPLED MODAL RESPONSE HISTORY ANALYSIS: BASIC ELEMENTS

2.1. INTRODUCTION

As stated in the precedent chapter, simplified methods for the assessment of seismic response are a current necessity for the earthquake engineering domain, particularly when large scale studies are to be carried out. As a contribution to the development of such simplified methods, a pseudo-adaptive method (PSA) is proposed in this chapter. It is derived from the UMRHA method given its straightforwardness and it provides the improvement of incorporating an energy-based approach to build the capacity curve and a pseudo-adaptive feature to consider changes in modal shapes after yielding. It is intended to be an alternative to fully adaptive strategies since it does not require the force vectors to be updated at each step in the pushover analysis for considering modal changes. A complete procedure is established to estimate global responses as storey displacements and drifts, as well as internal forces and component rotations. It is then illustrated with an application example.

2.2. BASIC ELEMENTS

Among the existing methods to estimate seismic response, the MPA (the original and the modified versions as well) has been a reference method since it is able to reflect higher mode effects on response maintaining a straightforward implementation. As already discussed, MPA comes from the UMRHA method which has its basis on the modal response analysis. It gives the UMRHA the advantage of considering the effect of ground motion characteristics in the response.

Thereby, retaining the fundamental features of UMRHA, this proposal presents two main enhancements which overcome two shortcomings already discussed, having at the same time reasonable analysis duration time.

2.2.1. Adaptation of the Energy-based approach to develop the capacity curve

According to the first chapter, within the framework of pushover-based methods, the representation of a MDOF system with an equivalent SDOF system is achieved by means of the capacity curve. This curve is intended to give a measure of the global lateral capacity, in terms of force and deformation. Concerning the deformational properties, the roof displacement is the most used parameter to represent the global deformational capacity of the system, even in multi-mode approaches despite the fact that storey displacements are not proportional to roof displacement beyond the elastic limit. In fact, any arbitrarily chosen floor displacement could not give a reliable measure of the global capacity of deformation. Hence, more rational procedures are required to express deformational global lateral properties.

Accordingly, admitting that more appropriate capacity curves could be developed using an equivalent displacement instead of using just the roof displacement, the alternative capacity curve proposed by Hernandez-Montes *et al*. [2004] is adapted here. Thus, the capacity curve abscissa D_{eq}, is computed by means of Equations (1.34) to (1.36), repeated below for convenience:

$$\Delta D_{eq,n}^{i} = \frac{\Delta E_{n}^{i}}{V_{bn}^{i}} \tag{1.34}$$

$$\Delta E_{n}^{i} = \sum_{j=1}^{S} F_{n,j}^{i} \Delta u_{n,j}^{i} \tag{1.35}$$

$$D_{eq,n}^{i} = D_{eq,n}^{i-1} + \Delta D_{eq,n}^{i} \tag{1.36}$$

The ordinate of the capacity curve as well as that of the capacity spectrum remain unchanged. It means that the resisting force indicator continues to be the shear force V_{bn} and the spectral acceleration S_a, is still computed as the ratio between the shear force and the effective modal mass. As stated before, this approach produces capacity spectra equivalent to those developed from roof displacement capacity curves within the elastic domain. When exceeding this limit, the energy based approach produces different yielding branches. Sometimes the differences are quite small, sometimes they are considerable enough to have a visible effect on response.

For illustration purposes, the capacity spectra (the conventional roof displacement-based and the energy-based) for two RC buildings are presented hereafter: Figure 2.1 illustrates the

first- and second-mode capacity spectra of a 4-storey frame and Figure 2.2 shows the capacity spectra of the first three modes of a 14-storey frame (for further details of these frames see section 3.2 Structural Models). In both cases, the pushover analyses were performed until the frame reached a predetermined roof displacement. In the case of the 14-storey frame, the roof displacements of the three modes were obtained from the UMRHA method, for a ground motion record scaled for reaching a roof drift of 2% of the building height (San Fernando, 1971 earthquake, station: Castaic, component: 021 [PEER, 2005]).

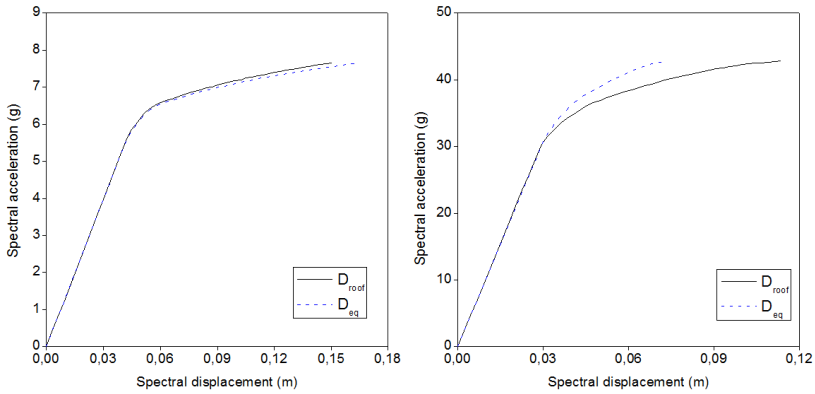

a) **b)**

Figure 2.1 Capacity spectra for a 4-storey RC frame: a) First mode and b) Second mode

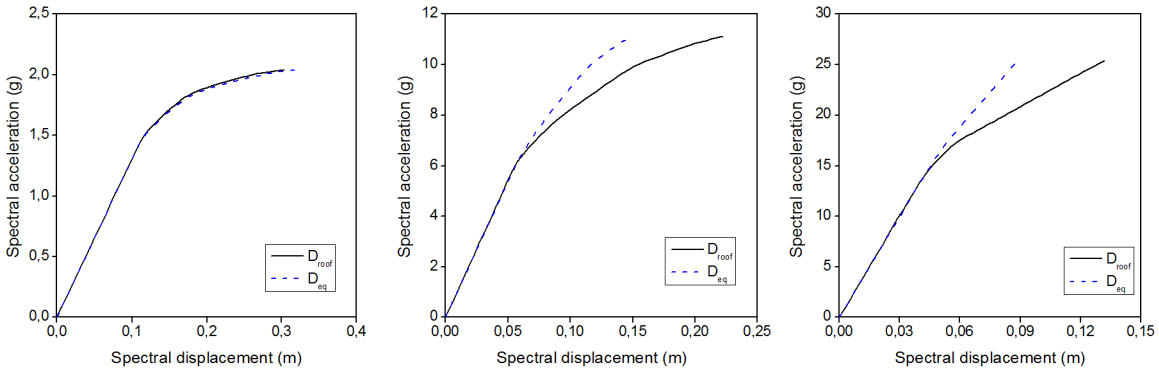

a) **b)** **c)**

Figure 2.2 Capacity spectra of a 14-storey RC frame for the a) First mode, b) Second mode and c) Third mode

According to the results for the first mode, both spectra express similar deformational capacity, and so, similar total absorbed energy, suggesting that for the first mode the use of roof displacement as global indicator may be appropriate, as already declared by Hernandez-Montes *et al*. [2004]. However, when working with higher modes, deformational capacities

are quite different between both spectra. Differences of peak spectral displacements are of about 54% for the second-mode curve of the 4-storey frame and of 48% and 50% for the second- and third-mode curves of the 14-storey frame. All variations are expressed with reference to the equivalent energy-based displacement D_{eq}.

These results may be explained by the fact that pushover analysis is applied as a force-based procedure. It means that a target roof displacement is fixed and a load profile is increasingly applied until reaching such displacement. Therefore, the roof displacement could not reflect the deformational properties of the remaining storeys beyond the elastic limit since it increases constantly while the others increase (or decrease) according to their current stiffness, strength and ductility. This trend may be observed in Figure 2.3a), where the series E1 and E2 represent two elastic stages on the pushover and NL1 to NL4 represent 4 points after yielding.

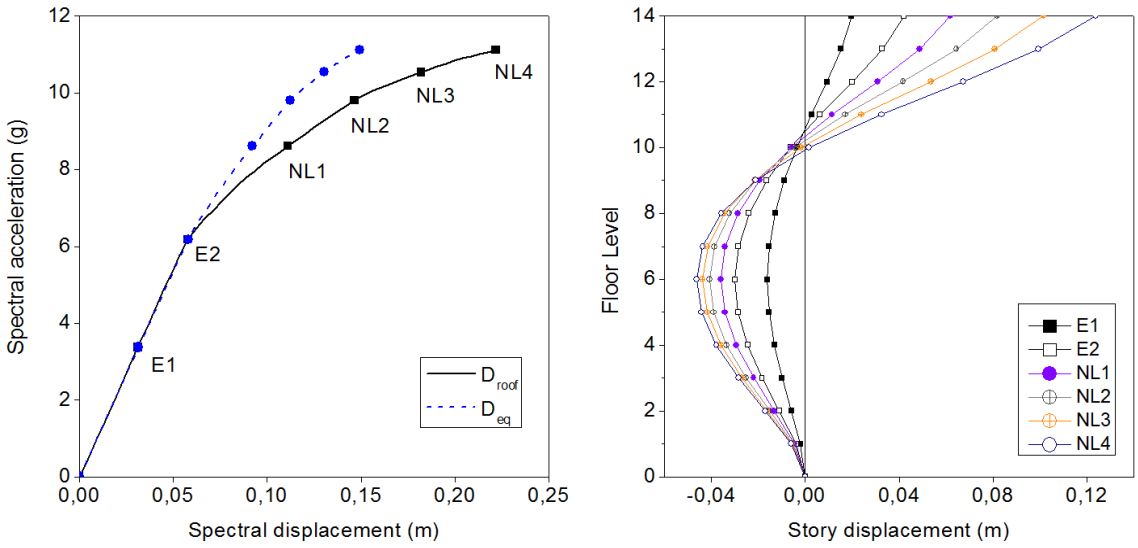

a) **b)**

Figure 2.3 a) Second mode capacity curve and b) Storey displacements during the second-mode pushover analysis of a 14-storey frame

It may be observed that from the initial state up to E1 and E2, the increase in roof displacement is proportional to the rest of displacements, see Figure 2.3b). Nevertheless, from E2 up to NL1 and so on, until NL4, the increase in roof displacement is quite large in comparison to what happens to the rest of the structure, hence the more rigid capacity spectra produced by the energy-based approach. Of course, the use of a force-based pushover is not the only cause for which the responses are not proportional to roof displacement. Actually,

any load profile would produce non-proportional displacements when the elastic limit is exceeded; therefore describing lateral behaviour by only one displacement seems to be unrealistic.

In addition, the 4-storey frame response being dominated by the first-mode, the contribution of the second mode may be neglected in most cases. Whenever it is required, deformational demands for the second mode will probably not reach the inelastic behaviour, so the conventional approach in this particular case may be sufficient. On the contrary, for higher buildings as is the case of the 14-storey frame, or for irregular buildings, the contributions of higher modes are significant in the response and usually, depending on the ground motion, they will be demanded to have nonlinear response. Therefore, for being certain of having rational capacity curves in any case, the energy-based approach is adapted and implemented in order to obtain the capacity curve abscissa within the framework of the proposed strategy.

2.2.2. Pseudo-adaptive scheme for finding structural responses

As the principle of multimodal pushover based methods is modal analysis, changes in modal properties after yielding may have a significant effect on nonlinear response. Furthermore, this effect may become more important in presence of localized inelastic mechanisms like soft storeys, typical of first storeys of commercial buildings with open configurations at the ground floor for instance, or weak storeys caused by abrupt changes in strength. Also some gravity load designed buildings present inelastic mechanisms which may cause important changes in modal properties.

Consequently, the second proposed improvement consists of implementing a strategy for considering those effects in a simple way. In fact, actual modal properties after yielding are derived from the pushover analysis on the basis of storey displacements. It means that pushover analysis is completely performed with an invariant profile: $\mathbf{s}_n^* = \mathbf{m}\boldsymbol{\phi}_n$ and updated modal shapes are computed afterwards and considered in the modal response calculation. As a result, the PSA method takes benefit of invariant lateral load profiles and is able to reflect the effect of variations in modal shapes on the structural response.

For each mode in the linear domain, the modal shapes are proportional to the storey displacements produced by modal load profiles. The PSA proposal relies on the assumption

that even though the load profile is invariant and proportional to the elastic modal shape for the n-*th* mode, the storey displacement vector, $\mathbf{u}_n$, is approximately proportional to the actual modal shape at each pushover step after yielding and therefore it may give a measure of the actual stiffness [Jerez and Mebarki, 2009; In press]. It is worth saying that this hypothesis works with displacements produced only by lateral loads, hence when gravitational loads are present, their associated displacements should be subtracted after pushover analysis.

Accordingly, taking $\mathbf{u}_n$ as an arbitrarily modal shape, the orthonormalized modal shape may be obtained by the equation (2.1) [Clough and Penzien, 1993]. Then, it is considered as the approximate modal shape $\boldsymbol{\phi}'_n$:

$$\boldsymbol{\phi}'_n = \frac{\mathbf{u}_n}{\sqrt{\mathbf{u}_n^T \mathbf{m}\, \mathbf{u}_n}} \tag{2.1}$$

The corresponding modal participation factor may be computed from classic expressions as [Jerez and Mebarki, 2010]:

$$\Gamma'_n = \frac{(\boldsymbol{\phi}'_n)^T \mathbf{m}\boldsymbol{\iota}}{(\boldsymbol{\phi}'_n)^T \mathbf{m}\boldsymbol{\phi}'_n} \tag{2.2}$$

As stated in the precedent chapter, a comparable expression to compute modified modes was already proposed within the framework of fully adaptive approaches [Li and Ellingwood, 2005; Galasco, *et al.*, 2006] . In the present case, for each step after yielding in the pushover analysis, the equivalent energy based displacement, $D_{eq,n}$, has an associated approximate mode and its corresponding modal participation factor. This database becomes the support for finding the variation of modal properties, relating the history of responses for the equivalent SDOF $D_n(t)$ to $D_{eq,n}$.

Once built this database, storey displacements and drifts may be computed with the conventional equations of the modal analysis, derived by replacing the elastic modal properties $\boldsymbol{\phi}_n$ and Γ_n by the approximate ones recently obtained, $\boldsymbol{\phi}'_n$ and Γ'_n:

$$\mathbf{u}_n(t) = \Gamma'_n \boldsymbol{\phi}'_n D_n(t) \tag{2.3}$$

$$\Delta_{j,n}(t) = \Gamma'_n (\phi'_{j,n} - \phi'_{j-1,n}) D_n(t) \tag{2.4}$$

Thereby, following the assumption of the UMRHA method, of the superposition principle being still valid, the total response may be computed from:

$$\mathbf{u}(t) = \sum_{n=1}^{N} \mathbf{u}_n(t) = \sum_{n=1}^{N} \Gamma_n' \boldsymbol{\phi}_n' D_n(t) \tag{2.5}$$

$$\Delta_j(t) = \sum_{n=1}^{N} \Delta_{jn}(t) = \sum_{n=1}^{N} \Gamma_n' (\phi_{jn}' - \phi_{j-1,n}') D_n(t) \tag{2.6}$$

The peak responses are obtained from maximum absolute values of total responses. They are produced only by dynamic effects so if gravitational loads have been considered, the following equation is to be employed for any response quantity *R*:

$$R_{peak} = max(abs(R_g + R_d), abs(R_g - R_d)) \tag{2.7}$$

Where R_g represents the response under gravity loads and R_d the dynamic peak response (e.g. in the case of displacements $R_g = \mathbf{u}_g$ and $R_d = \mathbf{u}(t)$).

2.2.3. Gravity load effects

Sometimes, only the first mode capacity curve is built by taking into account gravity loads, as it was stated by Chopra and Goel [2001]. However, for some structures (e.g. gravity load designed buildings, GLD) the omission of gravity loads in the pushover analysis of higher modes causes imprecise, stiffer and stronger capacity curves. Differences may sometimes be as low as 4% in strength (Figure 2.4a). Sometimes, they may also cause important changes of the inelastic mechanism as shown in Figure 3 (b), for a gravity load design building with poor detailing and no ductility capacity. Consequently, for a more accurate evaluation of capacity, all the studied modes must take account of the gravity load effects, as it was also established later by Goel and Chopra [2004].

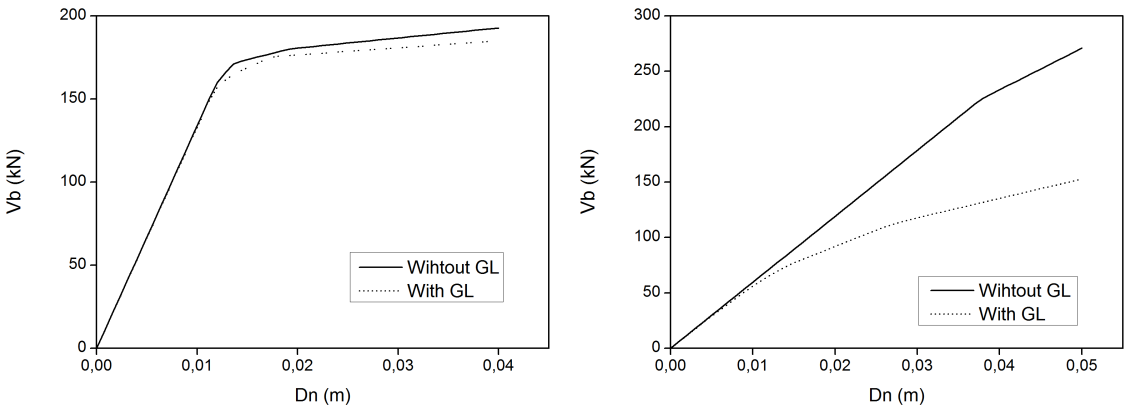

(a) **(b)**

Figure 2.4 Second mode capacity curves of a 4- and a 7-storey GLD buildings

2.2.4. Internal forces and component rotations

Getting accurate estimates of member forces and rotations has always been a major challenge of pushover based methods since there is no explicit relationship between those response quantities and the equivalent SDOF modal displacement D_n. It means that it is not possible to estimate these quantities in the same way than for storey displacements and drifts. Methods like the CSM or any other first mode based nonlinear static procedure propose to compute other response quantities like internal forces from the pushover analysis: once the performance point is known, any response quantity may be extracted from the data recorded during pushover analysis, for the step associated to the performance point.

When working with multi-mode procedures, these so computed quantities would be combined by an appropriate modal combination rule. However it has been found out that such an approach has not been completely successful as reported in the literature, since the obtained forces might exceed the members capacity [Goel and Chopra, 2005]. As a result, the same authors proposed a technique to estimate member forces on the basis of member end deformations computed from the pushover analysis. This procedure is applied only if the forces calculated by modal combination do exceed the member capacity. According to the presented results, this solution seems to produce better estimates than those already produced by the initial MPA procedure. Nevertheless, mixing two procedures, retaining in some cases the peak modal combination and for the others the deformation-based computation, is not reliable. In fact, the proven shortcomings of modal combination of forces are sufficient for not using this procedure.

The proposal presented in this study has its basis on the conventional approach but aims to estimate the modal history of responses to avoid modal combination. Thereby, when each pushover analysis is performed, a set of predefined response parameters is stored e.g. storey displacements, plastic hinge deformations, internal forces. The equivalent energy-based displacement $D_{eq,n}$ as well as the approximate modes are computed on the basis of this set of response parameters. Thus, similarly to what is made for finding the modal shapes history through the association between $D_{eq,n}$, and $D_n(t)$, the time-variation of any response may be obtained for each mode by relating $D_n(t)$ to $D_{eq,n}$ and then to the required response. Peak force responses may now be computed following the same principles of total displacements: superposition of modal responses and computation of maximum values.

2.3. PROCEDURE

In order to have this strategy clear and ready for application, the basic procedure is explained herein [Jerez and Mebarki, In press]:

2.3.1. Initial steps

Once the complete model of the building is made, compute the elastic modal properties $\boldsymbol{\phi}_n$ and Γ_n. If gravitational loads are to be considered, perform a gravity load analysis and record storey displacements ($\mathbf{u}_g$), storey drifts ($\boldsymbol{\Delta}_g$) and any other required quantity r_g.

2.3.2. Pushover analysis

1. For the n*th*- mode, perform the pushover analysis until a roof displacement u_{rn} for a force distribution $\mathbf{s}_n^* = \mathbf{m}\boldsymbol{\phi}_n$. Record the base shear, $V_{b,n}$, the storey displacements, $\mathbf{u}_t$, and any other required response quantity, r_n.
2. Determine the storey displacements due to lateral loads following Equation (2.8), where $\mathbf{u}_g$ represents the gravity loads, if any.

$$\mathbf{u}_n = \mathbf{u}_t - \mathbf{u}_g \tag{2.8}$$

3. Compute the modified modal shapes and their associated modal participation factors by Equations (2.1) and (2.2).
4. Calculate the equivalent displacement $D_{eq,n}$ by means of Equations (1.34) to (1.36).
5. Construct the capacity curve $V_{bn} - D_{eq,n}$ and idealize it as a bilinear curve.
6. Convert the capacity curve into the capacity spectrum, computing the spectral acceleration as the ratio between V_{bn} and the effective modal mass, and let D_n, the spectral displacement, be equal to $D_{eq,n}$.

2.3.3. Time history responses

7. Compute the deformation history $D_n(t)$, for the n*th*-mode with unitary mass and stiffness defined by the force-deformation relationship (F_{sn}/L_n) found in step 6, solving the classic dynamic equation by any conventional method:

$$\ddot{D}_n + 2\zeta_n \omega_n \dot{D}_n + \frac{F_{sn}}{L_n} = -\ddot{u}_g(t) \tag{2.9}$$

For the applications presented in this chapter and the following one, the hysteretic properties of the equivalent SDOF system are represented by an elastic-plastic with strain hardening hysteretic model.

8. Determine storey displacements and storey drifts with Equations (2.3) and (2.4). For this step to be performed it is necessary to relate each $D_n(t)$ to $D_{eq,n}$ in the pushover database in order to have the corresponding approximate modal shape ϕ'_n.
9. Repeat the steps 1 to 0 for as many modes as necessary for performing an accurate analysis.

2.3.4. Peak responses

10. Superpose modal responses (e.g. following Equation (2.5) for storey displacements).
11. Calculate peak responses according to the Equation (2.7).

This procedure was implemented in a combined tool which uses MATLAB and OpenSees platforms for all the structural analyses, linear, nonlinear static and nonlinear dynamic, as explained thereafter. It is first applied to a single building in this chapter for illustration purposes and then a broader validation is performed over more building models in the next chapter.

2.4. GENERAL MODELLING

The numerical models were simulated using OpenSees platform for the analysis [Mazzoni *et al.*, 2007] and MATLAB for the pre- and post-processing [The MathWorks, 2007]. For the modelling and design of some of the validation buildings SAP2000 and ETABS packages have been used [Computers and Structures Inc., 2003]. P-delta effects were considered for all the methods under study. Soil-structure interaction is beyond the scope of the present study, therefore it has not been taken into account; hence the supports were modelled as infinitely rigid.

2.4.1. Modelling of nonlinear behaviour of components

As stated before, fibre modelling has become a widely used approach for representing the nonlinear behaviour of frame elements since it can take into account the distribution of longitudinal reinforcement, the properties of confined and unconfined concrete and a direct interaction between axial load and bending moment. Nevertheless, the increase in the analysis duration time being a major objection, the modelling through global moment curvature relationships remains also an appropriate choice depending on the main objectives of the analysis. In fact, for a number of practical cases, global results obtained by using moment-curvature relationships are similar to those obtained by fibre modelling, as it is shown in Figure 2.5, where the capacity curve for a one storey frame was developed following both approaches.

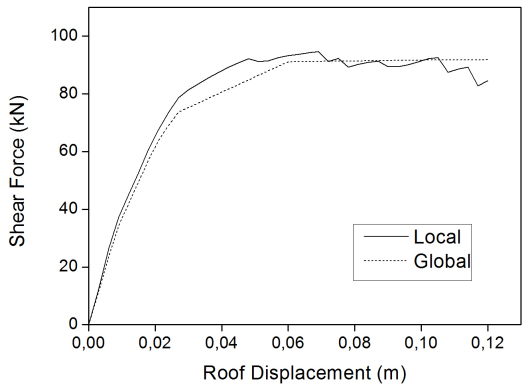

Figure 2.5 Capacity curve of a 1 storey frame obtained by local (Fibre model) and global (Moment – curvature relationship) modelling of elements

Furthermore, Hamza *et al*. [2005] and Lee and Mosalam [2006] have found similar results in the framework of probabilistic approaches for estimating seismic response of RC frames. Thereby, when time analysis duration is a major concern as is the case of probabilistic approaches requiring a large number of analyses, the modelling of nonlinear behaviour by means of a global approach seems an appropriate decision.

Accordingly, the nonlinear behaviour of elements was represented by means of moment-curvature relationships. These curves were obtained from a fibre element analysis of each element isolated, taking into account the vertical loads when they were present and significant, as is the case of columns.

2.4.1.1. Constitutive models

Beams and columns were modelled as containing three materials: unconfined concrete for the cover, confined concrete for the element core and reinforcing steel. Both, the unconfined and confined concrete were represented by the *concrete01* model, with degraded linear unloading/loading stiffness, which is based on a modified version of the Kent-Park model [Scott *et al.*, 1982], see Figure 2.6a. f_{cc}, f_{cu}, ε_{cc} and ε_{cu} are respectively the compressive strengths and their associated strains for the confined and unconfined concrete, and ε_u is the concrete strain at crushing strength which is considered equal to 0.2 f_{cc} according to Kent and Park model [Kent and Park, 1971].

Steel material for reinforcing bars was modelled by a bilinear elastic-plastic material with strain-hardening, the *steel01* material, see Figure 2.6b. It is characterized by the Young modulus E, the yielding strength f_y and the post-yield slope α, considered equal to 0.01. Both models, the *concrete01* and *steel01* are available in OpenSees [Mazzoni, *et al.*, 2007].

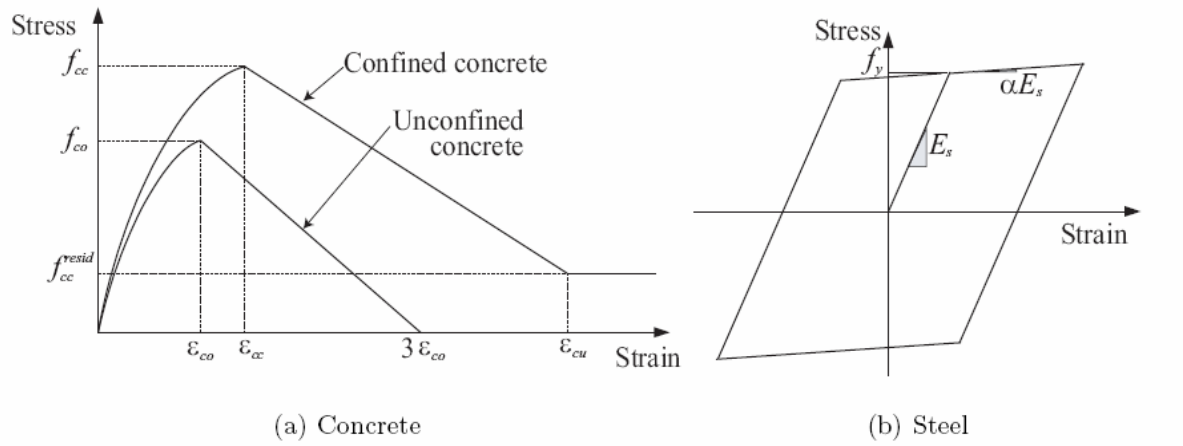

Figure 2.6 Concrete and steel models used for fibre modelling of components, from the OpenSees Library [Lee and Mosalam, 2006; Mazzoni, *et al.*, 2007]

2.4.1.2. Element modelling

Once the fibre analysis is made, the moment-curvature relationships were obtained and approximated as bilinear curves characterized by a yielding strength and deformation M_y, ϕ_y, a post-elastic slope *b*, and an ultimate strength and deformation M_u, ϕ_u, see Figure 2.7.

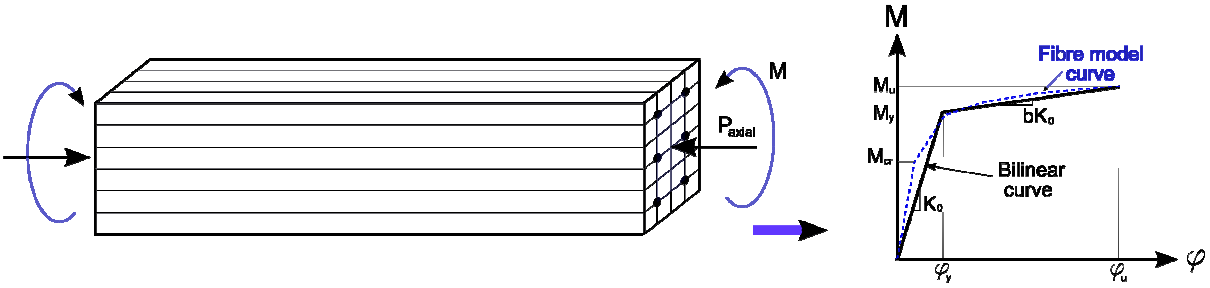

Figure 2.7 Developing of moment-curvature relationships

At the component level, each element was modelled through an available distributed plasticity model, the *nonlinear beamColumn* element which is based on a non-iterative force formulation accounting for the spread of plasticity along the element [Mazzoni, *et al.*, 2007]. For a bi-dimensional analysis, the section of each element (which is an *Euler-Bernoulli beam* element) is composed of three properties: the bending behaviour represented by the moment-curvature relationship obtained from the fibre model, and the axial and shear behaviour, both considered as elastic, hence represented only by their elastic stiffness. Brittle phenomena as shear failure in joints were not considered so joint strength was not modelled. Elements were supposed to be connected by rigid joints.

Plastic rotations are computed from the obtained curvature at a particular integration point by means of the product between the curvature ϕ_p and the equivalent plastic hinge length l_p:

$$\theta_p = \phi_p l_p \tag{2.10}$$

The plastic hinge length was obtained by means of the equation proposed by Paulay and Priestley [1992], which provides an estimate of this length as a function of the member length l, the diameter of reinforcing bars d_b and the reinforcing steel yielding strength f_y:

$$l_p = 0.08l + 0.022 d_b f_y \tag{2.11}$$

2.4.2. Stiffness of frame elements

For computing bending stresses and strains, the complete elastic stiffness must be reduced to account for the effect of initial cracking on the concrete. For this purpose, following a well known approach, when working in the elastic domain the reduction factors, shown in the Table 2-1, are considered [Paulay and Priestley, 1992]. There, A_g represents the section gross area, I_g the inertia of the gross concrete section, P the axial load supported by the column and

f'_c the compressive concrete strength.

Element	Range	Recommended Value
Rectangular beams	0.30 – 0.50 I_g	0.40 I_g
Columns, P > 0.5f'$_c$A$_g$	0.70 – 0.90 I_g	0.80 I_g
Columns, P = 0.2f'$_c$A$_g$	0.50 – 0.70 I_g	0.60 I_g
Columns, P = - 0.05f'$_c$A$_g$	0.30 – 0.50 I_g	0.40 I_g

Table 2-1 Effective Member Moment of Inertia, from [Paulay and Priestley, 1992]

In the nonlinear domain, these values are to be applied when components are modelled by elements characterized partly by their elastic stiffness or models where the plastic behaviour is concentrated at the member ends, keeping a central elastic section. However, the reduction is obtained automatically when using distributed plasticity models as the chosen *beamColumn* element. It was verified through the modelling of an 8 storey frame (whose details will be provided in the next chapter) with elastic elements reduced by the mentioned factors and also with the *beamColumn* element. Elastic modal properties are taken as indicators of stiffness. Very close results were obtained by the two approaches as shown in the Table 2-2. As a result, even for elastic analysis the distributed plasticity model was used to represent the components behaviour.

Component modelling	T1	T2	T3
Elastic with reduced inertia	2.43	0.79	0.45
Distributed plasticity model	2.40	0.85	0.49

Table 2-2 First three periods of vibration of the 8-storey frame computed by two different modelling techniques

2.4.3. Damping

Rayleigh damping approach was employed for modelling damping properties of all the analyzed buildings. The damping matrix is assumed to be proportional to a linear combination of both stiffness and mass matrices so that it may be expressed in terms of two proportionality constants α and β as [García, 1998]:

$$c = \alpha \mathbf{m} + \beta \mathbf{k} \tag{2.12}$$

When decoupling this equation by the matrix of modes, a diagonal matrix with $\alpha + \beta \omega_n^2$ as diagonal term is found. So a relationship between damping ratio and the angular frequency of each mode, ω_n, is derived as:

$$\zeta_i = \frac{\alpha}{2\omega_n} + \frac{\beta \omega_n}{2} \tag{2.13}$$

Therefore the coefficients α and β may be computed by means of a system of equations coming from two modes with known frequency and damping. In this case, for the NLTHA the damping ratio is supposed to be constant and equal to 5%, for the modes which contribute the most to response. Accordingly, α and β are obtained from the equation (2.14), where ζ represents the chosen damping ratio and ω_i and ω_j are the angular frequencies of the fundamental mode and the last mode considered relevant in the response.

$$\alpha = \frac{2\omega_i \omega_j}{\omega_i + \omega_j} \zeta \qquad \beta = \frac{2}{\omega_i + \omega_j} \zeta \tag{2.14}$$

Next, when performing the analysis over the equivalent modal SDOF systems, damping is supposed to be proportional to the mass matrix. In this case only one coefficient is required and it is computed by the equation (2.15) for being in accordance with the damping level considered in NLTHA for each mode.

$$\alpha_{SDOF}^{j} = \alpha + \beta \omega_n^2 \tag{2.15}$$

2.5. APPLICATION EXAMPLE

For illustration purposes, a 4-storey frame was analysed by the proposed PSA method. The frame is a gravity-load designed building (GLD) which was experimentally tested under seismic loads in the European Laboratory for Structural Assessment (ELSA) [Pinto *et al.*, 2002]. Figure 2.8 shows the general features of this frame. Further characteristics of this frame are presented in the APPENDIX A. It was considered in the present study in order to verify the efficiency of the pseudo-adaptive feature of PSA method when no seismic provisions are present and also when the usual principle of weak beams – strong columns is not fulfilled. Furthermore, it has a vertical irregularity due to the change in the stiffness and

strength of a strong column in the third floor. In fact, available full-scale experimental results report the presence of hinging at the third floor, which concentrates inelasticity and eventually might have led to the failure.

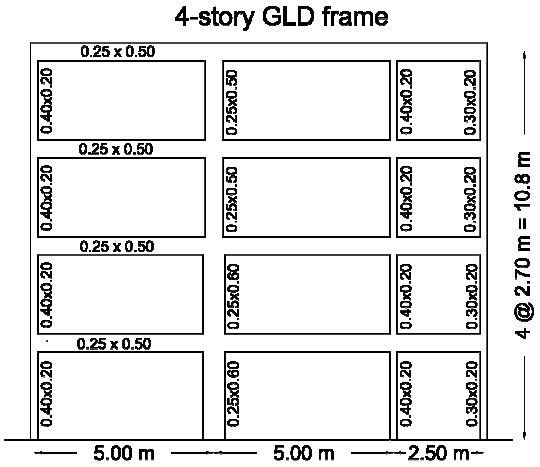

Figure 2.8 Elevation view of the 4-storey GLD frame

The frame was analysed under an artificially generated accelerogram with 475 years of return period and PGA of 0.22g for which experimental results are available [Pinto, *et al.*, 2002]. Although this signal produces slightly inelastic responses, the changes in modal shapes for these levels of inelasticity are significant as it may be observed in Figure 2.9, which illustrates the difference between the actual and the elastic first modal shape at the point of maximum deformation, under the mentioned ground motion.

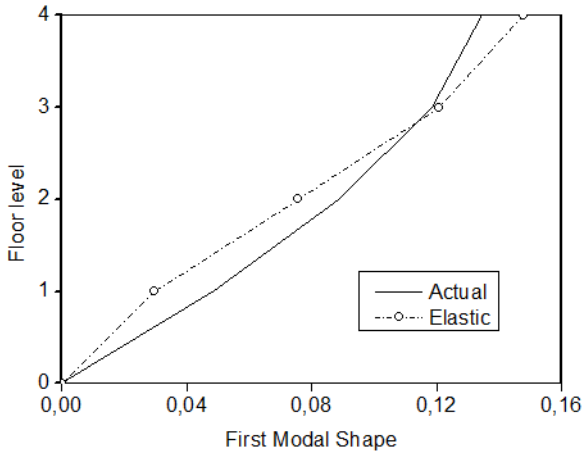

Figure 2.9 First modal shape at the maximum displacement produced by an artificial record (PGA=0.22g)

Figure 2.10 illustrates the maxima storey drifts and shear storey forces. A good agreement

between experimental and analytical results is observed for the studied quantities; in addition, the estimated roof displacement presents a relative difference of only 7.5% in comparison with the experimental one.

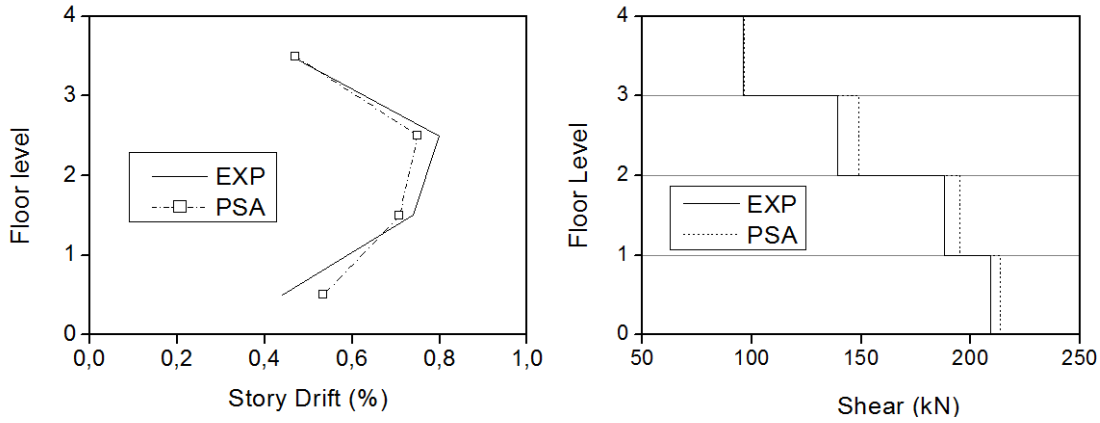

Figure 2.10 Experimental and analytical results using PSA method

The same frame was then subjected to three real ground motion records (for further details of these records see Table 3-1 Ground Motion set in the next chapter): "El Centro", "Corralitos" and "Takaratzu", from Imperial Valley, Loma Prieta and Kobe earthquakes respectively. These records were scaled so that roof displacement reaches 1% of the building height. The results were compared to those of NLTHA as a reference method and to MPA and UMRHA methods to evaluate the efficiency of the proposed method in reflecting the effect of modal shape changes in the response. Some of these results are presented hereafter; Figure 2.11 up to Figure 2.13 show the obtained storey displacements and drifts.

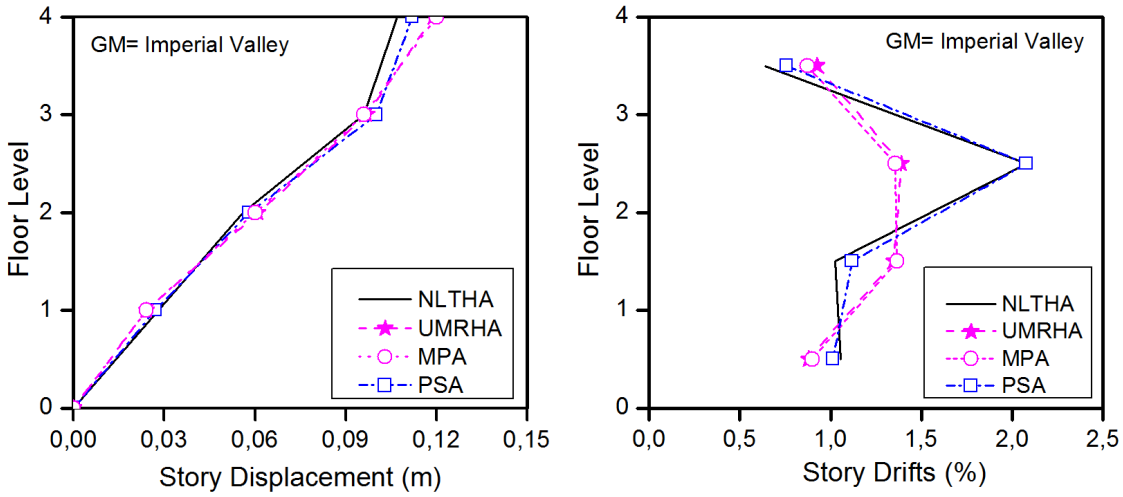

Figure 2.11 Displacements and drifts under "El Centro" record

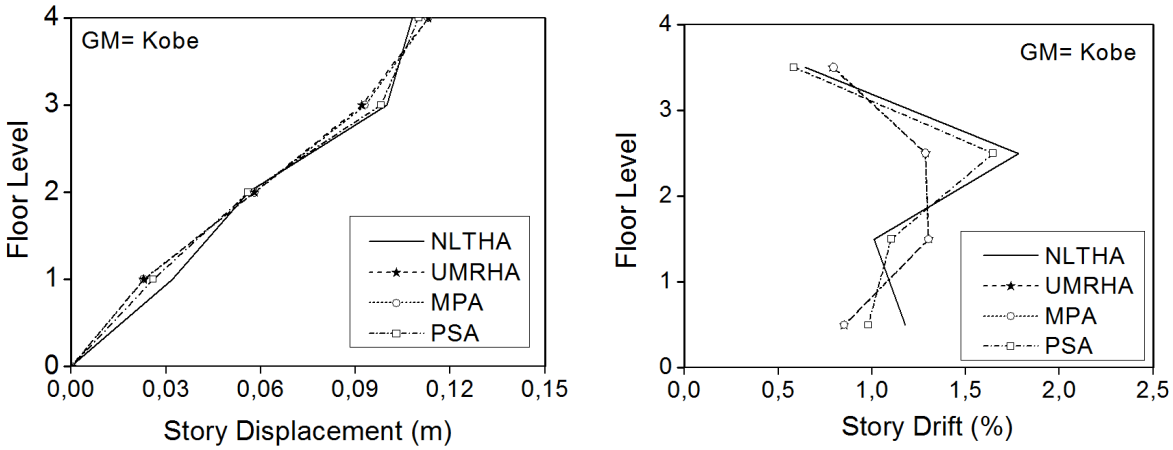

Figure 2.12 Displacements and drifts under "Takaratzu" record

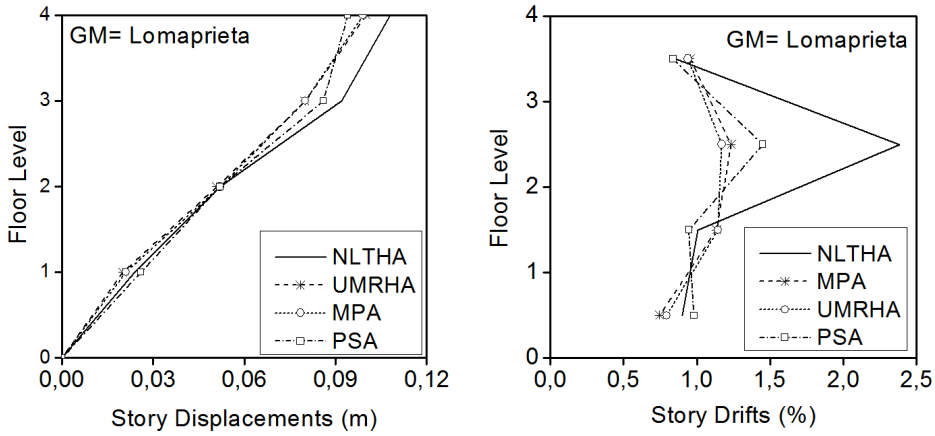

Figure 2.13 Displacements and drifts under "Corralitos" record

As expected, deep inelastic behaviour and a storey mechanism were developed as this frame has not a seismic design. Important variations between the actual and the elastic mode are found. These variations have not a significant effect on displacements since all the studies methods provide similar responses, whereas for storey drifts the effect is evident. Actually, the comparison of methods based on elastic modes (UMRHA and MPA) with the complete NLTHA shows that they do not succeed in estimating the concentration of relative displacement in the third floor due to the soft storey mechanism. Of course, this case is an extreme example as the building has not seismic design and has an important stiffness gradient between the second and the third floor. However it is useful to illustrate the drawbacks of methods working with elastic modes instead of real ones.

Regarding the formation of plastic hinges, usually pushover-based methods do not achieve

in estimating accurately their localization. In this study, a comparison is made between the plastic hinges distribution, obtained after a NLTHA and that obtained from PSA method, considering the N involved modes. The obtained results show that a suitable prediction of the plastic hinges distribution, as shown in Figure 2.14.

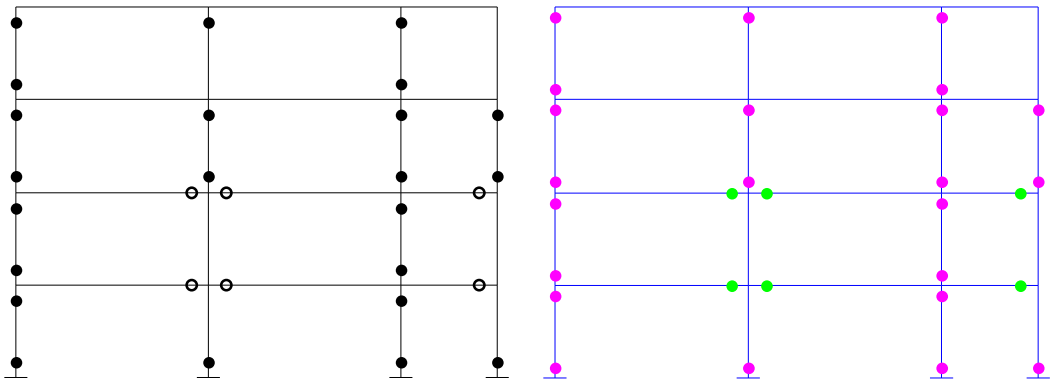

a) **b)**

Figure 2.14 Plastic hinges localization under "El Centro" record, estimated by: a) NLTHA and b) PSA method

Figure 2.15 illustrates the results of mean column rotations and storey shears. The advantage of the proposed method in estimating non linear responses is observed for two of the three studied cases. PSA is actually efficient as it provides good estimates of rotations, drifts and storey shears when a storey mechanism –which was first observed at the experimental test–, is present. It concentrates plastic deformation and generates important changes in modal shapes. Moreover, despite the poor results obtained by all the studied methods for the "Corralitos" record, PSA produces closer estimates of the studied responses than the other two methods.

It is worth saying that further inelastic response for this frame is not presented as it was not reached for none of the three records due to dynamic instability. In fact, this result was expected since numerical analyses of this building showed a lateral resistance of about 8% of its weight [Pinto, *et al.*, 2002], while it had been already subjected to 31% of its weight just for a roof drift of 1%.

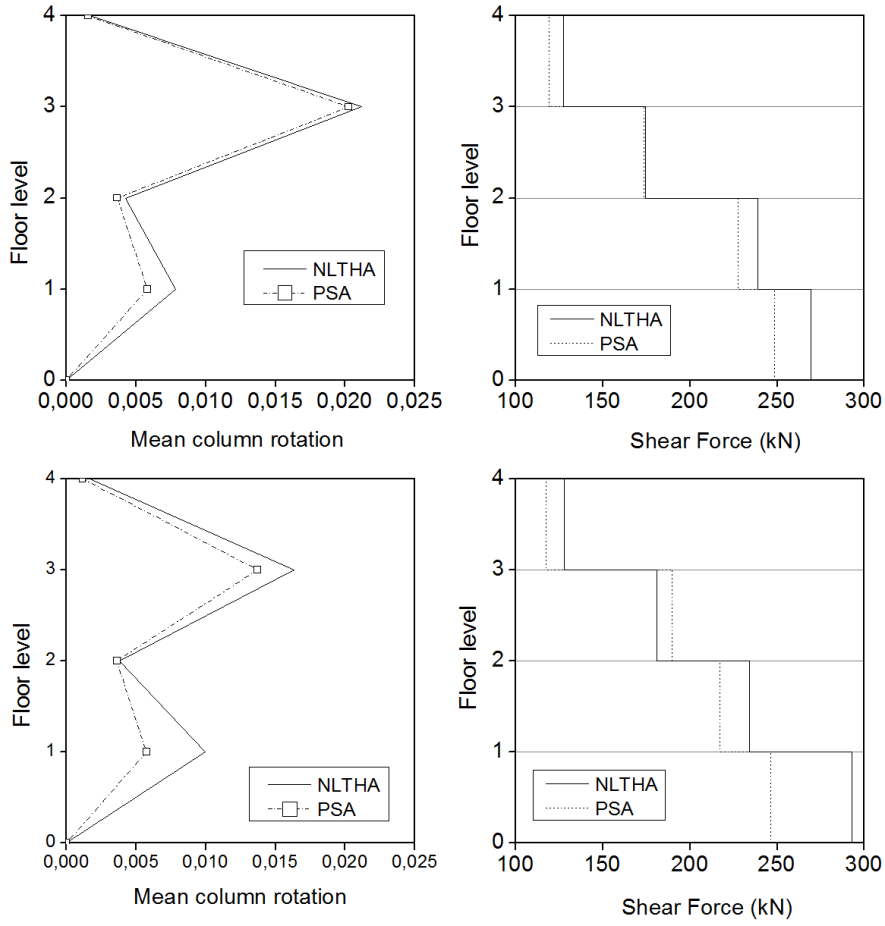

Figure 2.15 Mean column rotations and storey shears of the 4-storey GLD frame under "El centro" and "Takaratzu" records

2.6. SUMMARY AND CONCLUSIONS

A pseudo-adaptive uncoupled modal response history analysis (PSA) is proposed in this chapter for the estimation of seismic response of buildings. It has its basis on the UMRHA method so that seismic demands are computed on the basis of time history analysis of inelastic SDOF systems. Thus, PSA takes into account the dynamic characteristics of the acceleration records whereas the analysis duration time is reduced since time history analyses are carried out on SDOF systems (usually two or three) instead of MDOF systems.

Two main improvements are proposed. First, an energy-based approach to develop the capacity curve has been implemented. It allows a better representation of equivalent SDOF system properties, using the work done during pushover analysis to compute the capacity

curve abscissa. Second, effects of changes in modal properties after yielding are taken into account in a simple way, retaining the advantage offered by invariant lateral load profiles and estimating structural response with modified modal shapes calculated from storey displacements at each pushover step.

The whole procedure is illustrated with an example. It is a 4-storey, reinforced concrete low-rise building designed only for bearing gravity loads. It was experimentally tested at ELSA laboratory. PSA method is found to produce good estimations of all the studied parameters, even when a storey mechanism was present. Outcomes have been compared with reference results: NLTHA as well as available experimental results. The efficiency in estimating responses of higher buildings will be tested in the next chapter.

CHAPTER 3
PSA METHOD: APPLICATIONS AND NUMERICAL SIMULATIONS

3.1. INTRODUCTION

The basic elements as well as the underlying assumptions of the proposed PSA method were explained and tested by means of an application example in the precedent chapter. The obtained results seem to be promising since PSA method succeeds in producing acceptable estimates of important parameters as storey drifts and storey shears for that specific case. However, further validation is required for this method before being considered as a useful strategy for the estimation of buildings seismic response.

Consequently, this chapter aims to provide a further step for this objective to be achieved. The proposed validation includes the analysis of five seismic designed buildings, which are subjected to a set of six real ground motion records. Storey displacements and drifts, as well as rotations and storey shears have been selected as response parameters to be studied. The results have been compared to reference NLTHA results.

3.2. STRUCTURAL MODELS

3.2.1. Seismic designed buildings

Five different buildings are considered in order to evaluate the efficiency of the proposed method: a four-, a six-, an eight-, a ten- and a fourteen-storey reinforced concrete moment resisting frames. They are generic frames chosen for representing the behaviour of low- and medium-rise buildings. They present fundamental periods ranging from 0.5 sec to 2.25 sec. They were designed for seismic loads typical of medium (10- and 14-storey) and high (4- and 6-storey) seismic risk areas. The 10- and the 14-storey frames were designed following the Colombian code NSR-98 [AIS, 1998], while the 4- and 6-storey frames following the Mexican NTC and RCMCh codes [Uriostegui, 2005]. The 8-storey frame was adapted from a study about seismic collapse safety in modern RC buildings [Haselton and Deierlein, 2007].

Figure 3.1 Elevation view of the five validation models

3.3. GROUND MOTIONS

A set of six real strong ground motion records [PEER, 2005] were chosen. This set of records is selected in order to cause important inelastic responses and consider several PGA magnitudes as well as different frequency contents. Table 3-1 summarizes the main features of these records while Figure 3.2 shows the 5% damped acceleration spectra for each record as well as the localization of the vibration period for each of the six analyzed buildings. These spectra were derived with the SeismoSignal software [SeismoSoft Ltd., 2008].

Earthquake	Year	Station (Component)	Mw	PGA (g)
Imperial Valley	1940	El centro (180)	7.0	0.31
Loma Prieta	1989	Corralitos (000)	6.9	0.64
San Fernando	1971	Castaic (021)	6.6	0.32
Kobe	1995	Takaratzuka (000)	6.9	0.69
Erzincan	1992	Erzincan (NS)	6.9	0.52
Northridge	1994	Canyon country (270)	6.7	0.48

Table 3-1 Ground motion ensemble

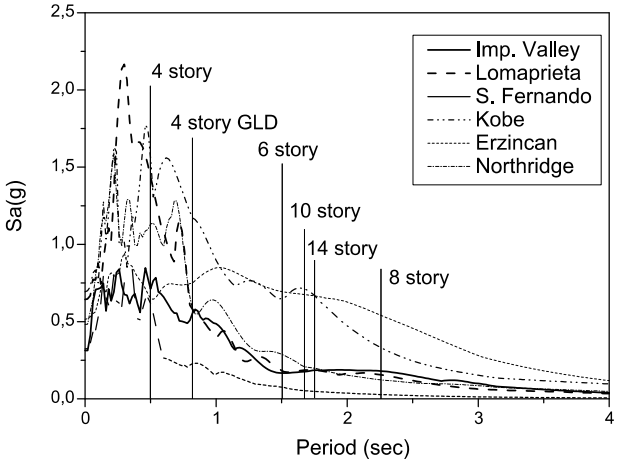

Figure 3.2 Response spectra (5% damped) of the six chosen records

3.3.1. Expected performance level

Concerning the response extent of each building under the chosen set of records, various approaches are possible for validation purposes: i) the application of each record as such, ii) scaling each record to reach a global response value or iii) to reach a local response value related to a performance indicator. Referring to the last scheme, usually local acceptability limits are established according to the expected performance level. However there is no

consensus concerning the appropriate values since deformational patterns depend on a number of factors like plastic hinging mechanisms, steel detailing and gravity load levels. Therefore some approaches propose particular limits for each building, which is appropriate for analysis of a single or a limited number of buildings [Kirçil and Polat, 2006; Kwon and Elnashai, 2006]. Meanwhile standards like ATC40 and FEMA356 are in agreement with values of 1% for immediate occupancy (IO) and 2% for life safety (LS) performance levels. In addition FEMA356 states 4% for collapse prevention (CP) [ATC, 1996; ASCE, 2000].

Since the main goal of the proposed validation is to evaluate the efficiency of the PSA method in estimating seismic responses, working with local responses associated to performance level limits is considered as unnecessary. Consequently, the roof drift was adopted as target deformation property for comparison purposes. Thus, the acceleration records were scaled so that models reach a roof drift of 0.5%, 1% and 2% of the building height *H*, referred hereafter as 0.5%H, 1%H and 2%H. This strategy is helpful in comparing the performance of buildings facing a particular record and guarantees at the same time the presence of responses ranging from elastic to important inelastic levels, e.g. a wide range of inter storey drifts, going from 0.2% to nearly 4% was found out.

3.4. RESULTS

3.4.1. Comparison of the proposed method with some existing methods

Peak responses from complete NLTHA are assumed as the reference results. The efficiency of the PSA method is investigated and the obtained results are compared to those obtained from the reference method and from two other current methods, i.e. MPA and UMRHA. Two indices are proposed in order to study the relative efficiency of the three methods in comparison to the reference one. For this purpose, a dimensionless index $I_{R,m}$, [Chintanapakdee and Chopra, 2003], is calculated as the ratio between the responses calculated respectively for the investigated method *m* (among PSA, MPA or UMRHA) and the reference (NLTHA) one:

$$I_{R,m} = \frac{R_m}{R_{NLTHA}} \tag{3.1}$$

It is intended to show trends about underestimation or overestimation of responses as well

as global results. Moreover, we suggest an index $\bar{\varepsilon}_m$, proposed to describe the global performance against the selected motions. It is defined as the mean value of the error over the building height [Jerez and Mebarki, In press]:

$$\varepsilon_i^m = \left| \frac{R_i^m - R_i^{NLTHA}}{R_i^{NLTHA}} \right| \qquad \bar{\varepsilon}_m = \frac{\sum_{i=1}^{S} \varepsilon_i^m}{S} \tag{3.2}$$

Where ε_i^m is the error at level *i* for the method being evaluated *m*, *NLTHA* is the reference method and *S* is the total number of storeys.

3.4.2. Number of modes

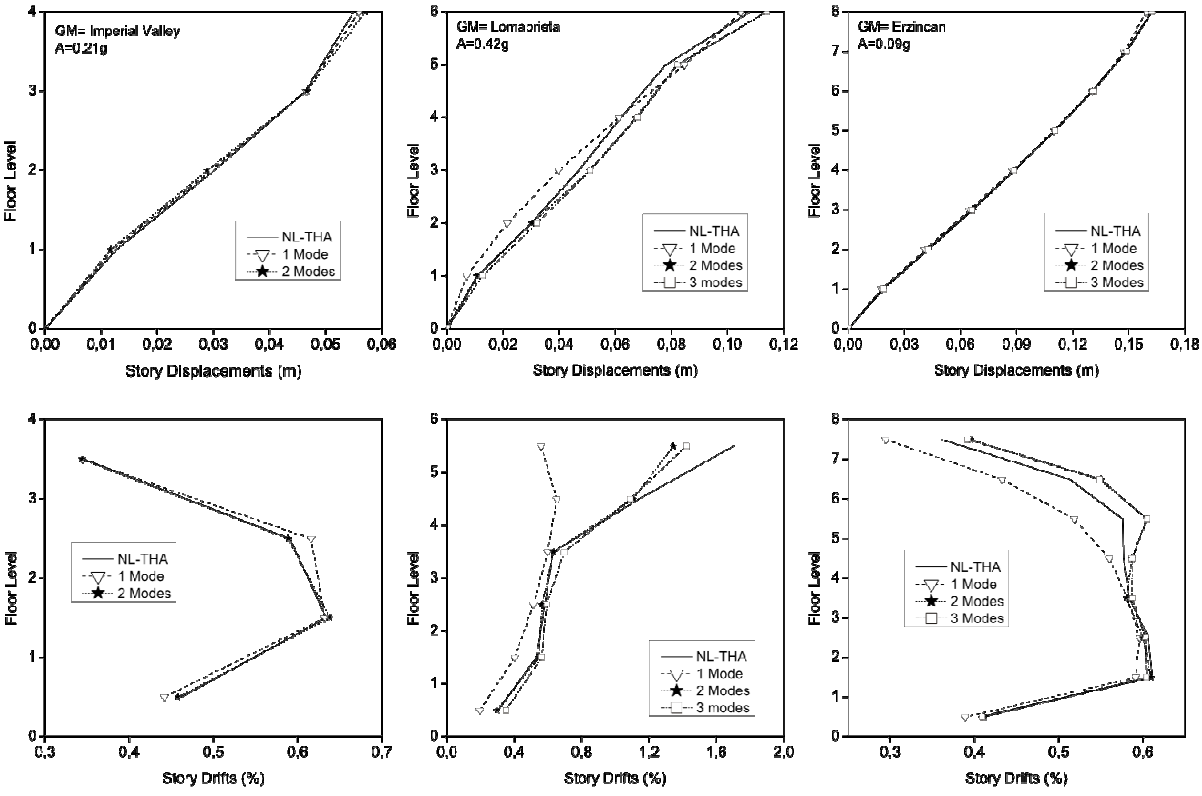

Figure 3.3 Responses of the 4-, 6, and 8-storey frames, for 0.5%*H*, for a variable number of modes involved

Concerning the number of modes required for obtaining an appropriate accuracy, the results suggest that two or three modes are in general required for estimating storey drifts, internal forces and rotations while the first mode is usually sufficient for storey

displacements, as already stated in other research studies [Chintanapakdee and Chopra, 2003]. This trend is observed in Figure 3.3 where the response of NLTHA is compared with that of the proposed method for various numbers of modes.

Four storey frames are usually dominated by first mode response. Consequently, a first-mode based procedure should be sufficient for estimating responses in those cases. However, when important changes in modal properties take place, one may consider a few additional modes in order to improve the general results. In accordance with these observations, two modes for the 4-storey frame and three for the-other frames are considered henceforth.

Most of codes provisions require that the considered modes contribute with at least 90% of the building mass when working with modal methods like the Response Spectrum Analysis. The stated number of modes involved in response calculations fulfils this requirement.

3.4.3. Low levels of deformation: Results for 0.5%H

The first level of global deformation (0.5%H) attempts to evaluate the performance of the proposed method when plastic hinging begins, usually at storey drift levels close to 1%. Nonetheless, larger storey drifts –meaning also higher inelasticity– have been reached at 0.5%H level, depending on the record and on the frame itself. This leads to larger responses and therefore larger errors, e.g. the 6-storey frame under Loma Prieta earthquake in Figure 3.3. Anyway, at these levels of deformation the proposed approach exhibits a very good accuracy according to Figure 3.3 and Figure 3.4 which show particular results for the five studied buildings. Thus, when compared to MPA and UMRHA methods, PSA produces in general better, or at least similar results, close enough of the reference NLTHA procedure.

Furthermore since the proposed procedure is a time-history process, the comparison with MPA and UMRHA methods in Figure 3.4 aims also to emphasize the effects of the computation of responses by means of SRSS combination of peak modal responses (MPA) instead of using direct superposition (UMRHA and PSA). According to these results, regardless of the approximate method, storey displacements are well estimated although UMRHA and the proposed PSA methods produce slightly better results than MPA. However, unlike displacements, the estimation of storey drifts presents significant differences between MPA results and those of the other two methods, which may become an important

disadvantage since storey drift is a widely used parameter to relate structural response to global damage, for instance.

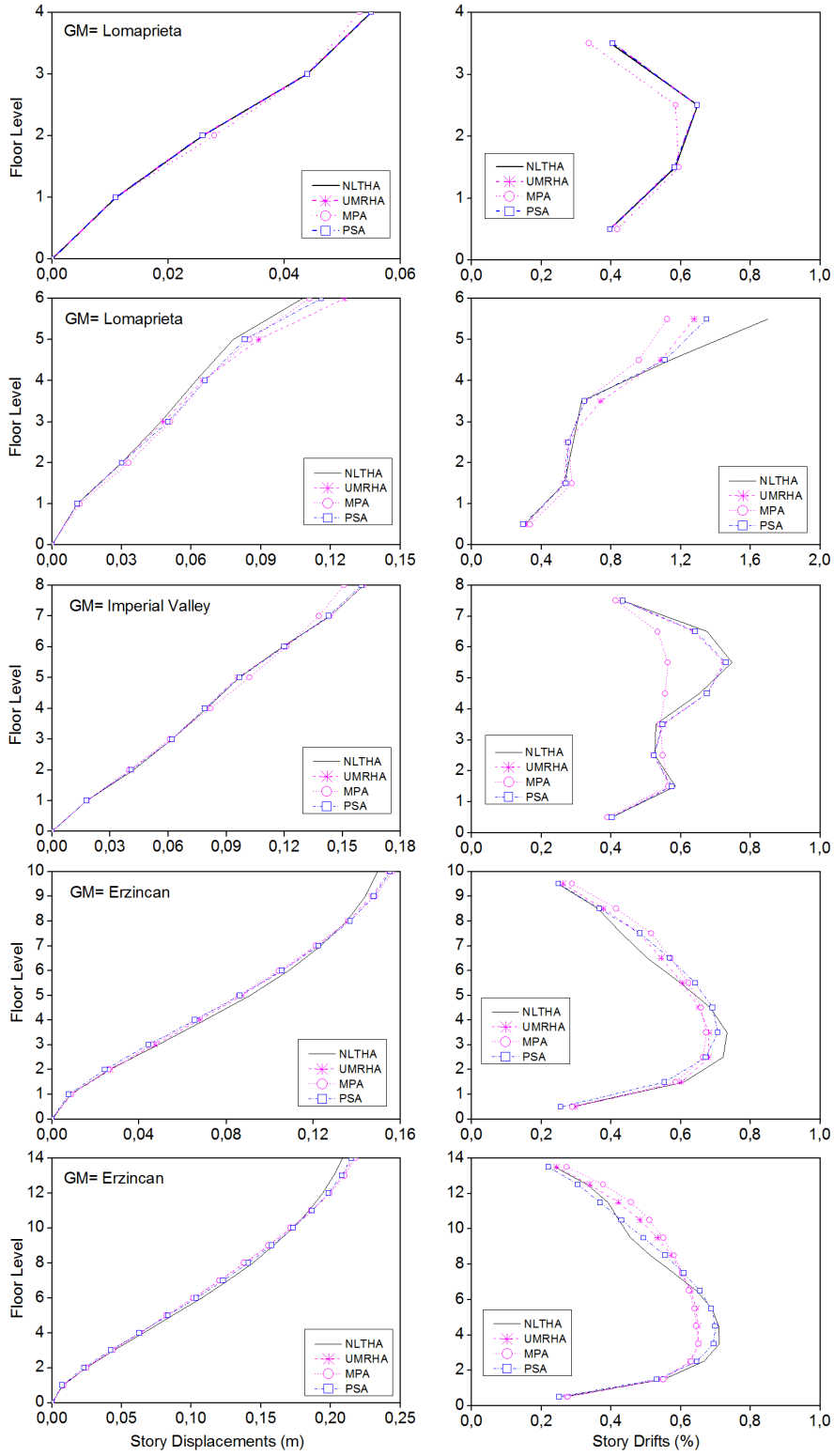

Figure 3.4 Response of the studied frames under some of the selected ground motions, for the 0.5% *H* level

On the basis of the these results one may say that more accurate results are obtained from methods based on calculation of the entire history of modal responses and the consequent superposition, since the effects of ground motion characteristics are considered in a better way. Moreover as NLTHA are performed over equivalent SDOF systems, the advantage could be taken with no much time addition. For instance, the total duration time required for the analysis of an 8-storey building is reduced as much as 4 times or even more when applying PSA (21 sec) instead of NLTHA (95sec), with the contribution of three modes and two iterations.

Global results of PSA method are presented through the mean drift index ($I_{\Delta,PSA}$) over the building height, for the five studied frames under the six ground motion records which have been sorted out as it was done in Table 1, see Figure 3.5. The observed trends in particular results are confirmed by these indices as they are close to 1 in most cases. Of course, there are cases presenting high variability or discrete results (e.g. Northridge earthquake for the 10-storey frame or Erzincan for the 6-storey frame) but general results are sufficiently good.

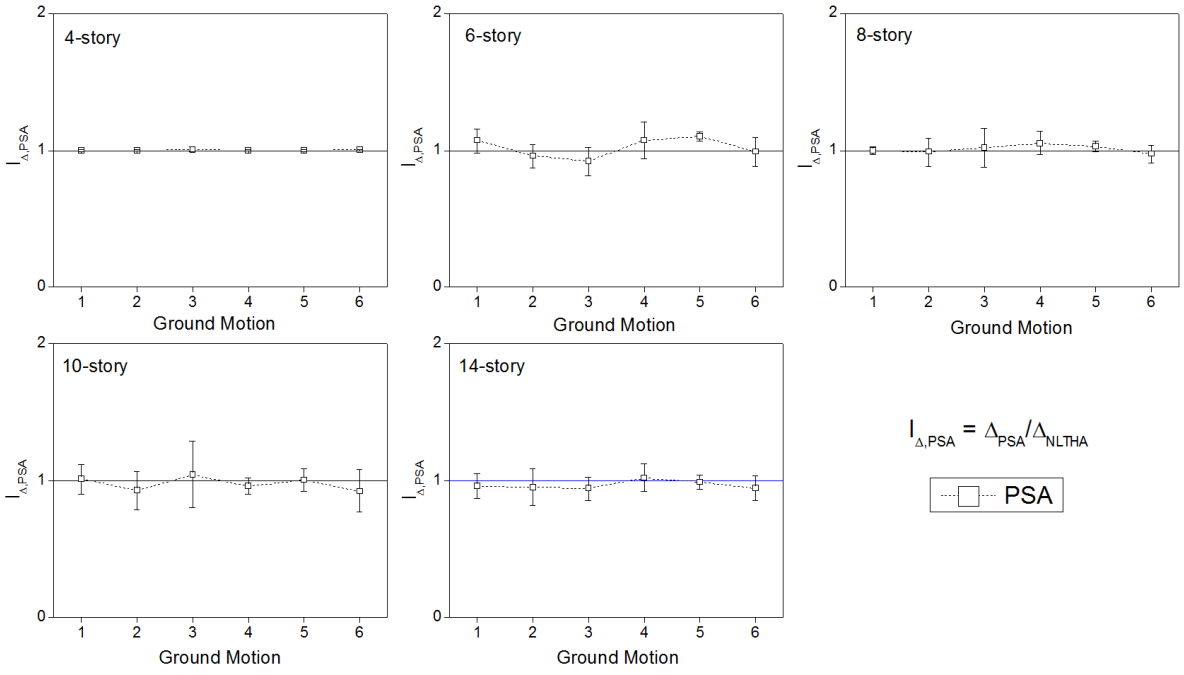

Figure 3.5 Mean drift indices and standard deviations for the five frames at 0.5%*H*

3.4.4. Results of 1%H

When going further to a roof drift level of 1%H, a wide range of responses is found. A slight inelastic behaviour is present in most cases with storey drifts ratios ranging between 1%

and 1.5%. For this deformation levels, PSA achieves in providing good estimates of the studied responses. Nevertheless, there exist also cases where large inelastic deformations are found. For these cases, particular characteristics of the studied frames in conjunction with those of the records are responsible for disparities between the expected slightly inelastic behaviour and the large concentrated deformations.

Figure 3.6 shows examples of storey drift responses at 1%H level, under Northridge, Imperial Valley and Erzincan records, where evident differences may be observed according to the record and the frame itself. In fact, results of PSA for the 4-, 6- and 10-storey frames are satisfactory, as well as those of the 14-storey frame under "el Centro" record, ranging between 0.4% and 1.8% of storey drifts. However, Northridge record, which tends to concentrate large deformations at the lower storeys and to excite higher modes at the same time, produced early hinging at the base and the beginning of a storey mechanism at the higher storeys on the 8- and the 14- storey frames. These large responses, which eventually lead to the failure at the 2%H level, were not predicted by any of the studied methods, although PSA manages to get the general trends.

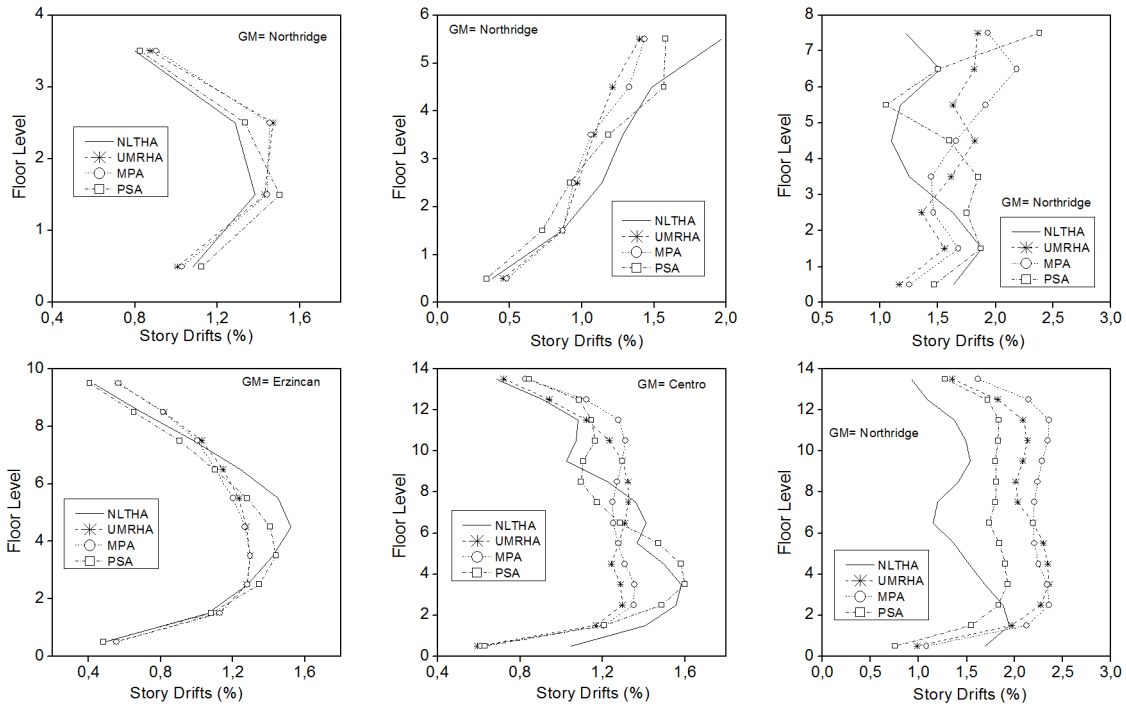

Figure 3.6 Examples of storey drift responses for the five studied frames at 1% H level

3.4.5. High levels of deformation: Results of 2%H

Far from the elastic domain, MID ranges from 2% up to 4% for a global displacement ratio of 2%, leading to important changes in modal shapes. Figure 3.7 confirms the influence of modal shape changes after yielding in the response of a seismic designed building. The first graph of each row represents the real, the elastic and the approximate first modal shapes at the 2%H level. For both responses, i.e. storey displacements and drifts, the estimation made by PSA method is very close to the NLTHA result.

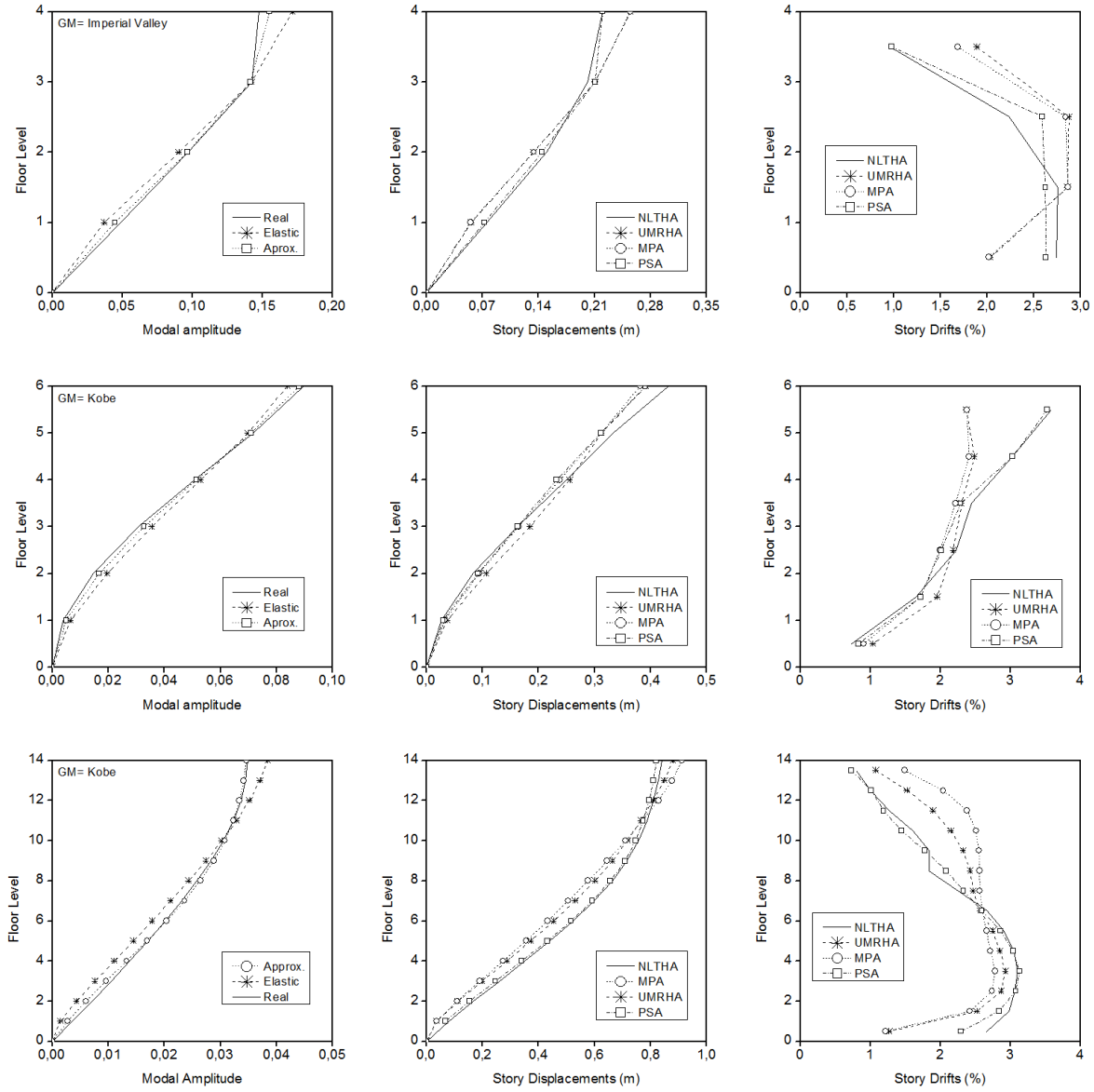

Figure 3.7 First modal shape, storey displacements and drifts for the 4-, 6- and 14-storey frames at 2% H level

Shear forces of the five buildings, for the 1%H and 2%H level, are presented in Figure 3.8 and Figure 3.9. The method is efficient though it might overestimate forces in higher storeys at 2%H level as observed in few cases for the 8- 10- and 14-storey buildings. Nevertheless in most cases, PSA is able to produce shear force estimates close to those of NLTHA.

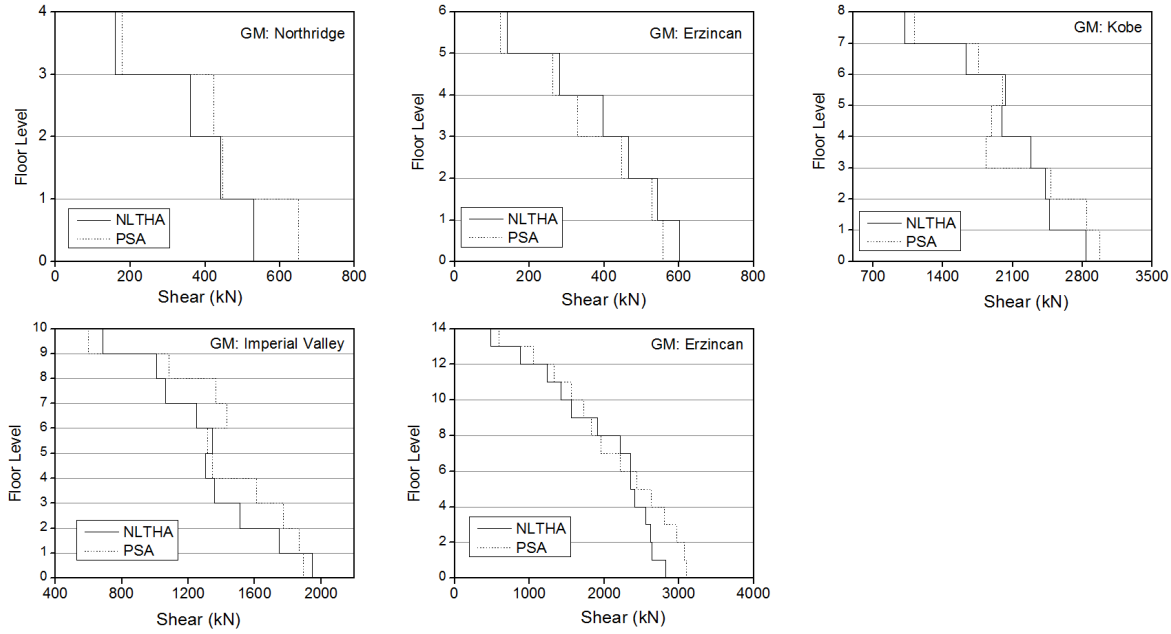

Figure 3.8 Shear storey forces at 1% H level

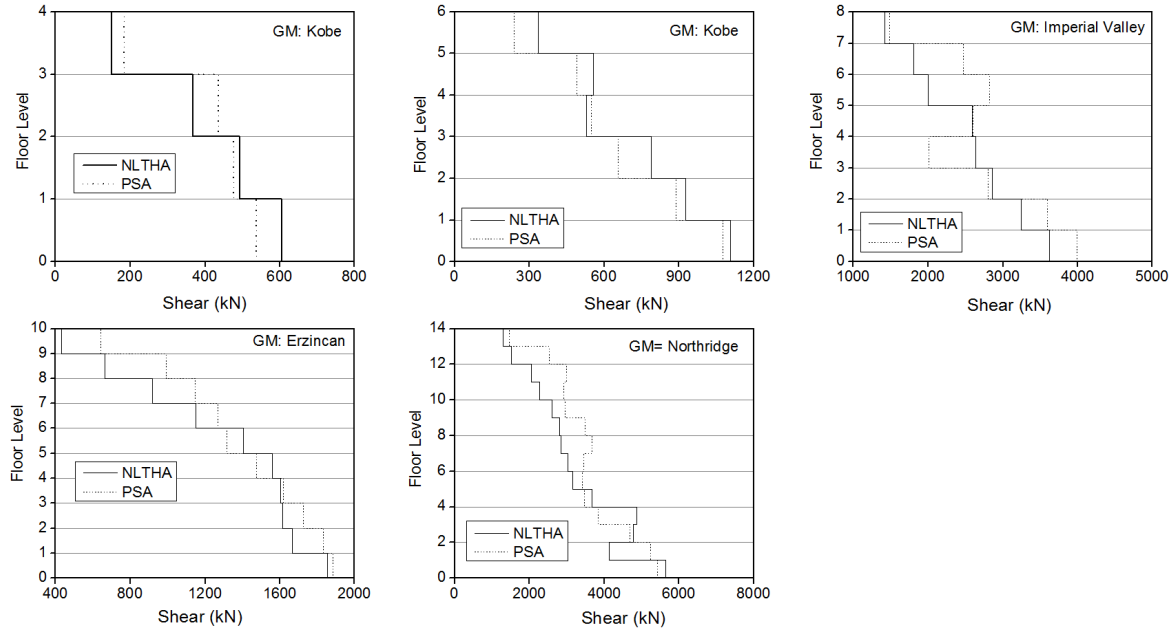

Figure 3.9 Shear storey forces at 2% H level

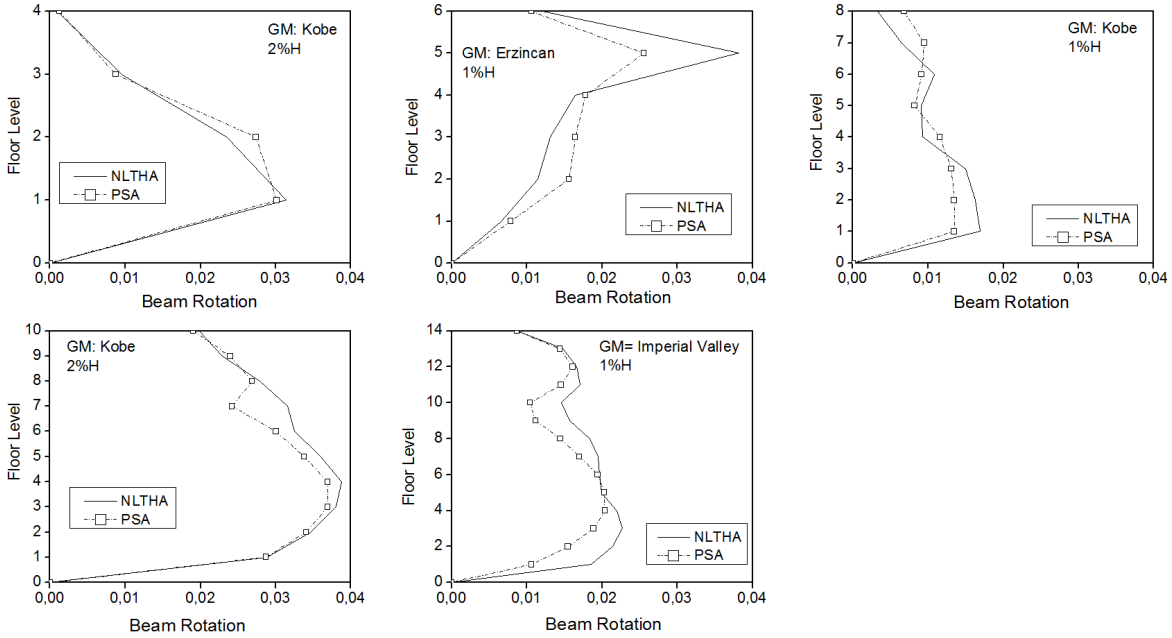

Figure 3.10 Rotations at the most demanded beam, at each storey

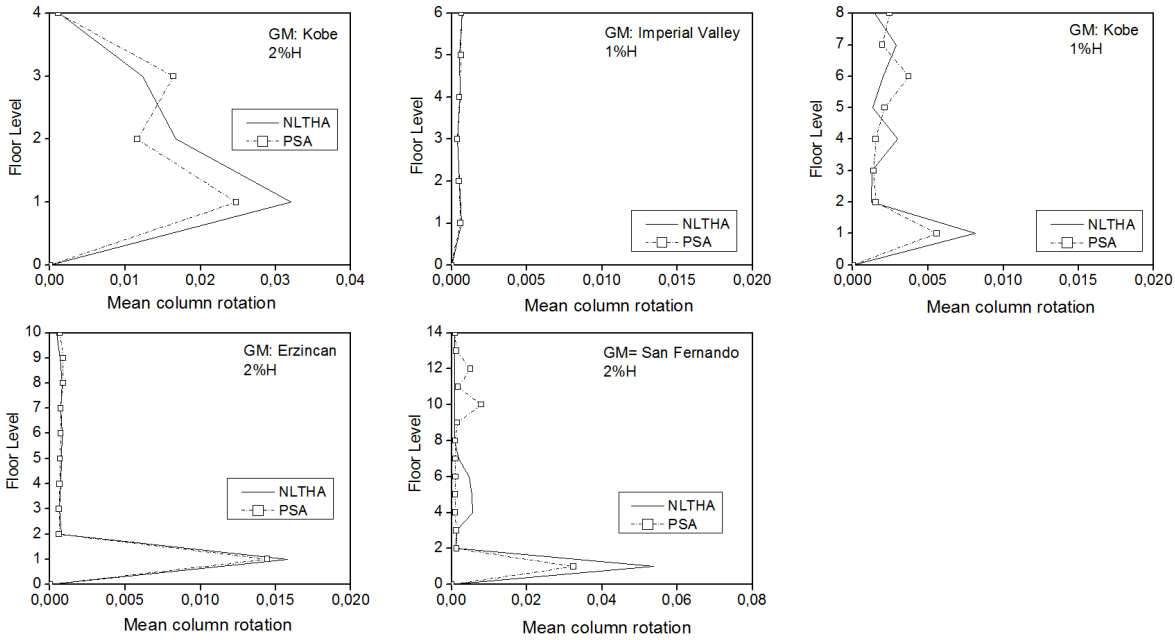

Figure 3.11 Mean column rotations at each storey

The efficiency in estimating plastic rotations is illustrated in Figure 3.10 and Figure 3.11 where beam and column plastic rotations are presented. The proposed method is very efficient in estimating beam rotations for inelastic levels of about 0.04 rad. Maximum relative errors

are lower than 20% in most of the studied cases at deformation levels of 2%H. For a few cases, the relative error in the plastic rotation reaches almost 30% for the upper beams. When dealing with column rotations, PSA predicts correctly the high concentrations of plastic rotation on lower storeys, as shown in Figure 3.11.

Figure 3.12 provides the measure of the global performance of PSA through the index $\overline{\varepsilon}_m$ for storey drifts, for the five frames under study and for the three levels of deformation. The results are satisfactory in most cases.

For low levels of deformation, the differences remain small ranging between 5% up to 10% or even lower as for the 4-storey frame. In the case of global deformation of 1%H, the trends are different for low-rise and medium-rise buildings: for the 4- and 6-storey frames errors are below 15% while for the other frames they are below 20% except for Northridge record, as already discussed.

As for any approximate method, PSA accuracy decreases as far as the response goes further in the inelastic domain so errors increase with deformation. When MID reaches values of about 3% and 4%, PSA provides differences around 20% for the 4-, 6- and 14-storey frames in most cases. For the other two buildings, performance is very variable and is intimately depending on the ground motions. They are especially large under Northridge and Imperial Valley records. This could be partly due to the particular characteristics of these records. Actually, close relationships between their main frequencies and those of the frames were found, e.g. $\omega_2 / \omega_{GM} = 1.06$ for the 10-storey frame and $\omega_3 / \omega_{GM} = 1.02$ for the 8-storey frame in the case of Northridge. Figure 3.13 shows the most extreme cases of large differences between the reference results and those of the approximate methods, under Northridge earthquake.

In fact, it is observed as a general inconvenient that large concentrated inelastic deformations produced by very particular contents in the earthquake signals are not always well predicted by static pushover-based methods with invariant load profiles. In those cases PSA achieves in getting with acceptable accuracy the general trends in comparison with other existing methods.

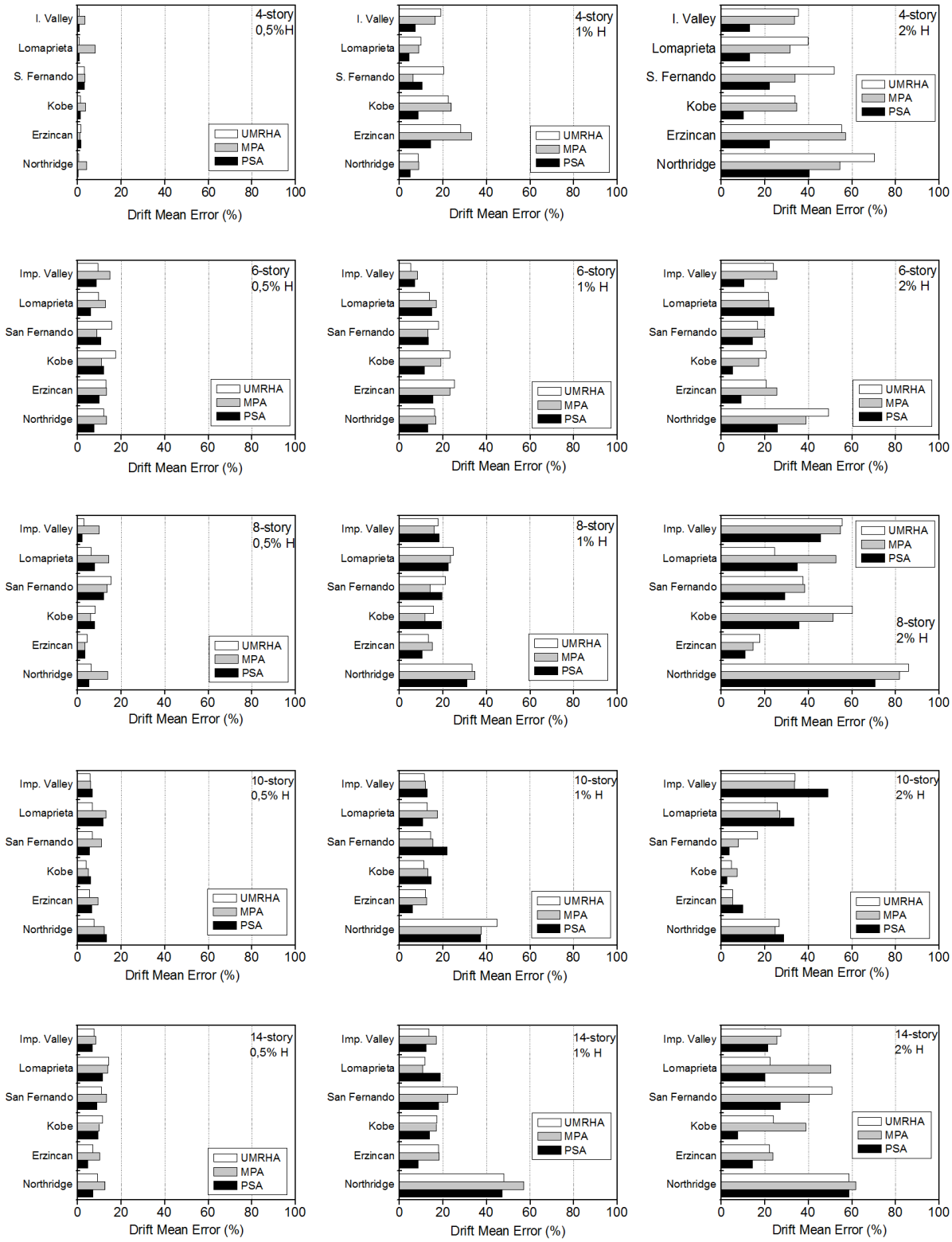

Figure 3.12 Drift mean errors ($\bar{\varepsilon}_m$) for the four buildings and the three levels of deformation

However, when dealing with large scale studies (reliability analysis at urban scales for instance) a preliminary analysis under some reference records should be performed in order to identify the presence of records producing significant concentrations of inelastic deformations. That being the case, maybe updating load profiles at key stages would be required, when exceeding specified limits of deformation for instance; or maybe a complete NLTHA remains the unique choice when good accuracy is requested.

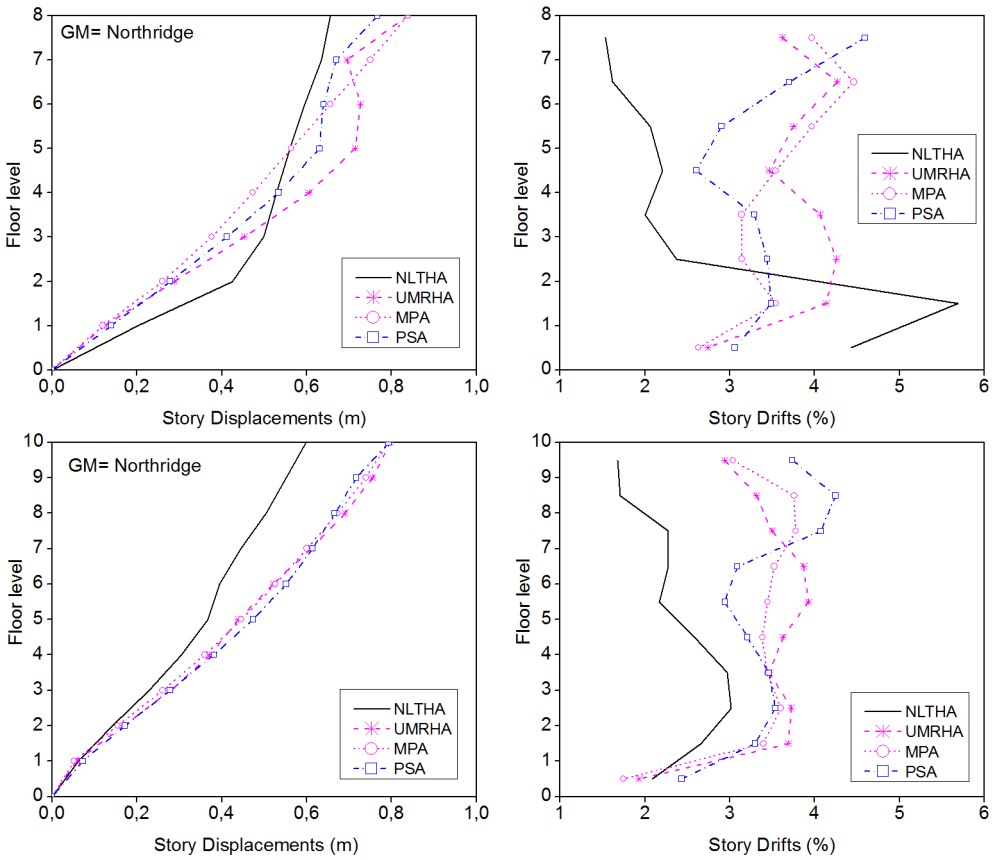

Figure 3.13 Response of the 8- and the 10-storey frames under Northridge record, at 2%H level

Returning to Figure 3.12, when looking at each frame separately it is apparent that PSA has a significant advantage over the other methods studied for the 4-storey frame for 1%*H* and 2%*H* levels of deformation. In the case of 0.5%H results are similar to UMRHA and definitively better than MPA. This observation may also be extended to the 6-, 8- and 14-storey frames chiefly at 2%*H* level. This behaviour is probably due to the fact that changes in modal shapes are more explicit at higher levels of inelasticity and therefore they have a major influence in the response. For the 10-storey frame results are modest and there is no clear

trend. In addition, the 4- and 6-storey buildings are designed for a high seismic risk area while the 10- and 14- are designed for a medium seismic risk area. The 8 storey building is designed only for 0.05 of its weight. This may also explain the differences in the response: for the 1% roof drift level, results of the five frames are comparable, better for the low-rise and acceptable for the medium-rise buildings, except for Northridge record. However, when dealing with more inelastic demand at 2% roof drift level, results are completely different, according to their seismic design: low-rise buildings present differences of about 10%, less than 15%, the 10- and 14-storey frames show differences around 20% and the 8-storey frame produced the highest differences for this level of deformation, rounding 30% except for Erzincan record.

Since the proposed procedure is a time-history based technique, comparison with MPA and UMRHA aims also to show the effect of computing the response quantities by means of SRSS combination of peak modal responses (MPA) instead of using direct superposition (UMRHA and PSA). Significant differences between MPA and time-history based methods can be noticed, particularly for storey drifts and for low levels of deformation. This may become an important drawback since storey drift is a widely used parameter to relate structural response to damage.

One may notice that particular features of the frames as well as of the ground motion records may produce large responses. Nevertheless, PSA method succeeds in getting closer to NLTHA results for a great number of the investigated cases.

3.5. SUMMARY AND CONCLUSIONS

A pseudo-adaptive uncoupled modal response history analysis (PSA) has been proposed in this chapter. As proved by some specific examples as well as by general results, considering real modal properties is a key issue for simplified methods based on modal analysis. Therefore, as an alternative to fully adaptive methods, PSA is intended to take into account the changes in modal properties by means of its pseudo-adaptive character.

Individual and overall results, mainly for low levels of deformation, demonstrate the convenience of a time history approach based on superposition of responses. It may improve mean estimations of response while keeping a reasonable time of analysis because NLTHA is performed over SDOF models. In most cases, PSA method succeeds in producing acceptable

estimates of inelastic responses.

For high levels of inelastic response, the proposed method provides better, or at least similar, results than other existing and widely used approximate methods. It gives acceptable estimates of the investigated parameters, as they are very close to those provided by the reference method, i.e. NLTHA (Non Linear Time History Analysis). Storey displacements, inter storey drifts, beam and column rotations and shear forces are considered for comparison purposes. Since storey drift is perhaps the most used parameter as it is intimately related to the damage, it is significant to find that PSA achieves in yielding good evaluation of it, as confirmed by the median values of errors. Shear forces and element rotations are also well predicted on the whole by PSA method. However, estimation of displacements is in some cases not very efficient as it is frequently the case for other existing simplified methods.

Of course, as an approximate method, the proposed method PSA has also its own limits. Its validity and general accuracy may be checked with a wide study including, for instance, infilled frames. Moreover, since particular features of real ground motion records have a significant effect on structural response, more adapted methods for selecting them should be used. Synthetic records are also an option for such study. However, the proposed procedure gives acceptable estimates of structural response with very few additional calculations. The fact that the calculation duration time is reduced and that it is possible to consider modal changes whereas an invariant load profile is assumed, gives attractive advantages to the proposed PSA method.

Consequently, as neither eigenvalue analysis nor updating of load profiles are needed during pushover analysis, open source or special software platforms are not required for the use of PSA method. This may be an important feature for current engineering practice and also for reliability and vulnerability studies as well as post-quake damage evaluations at large scales such as urban scale.

PART II
DAMAGE EVALUATION

CHAPTER 4
SEISMIC DAMAGE ASSESSMENT

4.1. INTRODUCION

Extended and greatly populated areas are being struck by natural disasters very frequently. Earthquakes are among the events causing extensive damage in buildings, in structural as well as non structural elements. These damage levels have consequences on the occupation and on the reconstruction costs. This emphasizes the need to have a rigorous assessment of the damage levels.

Damage, as well as damage measures have been the subject of a wide number of research works in the last three decades and have been defined in several ways. A damage measure may be a function of the remaining life span of the structure, of microstructure measures which account for real defaults in a representative volume, of variations in physical properties as density and, of variations in mechanical properties [Besson *et al.*, 2001]. In addition, some measures have been expressed in terms of economical indices as a function of repair costs [Kappos *et al.*, 1998] or have been related to residual probabilities of failure [Mebarki and Laribi, 2008].

This chapter aims to provide a brief definition of fundamental concepts associated to damage assessment at all levels as well as a summary of some methods available for this purpose.

4.2. STRUCTURAL DAMAGE: BASIC ELEMENTS

4.2.1. Definition

As a general phenomenon, damage may be defined as an irreversible physical deterioration affecting the usefulness or the functionality of a system or its sub-systems. Particularly, according to FEMA 306, when dealing with structural seismic damage, a definition implies the existence of physical evidence about inelastic deformation caused by a damaging earthquake [ATC, 1998a]. Therefore, as it will be pointed out later, damage indices

and mechanical states are usually related to measures of inelastic deformation.

4.2.2. Damaged components

Before dealing with damage measures and identification parameters, a classification of damaged components is necessary. The classification is made on the basis of the function of the elements under study. When a building withstands an earthquake, all the components are concerned: structural and non structural components (including mechanical and electrical equipment and piping) as well as foundation elements. The involved components govern the required damage indicator according to their sensibility to the different expressions of seismic response. For instance, storey drifts are known to be a good indicator of damage of non structural components, which used to be highly sensible to relative deformation. It is the case of infill walls, door and window frames and cladding or glazing elements. For that reason, each group of elements requires a specific study of damage assessment, even if, at the end, a global measure will be produced.

According to the main objectives of this study, only structural components will be considered hereafter since the damage under study concerns the mechanical capacity, regardless of the global utility and functionality of the buildings, in which case even the non structural components should be involved.

4.2.3. Main causes and expressions of damage (visual and functional indicators)

For a particular system –a building for example– the common causes of damage are the various actions supported during its lifetime, applied suddenly or steadily with different intensities and time duration. More precisely, according to experimental studies, structural seismic damage is the result of the large nonlinear deformations and the energy dissipation as well as the fatigue due to cyclic loading inherent to earthquake actions [Park and Ang, 1985]. This results in functional expressions as stiffness and strength deterioration affecting the lateral performance, as well as the possibility of bearing vertical loads, leading sometimes to the failure. Usual visible indicators of damage are the presence of permanent deformations and patterns of cracks or deformation specific to the material and the particular stress state.

Thereby, pure tension, bending and shear stresses lead to differently oriented cracks on elements, see Figure 4.1a. Compression states generate crushing of concrete and buckling of

steel reinforcement in the case of reinforced concrete structures (see Figure 4.1b) or local buckling in the case of steel structures. Presence of out of plane deformations is also common on wall elements, among a large number of visible signs. All these physical effects must be represented by a suitable parameter which will be inevitably related to these expressions of permanent deformation.

a) **b)**

Figure 4.1 Examples of visual expressions of damage. a) Shear cracks in a beam-column joint (Photography taken by the author) b) Bucking of reinforced bars caused by lack of confinement [Pujol *et al.*, 1999]

4.2.4. Damage classification

As stated before, damage may be defined from material or component level, referenced as local damage, up to structural level referenced as global damage. These damage levels control the nature of variables representing the phenomenon itself. Thus, local damage may be evaluated on the basis of end rotations for example, whereas global damage requires an overall indicator such as a global displacement limit or a vibration frequency of the system.

4.2.5. Representations of damage

Dealing with complex phenomena such as structural damage requires several hypotheses and simplifications. Furthermore, a suitable representation means necessarily objective and quantitative damage measuring. In practice, several approaches are available involving either

scalar or vectorial variables obtained by direct or indirect measures that express damage effects.

4.2.5.1. Direct measures

The direct measures concern the physical or mechanical properties which have been affected by the earthquake, i.e. quantities directly related to the visible signs of damage such as:

- Measures of physical properties variation such as density or resistivity [Besson, *et al.*, 2001].
- Microstructural measures which provide an evaluation of actual flaws per unit volume, as indicator of physical degradation [Besson, *et al.*, 2001].
- Measures of the changes in mechanical properties such as stiffness or strength
- Measures of the variation of the maximal available values of a demand parameter such as ductility, deformation or strength.

4.2.5.2. Indirect measures

These are quantities intended to represent damage by means of the effects on other properties or attributes which are not directly related to the physical signs, such as the economic loss represented by a parameter such as the repair or the strengthening cost.

4.2.6. Damage states

The damage state identification is the first step in order to classify damage by means of a qualitative physical evaluation of the earthquake effects. Usually damage states are intended to be the basis of decision-making tools about the residual capacity of the component or system. They may be associated to the direct observation of the damage evidence (like the extent and magnitude of cracks, deformations, etc.) or to the serviceability of the building after the earthquake. They may also be associated to damage indices, establishing therefore categories and ranges of the selected index according to different particular damage states, like those proposed by the ATC-13 [ATC, 1985]. According to Bonett [2003], a possible classification may be:

- According to observed damages: Damage states are established on the basis of direct observations of the different damage signs and may be expressed by means of an increasing damage scale: e.g. “No damage”, “slight”, “moderate”, “severe” and “complete”. The well known proposal of Park, Ang and Wen is an example of this approach [Park *et al.*, 1987].
- According to the required repair or even the possibility of repair, damage states may be: “No damage or slight”, “repairable”, “no repairable” and “collapse”.
- A combination of the latter two approaches. They define damage states based on all the mentioned aspects (observed structural and non-structural damages, serviceability, repair costs and risk for the inhabitants), e.g. the ATC-40 limit damage states [ATC, 1996].

The main disadvantage of damage states concerns their subjective character since they rely on engineering judgment or expertise, regardless of any explicit or direct structural calculation.

4.2.7. Damage indices

Indices are intended to quantify damage according to a given number of criteria. Most of them are intimately related to damage representations and usually require the development of a model to represent the structural behaviour of the component. When based on direct representations, they express the deterioration level of a specific property by means of a variable, usually normalized by the initial or reference value of the studied parameter such that it takes theoretical values from 0 indicating no damage up to 1, meaning complete damage. If they are based on indirect measures, they will usually have magnitudes ranging between two bounds associated also to no damage and complete damage. Methods for getting damage indices will be explained afterwards.

4.2.8. Damage models

Local damage index definition often requires the development of damage models, which are analytical representations of real damage at the component level. According to whether cyclic loading effects are considered or not, damage models may be cumulative or non cumulative [Williams and Sexsmith, 1995]. Non cumulative models estimate damage indices

on the basis of monotonic, static properties of the member whereas cumulative models consider both, monotonic effects and energy dissipation and fatigue due to cyclic loading. Examples of cumulative damage models are the model proposed by Krawinkler and Zohrei [1983], for application on steel structures and the Park and Ang model [1985], calibrated with a large number of experimental tests on reinforced concrete specimens. In fact, it was one of the first proposals for establishing a local damage index considering the effect of excessive deformation and repeated cyclic loading, both related by a linear function [Park and Ang, 1985]:

$$D = \frac{\delta_M}{\delta_u} + \frac{\beta}{Q_y \delta_u} \int dE \tag{4.1}$$

Where: δ_M is the maximum deformation under the earthquake, δ_u is the ultimate deformation under monotonic loading, Q_y is the calculated yield strength, dE represents the incremental absorbed hysteretic energy and β a non-negative parameter. This index was also used to associate damage degrees and damage states with observed seismic damage, as shown in Figure 4.2. Of course the structures represented by B, G and A letters are reported to have collapsed, so consistently D>1 [Park *et al.*, 1985].

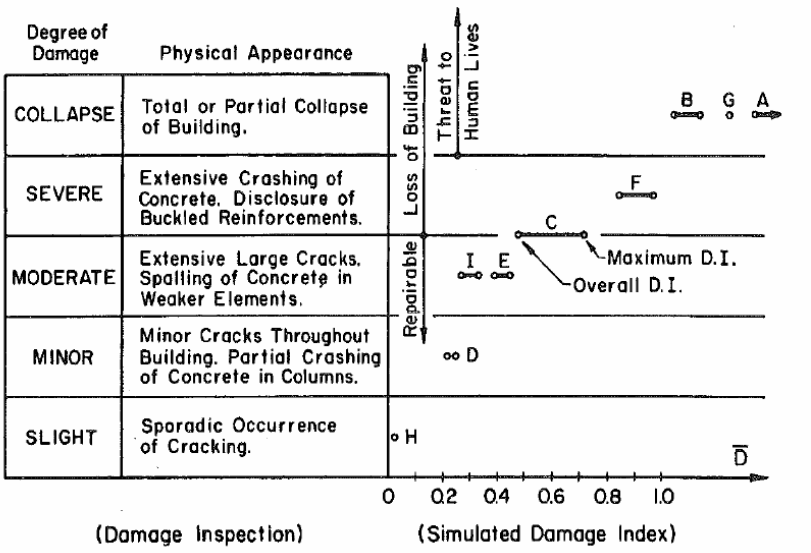

Figure 4.2 Relationship between damage indices and observed damage. [Park, *et al.*, 1985]

This index has been the basis of numerous approaches [Reinhorn *et al.*, 1992; Fajfar and Gašperšič, 1996; Chai, 1999] and it is still widely used as reference method since it relies

directly on the main causes of damage. Nevertheless, it is difficult to apply in many practical cases, e.g. post-seismic evaluation, since it requires detailed information about the monotonic and dynamic behaviour of elements as well as the detailed data about the constitutive materials and reinforcement, joints, etc.

4.3. DAMAGE INDICATORS BASED ON MEASURES OF MECHANICAL PROPERTIES

Considering the nature of structural seismic damage, the identification should be related to a deformation parameter, to the absorbed and dissipated energy as well as to strength and stiffness loss. However, despite the current appropriate understanding of the phenomenon itself, there is no consensus neither about a unique and reliable identification parameter nor a method for its estimation. Moreover, structural damage depends on the material, on the component and on the predominant force the component is submitted to, either axial force, bending or shear or their combination [Colombo and Negro, 2005].

Using the thermodynamics principles and by means of continuum damage mechanics theory, a suitable measure of local damage has been proposed. It relies on the representation of the macroscopic variation of mechanical properties such as Young modulus, potential energy, etc. It is expressed as a variable D –a scalar quantity when damage is considered as isotropic– ranging from 0 when no damage exists, up to 1 when damage is considered complete [Lemaitre, 1985; Besson, *et al.*, 2001]. This index is better understood through the concept of effective stress, expressed by Kachanov (quoted by Lemaitre [1985]).

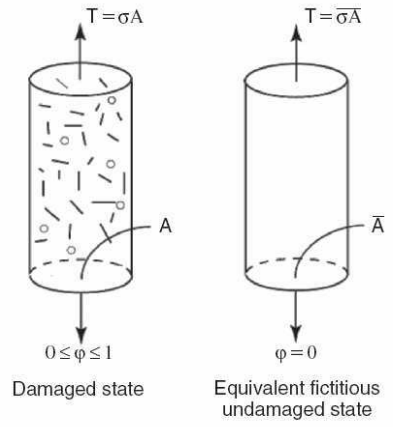

Figure 4.3 Concept of effective stress [Voyiadjis, 2005].

In fact, the damage variable accounts for the macroscopic effect of damage on the initial undamaged area *A* (see Figure 4.3), by means of the following relationship:

$$D = \frac{A - A_d}{A} \rightarrow A_d = A(1 - D) \tag{4.2}$$

Where A_d represents the damaged area and D would have theoretical values between 0 and 1. Then, for the axial case, the stress caused by the force F on the damaged area is known as the effective stress, $\tilde{\sigma}$, computed as a function of D and the apparent stress σ on the total area A [Lemaitre, 1985]:

$$\tilde{\sigma} = \frac{\sigma}{(1 - D)} \tag{4.3}$$

Thereby, applying the hypothesis of strain equivalence[3] on the elastic strain energy of the damaged body, the Young's modulus of the damaged state E_d may also be expressed as a function of *D* and the initial Young's modulus *E*:

$$E_d = E(1 - D) \tag{4.4}$$

As a result, a straightforward formulation for expressing damage effects is available. It allows to estimate damaged properties provided the index D, or obtaining directly a measure of the damage when the initial and damaged states of a mechanical property are known.

4.3.1. Damage assessment by means of variations in the lateral force –displacement relationship

Following this general framework, several approaches have been presented for computing D, obtaining the deterioration of mechanical properties in different ways, as it is illustrated in Figure 4.4.

[3] This hypothesis states that 'any strain constitutive equation of a damaged body derives from the same function as for a virgin material, except that the stress is replaced by the effective stress'. [Lemaitre, 1985]

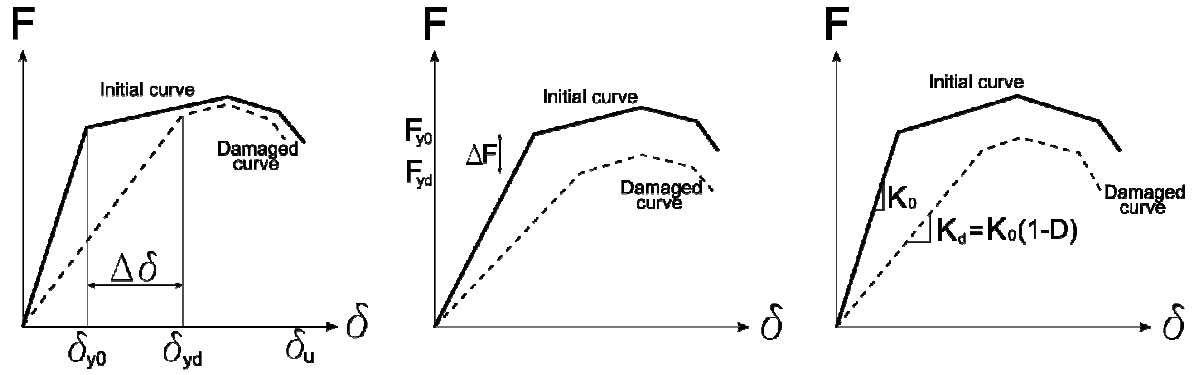

Figure 4.4 Different strategies for damage identification: a) Change in displacement patterns, b) Reduction in bearing capacity and c) Reduction in stiffness

4.3.1.1. Variation in the displacement response

This procedure is illustrated in Figure 4.4a, where the increase –or decrease– in ductility levels may be the base for an indicator of damage. In general D may then be computed as a function of a reference displacement, e.g. yield or peak displacement, at the initial (δ_{y0}) and at the damaged state (δ_{yd}):

$$D = 1 - \frac{\delta_{y0}}{\delta_{yd}} \tag{4.5}$$

An example of such an approach is the proposal of Jeong and Elnashai [2006] for computing damage indices of planar frames considering out of plane deformations, within a 3D damage framework. Another example is the procedure established in the FEMA306 guidelines [ATC, 1998a], which is a performance-based technique, explained in detail hereafter.

4.3.1.2. Decrease in bearing capacity

According to this approach, damage is supposed to be adequately defined by the reduction in strength. Thus D may be defined by the variation between the initial (F_{yo}) and the damaged (F_{yd}) yielding strength:

$$D = 1 - \frac{F_{yd}}{F_{yo}} \tag{4.6}$$

Since damage indices depend intimately on the structural material, a proposal following this strategy was presented as an attempt to define a generalised damage index which may be used for any structure regardless of the material. It has the mathematical form of the Equation (4.6) where the forces or moments representing the bearing capacity vary according to the structural material [Colombo and Negro, 2005].

4.3.1.3. Variation in modal properties

Unlike the latter two approaches, which may be applied to obtain local or global damage indicators, the procedures based on the computation of modal properties are mainly indicated for obtaining directly global damage indices, i.e. without computing explicitly local damage indices. The average damage of the structure is supposed to be represented by the lengthening in the fundamental period (T_0), called the *maximum softening,* δ_M, according to DiPasquake and Cakmak [1990]. It is obtained by Equation (4.7), where $(T_0)_{initial}$ and $(T_0)_{max}$ represent the initial and the maximum estimated fundamental periods. Also the combined variation of the period of the first and second modes [Nielsen *et al.*, 1992] as well as the variation between the undamaged and damaged largest eigenvalue have been used as indicators of global damage [Molinari *et al.*, 2009].

$$\delta_M = 1 - \frac{(T_0)_{initial}}{(T_0)_{\max}} \tag{4.7}$$

4.3.1.4. Stiffness reduction

Damage may also be represented by the decrease in the elastic slope of the curve representing the overall (or local) behaviour of the structure (or component). Thus, D depends on the initial undamaged stiffness K_0 and the damaged stiffness K_d:

$$D = 1 - \frac{K_d}{K_o} \tag{4.8}$$

This approach is closely related to that of the variation in modal properties, since they become equivalent when applied to elastic structures under the assumption of having an invariant mass matrix before and after damage is taking place. Both strategies are often used for identification and localization of structural damage in experimental studies based on finite

element model updating techniques [Simoen *et al.*, 2010].

4.3.2. Performance-based damage assessment

On the basis of performance-based engineering, this kind of approach is intended to evaluate the effects of seismic damage through the building performance loss. In fact, it consists in assessing the changes in the future performance of the building, under the performance ground motion, as established by FEMA306 guidelines [ATC, 1998a]. According to this document, decisions about serviceability or repair depend on a variable relating the global displacement capacity d_c to the global displacement demand d_d, for the undamaged (pre-event) and damaged states, see Figure 4.5. The variable is called the performance index *P*, computed from:

$$P = \frac{d_c}{d_d} \tag{4.9}$$

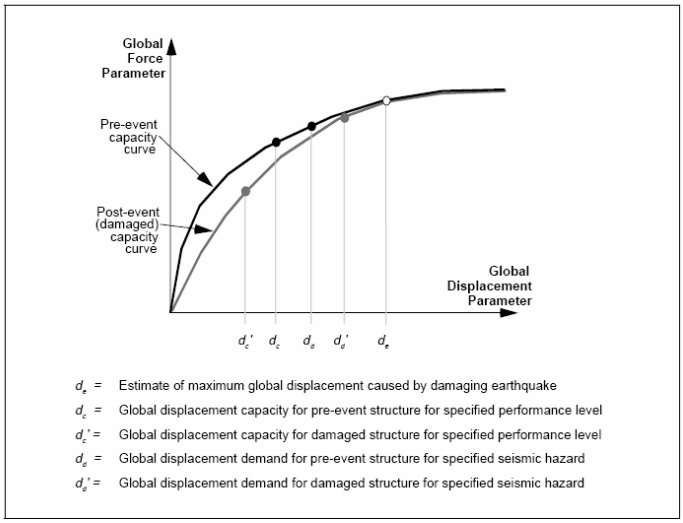

Figure 4.5 Displacement parameters for Damage Evaluation. Taken from FEMA306 [ATC, 1998a]

Of course, the capacity parameters (d_c and d_c') are global displacement limits determined by the performance objective. Actually, each one represents the displacement for which a performance objective (IO, LS or CP, according to §1.2.6 PBE) is attained, for a given level of seismic hazard. Values of variable P provide the ability of the building to meet a performance objective (P<1 means non compliant and P=1 or P>1, compliant) and also allow to obtain the loss of performance capacity as a damage measure.

Within a similar performance-based framework, Barbat *et al*. [2008] and Lagomarsino and Giovinnazi [2006] proposed a vulnerability and damage evaluation technique on the basis of the CSM method for obtaining the performance point and the definition of damage state thresholds. The final objective is to express the vulnerability as the probability of reaching a particular damage state given a specified hazard level by means of fragility curves. Actually, these curves provide directly the probability of exceeding a defined damage level as a function of an earthquake parameter indicator such as the peak ground acceleration PGA or a spectral displacement. Fragility curves are usually generated from a large number of structural response data. This information comes from different sources: field assessment results, experimental data, expert's opinion or analytical results (usually from nonlinear methods) [Agnanos *et al.*, 1995; Bonett, 2003]. Regardless of the source, these data are usually fitted under the assumption of the probability following a lognormal distribution, as shown in Figure 4.6.

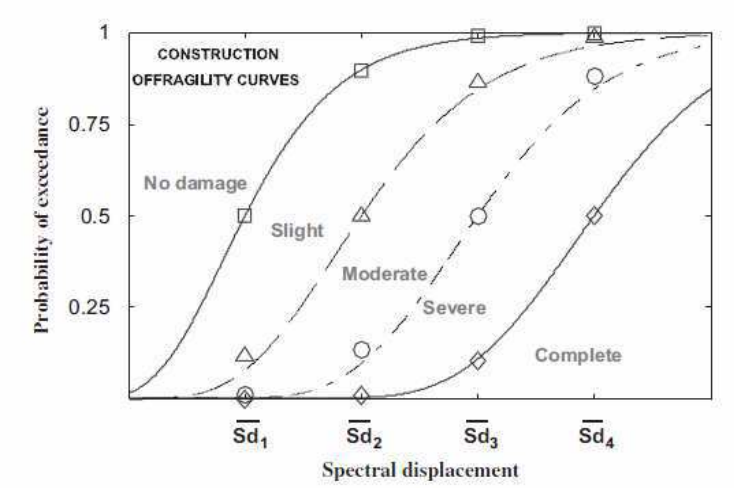

Figure 4.6 Example of a fragility curve [Barbat, *et al.*, 2008]

4.4. GLOBAL DAMAGE EVALUATION BY MEANS OF LOCAL DAMAGE OF COMPONENTS

With the exception of the methods based on modal properties variations, most procedures intended to estimate global damage suggest computing global indices as an average of local ones, the average criterion being the main difference between them. In general, the following expression is used to estimate the global damage D of a system consisting of N components with local damage indices D_i [Chai, 1999]:

$$D = \sum_{i}^{N} \lambda_i D_i; \quad \lambda_i = \frac{W_i}{\sum_{i}^{N} W_i} \tag{4.10}$$

Where: i represents each of the N elements composing the system (it may be an element in a storey –or in a building– or a storey in the whole building, depending on the study level); λ_i is the averaging factor and W_i stands for the value of the averaging criterion for the element i.

According to Ang [1988], a global indicator of damage must reflect the damage concentration in weak regions of the building, as well as its spatial distribution. Therefore, since damage distribution is known to be related to absorbed energy distribution, the total absorbed energy E_i at each storey is used as averaging criterion (W_i=E_i). Then, D_i is computed by the Park and Ang approach (see § 4.2.8).

Working also on the basis of total elastic strain energy, a global index is determined as a weighted average of energy-based local indices in a finite volume of a structure. In fact, it is a macroscopic extension of a proposed local (finite-element based) damage approach. Thus, since the term 'local' may represent a single finite element, the proposed index has the advantage of being suitable for application to an element, a section, or the entire structure [Hanganu *et al.*, 2002]. Within the same framework, Scotta *et al*. [2009] proposed a section index based on a fibre approach and a global index for RC structures. In both cases, this kind of proposals are particularly adapted to detailed studies within a finite element framework, where local indices are computed on the basis of deterioration at the material level.

From Bracci *et al*. [1989] a weighting factor should consider the consequences of significant damage in lower storeys on the structural collapse. Accordingly, W_i is defined as the tributary gravity load supported by each element. Such a scheme seems rational since it considers simultaneously that damage in lower storeys and in columns has a larger influence on global damage than that of higher storeys, for instance.

Relying also on gravity loads as averaging criterion, Jeong and Elnashai [2006] proposed a 3D global index computed as the weighted average of the damage indices of planar frames. In this case the weighting factor depends on the gravity load (w_i) carried by the influence area (A_{Ci}) of each frame of the 3D structure: $W_i = w_i A_{Ci}$; A_{Ci} is a function of damage itself since it accounts for the redistribution of load bearing capacities due to damage in local components, i.e. a frame in this case. Despite using a more rational weighting factor, this strategy is

indicated mainly for damage prediction as it may be difficult to apply when dealing with post-seismic evaluation, since the required information for obtaining the influence area is not usually available.

Amziane and Dubé [2008] stated that a component damage is mainly due to the deterioration developed in plastic hinges but it may also be affected by less damaged areas other than plastic hinges. Hence they propose both sources of damage to be considered. Thereby, global index D is computed as a simple average of local indices from all the damaged areas:

$$D = \frac{\sum_{i=1}^{m} D_i + \sum_{j} D_j}{m + \sum_{j} D_j} \tag{4.11}$$

Where: i represents the i-th element with a developing plastic hinge, j the j-th element with damage due to other source than plastic hinge development and m the number of critical sections where plastic hinging is present. It is noteworthy to point out that unlike precedent approaches, all the components have the same weight on global damage which may be an advantage concerning the simplicity for application purposes but it may also underestimate global damage when it is concentrated on key components of the load bearing system.

Recently, a proposal for a local damage index accounting for the shear or flexural failure of a reinforced concrete member has been presented by Mergos and Kappos [2010]. The damage of a component is supposed to be the result of the combined effect of flexural damage and shear damage; hence a combined relationship is taken as the base to develop the total damage D_{tot}:

$$D_{tot} = 1 - \left(1 - D_{fl}\right)^{\alpha} \cdot \left(1 - D_{sh}\right)^{\gamma} \tag{4.12}$$

D_{fl} and D_{sh} stand for the flexural and the shear damage indices respectively and α and γ are exponent factors representing the importance of flexural and shear damage index on the total local index. It is important to point out the fact that unlike the average-based approaches, the contribution of the components to the total damage is considered by some kind of importance factors. However they conclude that these factors must be both equal to 1 because of mathematical matters.

4.5. POST-SEISMIC EVALUATION OF DAMAGE

Strong earthquakes have significant consequences at several levels. Immediate effects are visible on the victims and the damage suffered by the infrastructure, long term consequences may include human displacement, indebtedness or even impoverishment depending on the localization of the affected region. Technical and economical measures need to be taken in the short term, aiming at the reduction of the earthquake's impact on the concerned environment and of course on the global situation of the affected zone or country. One of the important measures concerns the post-seismic evaluation of damage regarding the affected infrastructure. It is intended in the short term to produce habitability decisions (occupancy in regard to possible aftershocks or for permanent occupation) and for the global assessment of physical and economical losses with reconstruction purposes.

Methods for post-seismic evaluation of damage may be classified into rapid methods, aiming at taking in-place decisions about occupancy and identifying potentially dangerous conditions, and detailed methods, for further investigation on the serviceability state of the building. Most rapid methods use evaluation forms which must be filled by trained staff (engineers usually) on the basis of observed damages, apparent characteristics of the structure and pre-existent available information. An example of these forms is illustrated in APPENDIX B. Regularly, occupancy decisions are taken on the basis of global damage category or index, obtained from damage states based on visual inspection and visible damage signs (cracks, buckling, etc.). Of course the methodology varies according to the region or country of application. An example of these methods is the ATC-20 procedure [ATC, 1995], implemented in the United States and tested for the first time in its early version after the Loma Prieta earthquake. Now it has been improved and also implemented to be applied on PDA devices.

When rapid methods state the necessity of further evaluation, detailed methods are considered in order to make better evaluations of the earthquake effects and state about the need and/or possibility of repair or strengthening. Therefore, these methods rely on evaluations of the damage effects on the mechanical properties of the building, as it is the case for the performance-based damage evaluation procedures of FEMA 306 guidelines [ATC, 1998a], which have already been discussed (see §4.3.2).

4.5.1. A probability-based approach

An integrated methodology within a probabilistic framework was proposed to estimate global damage of buildings [Mebarki and Laribi, 2008]. Since it is intended for application in post-earthquake seismic evaluation, overall damage index is computed from observed damage in structural as well as non structural components. The results were compared with a database of experimental field evaluations corresponding to the 2003 Bourmedes Earthquake (Mw=6.8, Algeria) finding a good accordance. The methodology has three main ordered stages: The estimation of the residual probability of failure for each component (structural and non-structural), the estimation of the overall probability of failure and the determination of the global damage index.

First stage requires the previous classic qualitative evaluation, where a damage category D_c is assigned to each component on the basis of observed signs of damage. Next, for estimating the residual probability of failure P_f for each component, a relationship between D_c and P_f is required. This relationship relies on the assumption of a correspondence between P_f and D_c, expressed as [Mebarki, 2006]:

$$P_f = \begin{cases} 0: no\ damage \\ 1: complete\ damage \end{cases} \quad \text{since} \quad \begin{cases} D_c(1): no\ damage \\ D_c(N_D): complete\ damage \end{cases} \tag{4.13}$$

This way, by means of a postulated relationship *f(.)* between these two parameters, $P_f = f(D_c)$, the qualitative damage expressed by the categories D_c is transformed into residual probability of failure, making thus possible the establishment of a quantitative parameter. Among the six tested relationships, two have been found to produce inaccurate results, a linear and an N-power relationship.

The second stage requires a relationship expressing global probability of failure as a function of elemental probabilities of failure. Under the assumption of the failure events being statistically independent, global failure is supposed to occur when either the structural or the non structural failure occurs. This relation is then expressed as [Mebarki *et al.*, Pending]:

$$P_f = 1-(1-P_s)(1-P_{ns}) \tag{4.14}$$

P stands for probability of failure and the indices *s* and *ns* represents the structural and non-structural components. For structural failure probability two probabilistic combinations (representing two likely failure mechanisms) were postulated and tested. The better

combination was the one based on the assumption of structural failure happens when either foundation or vertical bearing components or horizontal components fails.

Finally, third stage computes the global damage on the basis of the global probability of failure already obtained, by means of the inverse of the relation obtained at the first stage:

$$D_g = f^{-1}(P_f) \tag{4.15}$$

This approach has the advantage of transforming, in a simple way, qualitative measures of damage into a quantitative index. It may be implemented in the post-earthquake assessment process to be a support of the tagging tasks when performing forensic evaluations.

4.6. SUMMARY AND CONCLUSION

The fundamentals of damage representation and damage evaluation have been briefly revised. Nowadays, it can be said that the phenomenon itself is adequately understood. Numerous attempts for finding objective, accurate measures of damage as well as evaluation methods have been developed. Damage may be studied from very different approaches depending on the evaluation level. Thereby, for prediction purposes detailed analyses based on finite element method are used in order to generate fragility curves, as functions of the expected seismic hazard, for example. For post-earthquake assessment, the first step consists, usually, in assessing the damage category which classifies the damaged structure on the basis of observed damage, in order to decide whether the building should be evacuated until it is repaired or demolished, for instance.

When further evaluation is required, detailed methods, such as performance based techniques, need to be used. In any case, detailed procedures always require reliable mechanical models, which are able to represent the main causes of damage: large inelastic deformations dissipating seismic energy, leading sometimes to the fatigue of materials. Also, treatment is different whether it is about local damage or global damage. Most proposals rely on averaging local damage measures in order to find global indices.

As pointed out in this chapter, a unique and reliable damage measure is still lacking despite the numerous available proposals. Some measures have the disadvantage of being subjective; others require detailed information that is not always available for rapid assessment programs. With the aim of improving the rapid post-seismic assessment

procedures, a strategy for global damage evaluation is developed and presented in the next chapter.

CHAPTER 5
GLOBAL DAMAGE INDICES: A PROBABILITY – BASED APPROACH

5.1. INTRODUCTION

Generally, post-seismic evaluation of structures is intended to take the decision of whether a building should remain in use or be evacuated. Furthermore, it aims to determine whether a repair action –rehabilitation or strengthening– is required or a demolition is compulsory. In any case, the decision must be taken in the short term, a few hours or days after the quake occurrence. Therefore, a reliable but readily global damage measure and a clear criterion of selection are necessary to undertake such actions.

Thus, this chapter aims to propose a strategy for post-seismic evaluation of structural damage. It is intended to be a step forward on the implementation of a decision-making tool which permits to do objective and accurate assessments of global structural damage based on damage of components. Thereby, global damage is related to local damage at a storey- and at a component-level, by means of a postulated relationship between the post-quake damage and the residual probability of failure against any future scenario of loading. Three factors are proposed to reflect the weight of component damage at the two mentioned levels. The efficiency and accuracy of the proposed method is evaluated by running this approach in the case of four reinforced concrete frames. The obtained results are discussed and compared with a mechanical approach and also with the damage results calculated by some dynamic analyses.

5.2. RESIDUAL PROBABILITY OF FAILURE

The strategy proposed in this study is motivated partly by the integrated methodology presented by Mebarki and Laribi [2008], since it is also based on a relationship between residual probability of failure and damage. In its first version it is applicable only to structural components. In the present chapter, the combinations of the building components are treated

differently. Actually, it is limited to frame buildings which are considered first as arrangements of storeys, which are in turn composed of beams and columns. Thus, all along the following sections two levels of study will be referenced: the storey level, depending on beams and columns, and the building level, depending on storeys.

5.2.1. Probability of failure: at storey level

First of all, an expression for the probability of failure of a system, as a function of the probabilities of failure of its components is required. Thus, let E_i be the event "failure of the i-*th* component or system" and P_i be the probability of that event occurrence. An expression for the probability of failure of a storey requires a detailed inelastic study on the possible failure mechanisms. The two classic probabilistic combinations, series and parallel, might both be unrealistic. The series combination implies that the storey fails when any of the components fails. It is then too conservative and it does not consider that vertical components may have more effect on the storey behaviour, for instance. The parallel combination, involves the necessity of all the components failing to cause the system's failure. It is hence non-conservative as the storey would have failed before the whole components reach their failure.

Nevertheless, for the purposes of this study the conservative approach will be used, so that each storey of the building is considered as a series system of beams and columns (see Figure 5.1), which means that failure occur whenever a beam or a column fails.

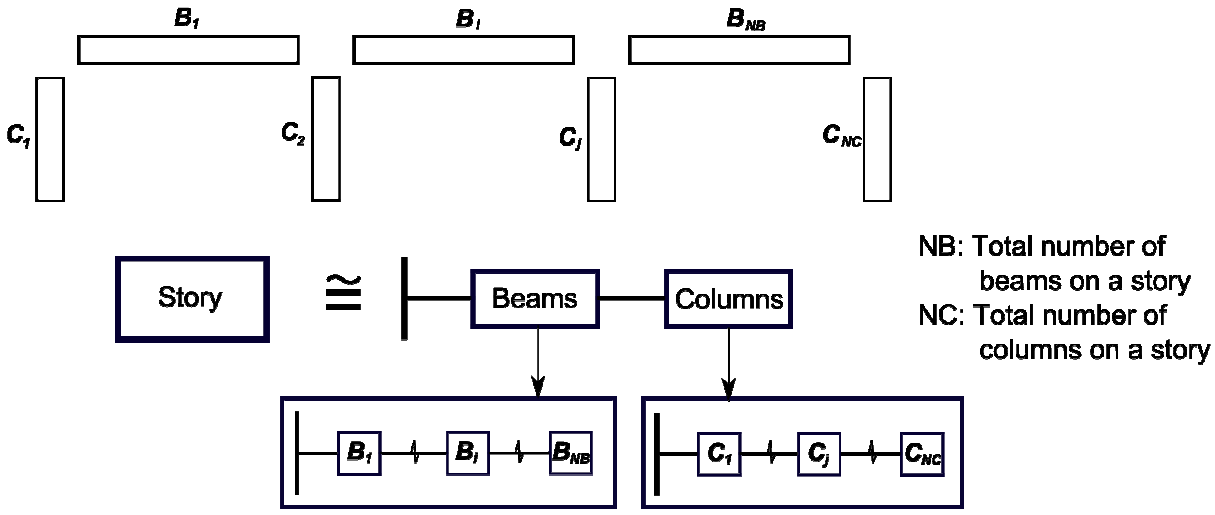

Figure 5.1 Storey series system of NB beams and NC columns

Thus the failure of a storey *k* may be expressed in terms of the events of failure at each general component:

$$E_k = E_b \cup \mathrm{E_c} \tag{5.1}$$

Indices *b* and *c* stand for beams and columns. Expressing the complementary event, which means the event "no failure in the storey *k*", it is found that:

$$\bar{E}_k = \bar{E}_b \cap \bar{\mathrm{E}}_c \tag{5.2}$$

In the former relationship E_c represents the failure of the columns in the storey, so E_c and its complementary event $\bar{E}_c$, are given by the following expressions in terms of each column in the storey:

$$E_c = E_{c,1} \cup E_{c,2} \cup ... E_{c,i} \cup ... \cup E_{c,Nc} \tag{5.3}$$

$$\bar{E}_c = \bar{E}_{c,1} \cap \bar{E}_{c,2} \cap ... \bar{E}_{c,i} \cap ... \cap \bar{E}_{c,Nc} \tag{5.4}$$

The index N_c represents the total number of columns in a storey. Now under the assumption that events are statistically independent, the relationship between the probabilities of occurrence of these events may be expressed as:

$$P(\bar{E}_c) = P(\bar{E}_{c,1}) \times P(\bar{E}_{c,2}) \times ... P(\bar{E}_{c,i}) \times ... \times P(\bar{E}_{c,Nc}) \tag{5.5}$$

Now, taking *P(E$_c$)* simply as P_c and considering that $P(E_c) + P(\bar{E}_c) = 1$, the following relationship is obtained for the probability of failure of columns:

$$(1 - P_c) = (1 - P_{c,1}) \times (1 - P_{c,2}) \times ... (1 - P_{c,i}) \times ... \times (1 - P_{c,Nc}) \tag{5.6}$$

$$(1 - P_c) = \prod_{i=1}^{Nc} (1 - P_{c,i}) \tag{5.7}$$

Likewise, for the N_b beam elements in a storey:

$$(1 - P_b) = \prod_{j=1}^{Nb} (1 - P_{b,j}) \tag{5.8}$$

Thus, under the same assumption of independence, Equation (5.2) leads to:

$$(1-P_k)=(1-P_c)\times(1-P_b) \tag{5.9}$$

Consequently the probability of failure of a storey may be computed as:

$$P_k=1-\left\{\prod_{i=1}^{Nb}(1-P_{b,i})\right\}\times\left\{\prod_{j=1}^{Nc}(1-P_{c,j})\right\} \tag{5.10}$$

5.2.2. Probability of failure: at the whole building level

When dealing with the global damage index of the whole building, an expression for the global probability of failure may also be found under the same assumption of having a series system of storeys (floors). Thus, the event failure of the system E_G is assumed to occur when any of the *NS* storeys fails, so:

$$E_G=E_1\cup E_2\cup\ldots E_k\cup\ldots\cup E_{NS} \tag{5.11}$$

Thus the event of not having a global failure may be expressed as:

$$\overline{E}_G=\overline{E}_1\cap\overline{E}_2\cap\ldots\overline{E}_k\cap\ldots\cap\overline{E}_{NS} \tag{5.12}$$

And the relationship between the probabilities of failure, under the hypothesis of probabilistic independence, is:

$$(1-P_G)=(1-P_1)\times(1-P_2)\times\ldots(1-P_k)\times\ldots\times(1-P_{NS}) \tag{5.13}$$

Subsequently, the probability of failure P_G of the whole system may be expressed as:

$$P_G=1-\prod_{k=1}^{NS}(1-P_k) \tag{5.14}$$

A very simple relation between global and local probabilities of failure has been established by means of consideration of a series system of storeys and of beams and columns at the two concerned levels. The series probabilistic combination of events is certainly not quite close of the real behaviour of a building. It has been adopted because of its simplicity of application, since there is a lack of detailed studies about failure mechanisms at a storey level. However, when relating residual probability of failure with damage, the established relationship in conjunction with the importance factors proposed in the following sections, give this proposal a theoretical basis more adapted to reality.

5.3. PROPOSAL OF A PROBABILITY-BASED STRATEGY FOR ESTIMATING GLOBAL DAMAGE INDICES

5.3.1. Relationship between damage and residual probability

Since damage always cause a degradation which may eventually lead to a failure, it is clear that there must exist a direct relationship between damage and probability of failure. A recent work proposed four possible relationships calibrated with forensic results of damage assessment [Mebarki and Laribi, 2008; Mebarki, *et al.*, Pending]. These mathematical functions stated a direct relation between residual probability of failure and damage, regardless of the nature of the component or the system being evaluated. Accordingly, a new direct relationship between P_n and D_n is assumed here [Mebarki *et al.*, 2010]. It depends on a factor α_n, intended to account for the significance of the component on the global system behaviour.

$$(1-P_n)=(1-D_n)^{\alpha_n} \tag{5.15}$$

$$P_n=1-(1-D_n)^{\alpha_n} \tag{5.16}$$

Here, P_n is the probability of failure of the n*th* element, D_n the damage index of the same element and α_n the importance factor, whose calculation is developed below. Figure 5.2 shows the variation of influence of the importance factor on the failure probability for given values of damage.

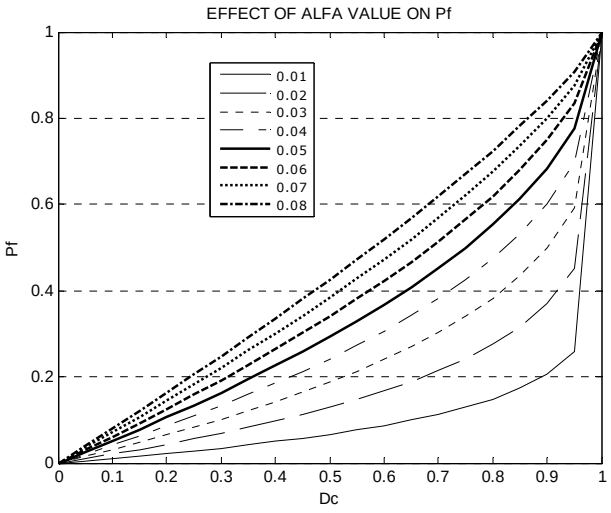

Figure 5.2 Effect of α value on the probability of failure

It may be observed that this Equation fulfils the correspondence between probability of failure and damage, already expressed in Equation (4.13). When there is no damage, the probability of failure is equal to zero and when the damage is considered as complete (D_n =1), P_n is equal to 1, regardless of the α_n value. Of course, close to the limit value of D_n =1, the behaviour is not so consistent since P_n goes abruptly from low values of 0.25 up to 1, for α_n =0.01.

5.3.2. Global damage index at a storey-level and at a building-level

Once the relationship between probability of failure and damage adopted, the damage of a storey may be estimated from the damage of the components –beams and columns–, by replacing Equation (5.15) into Equation (5.10):

$$D_k = 1 - \left\{ \prod_{i=1}^{Nb} (1 - D_{b,i})^{\alpha_{b,i}} \right\} \times \left\{ \prod_{j=1}^{Nc} (1 - D_{c,j})^{\alpha_{c,j}} \right\} \tag{5.17}$$

Subsequently, according to Equation (5.15) and defining the index β_k as the indicator of the importance of each storey *k* on the global behaviour of the building, the global damage index D_G is obtained as:

$$D_G = 1 - \prod_{k=1}^{NS} (1 - D_k)^{\beta_k} \tag{5.18}$$

These expressions (Equations (5.17) and (5.18)) are intended to compute the damage index D_k at each storey and the global damage index D_G as a function of the local damage at each component (beams and columns in this case) according to the assumption of uniform damage on each element. Three indices have been proposed: α_b and α_c for reflecting the significance of beams and columns and β_k for considering the influence of each storey on the whole behaviour. Therefore, it is also required to develop and calibrate the values and expressions of the fitting parameters or importance factors.

5.4. IMPORTANCE FACTORS

5.4.1. Damage assessment at the storey-level: α_b and α_c factors

As for any structural system, the seismic behaviour of a storey depends intimately on the

strength, stiffness and ductility of each component. The proposed factors should provide a measure of the importance of beams and columns on the overall behaviour of the storey. Thus, the effect of each of these elements needs to be separated in some way. This is a difficult task since their properties are usually interdependent. However, since damage may have a significant effect on lateral stiffness, for this strategy, the influence of each element class (i.e. beam, column) on the lateral stiffness of the storey is considered as indicator of the effect of the components local damage on the storey overall damage. Therefore, a relationship between the lateral stiffness of a storey and the relative stiffness of its components is required.

For the simplest case, a one-storey, one-bay frame with rigid supports, it is possible to derive, in the elastic range of behaviour, the following expression by neglecting the axial and shear deformations of elements:

$$K_L = \frac{24E}{L_c^2}\left[\frac{\rho_c^3 + 6.5\rho_b\rho_c^2 + 3\rho_b^2\rho_c}{4\rho_c^2 + 8\rho_b\rho_c + 3\rho_b^2}\right] \tag{5.19}$$

The terms $\rho_c = I_c/L_c$ and $\rho_b = I_b/L_b$ represent the relative stiffness of beams and columns, computed as the ratio between the second moment of area of the cross section, I and the element length L. As expected, from Equation (5.19) it is observed that getting an explicit, separate expression for the effect of beams and columns is a hard task, even in the simplest case, since beams and columns do interact. However, a relative influence of these components may be estimated considering that the lateral stiffness of a storey reaches its maximum value when beams are stiff enough to act as a fixed end of columns [Chopra, 2007]. Then the maximum lateral stiffness $K_{L,k}^{\max}$ of a storey is computed as:

$$K_{L,k}^{\max} = \frac{12E}{L_c^{\,3}}\left(\sum_{j=1}^{NC} I_{c,j}\right) \tag{5.20}$$

Where L_c is the storey height (the column's length) and $I_{c,j}$ represents the second moment of area of each column j cross section. According to Equation (5.20), lateral stiffness does not depend on the beam's length, as already stated by Chopra [2007]. For this case, one may say that columns have their maximum contribution, hence the maximum importance. On the opposite side, when stiffness of beams is almost negligible, so that there is no any restriction to lateral displacements, the minimum lateral stiffness value tends to:

$$K_{L,k}^{\min} = \frac{3E}{L_c^{\,3}}\left(\sum_{j=1}^{NC} I_{c,j}\right) \tag{5.21}$$

For the latter case, lateral stiffness value also depends only on columns stiffness. But, columns contribution is the smallest possible so that the associated importance must be the minimum. Now, since the current lateral stiffness K_L for a given configuration ranges between these two bounds, smaller than $K_{L,k}^{\max}$, the ratio between the real and the maximum stiffness may provide an estimate of the influence of columns on lateral stiffness, i.e. the α_c factor:

$$\alpha_c = \frac{K_L}{K_{L,k}^{\max}} \tag{5.22}$$

Of course this is a first approximation since the computation of the "real" influence is really more complex, and depends on all the connected elements to the columns under study. Thereby, as the summation of the importance factors for all the considered components must be equal to 1 regardless of the chosen property, the influence factor of beams is:

$$\alpha_b = 1 - \alpha_c \tag{5.23}$$

Defining the relationship between the second moments of area as $\rho = I_b/I_c$, it is observed from Figure 5.3a that α_c factor rises with increasing ρ, ranging between 0.25 and 1, when ρ_b goes from quite small (~ 0) up to large values (~∞) with respect to a fixed value of ρ_c, as stated by Chopra [2007] for a one storey frame. However, these factors are usually far from their bounds since current values of ρ are smaller as shown in Figure 5.3b:

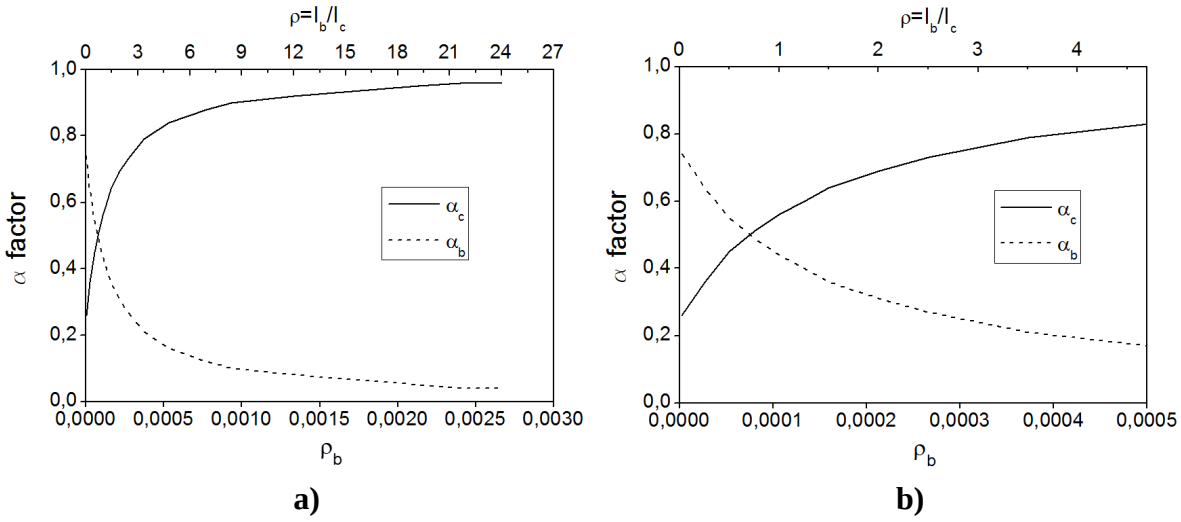

Figure 5.3 Effect of ρ_b and ρ on the α factors. a) Complete graph, b) Current values

Getting an explicit expression for lateral stiffness, as that of Equation (5.19), is not feasible for taller frames. Thereby, simplified expressions for K_L are required in order to compute the α_c factor. Several simplified relationships may be used to estimate the lateral stiffness of each storey as a function of the mechanical and geometrical properties of its components. In this case a version of the Wilbur's formulae has been used [Norris *et al.*, 1991; Bazán and Meli, 2002]. They depend on the storey being evaluated, thus for the first storey[4]:

$$R_1 = \frac{48E}{D_1 h_1} \quad D_1 = \frac{4h_1}{\sum K_{c1}} + \frac{h_1 + h_2}{\sum K_{t1} + \sum K_{c1}/12} \tag{5.24}$$

For the second storey:

$$R_2 = \frac{48E}{D_2 h_2} \quad D_2 = \frac{4h_2}{\sum K_{c2}} + \frac{h_1 + h_2}{\sum K_{t1} + \sum K_{c1}/12} + \frac{h_2 + h_3}{\sum K_{t2}} \tag{5.25}$$

And for intermediate storeys:

$$R_n = \frac{48E}{D_n h_n} \quad D_n = \frac{4h_n}{\sum K_{cn}} + \frac{h_m + h_n}{\sum K_{tm}} + \frac{h_n + h_o}{\sum K_{tn}} \tag{5.26}$$

Where: R_n is the lateral stiffness of the nth floor; E the Young modulus; K_{tn} and K_{cn} represent the relation I/L (Ratio between the second moment of area of the cross section and the element's length) for beams and columns respectively in the nth storey; m, n and o are three consecutive levels and h_n represents the storey height. When dealing with the last level h_m must be replaced by $2h_m$ and h_o by 0.

The assumptions underlying the development of these expressions are: i) they are valid on regular frames composed of constant inertia elements, ii) the axial deformations of the elements are neglected, iii) the columns develop points of inflection and iv) the rotation of each point as well as the shear force on the studied level and the two adjacent levels have the same value. Of course these assumptions, particularly the fourth one, are hardly true in most cases. Nevertheless, since only an estimate of the influence of elements on the lateral stiffness is required, their use is assumed as being suitable in this case.

[4] The notation used in Bazán and Meli [2002] for these formulae has been retained here.

5.4.2. Damage assessment at the building level: β factor

Concerning the influence of the storey damage on the global damage, a factor β is proposed. It is proportional to the gravitational load carried by each storey. As it is already stated in other works using averaging factors based on gravity loads carried by elements [J.M.Bracci, *et al.*, 1989; Jeong and Elnashai, 2006], such an index has the advantage of reflecting the risk and the consequences of collapse of elements on lower storeys. Defining W_k as the gravitational load carried by the storey being studied, that index is computed as:

$$\beta_k = \frac{W_k}{\sum_{k=1}^{NS} W_k}, \quad \sum \beta_k = 1 \tag{5.27}$$

As a result, all the parameters for computing the damage at each storey of the building as well as the global damage, by means of Equations (5.17) and (5.18) are defined. The factors α_b^i and α_c^i are computed by dividing the α_b and a_c factors by *NB* and *NC* respectively. This approach for the global damage index fulfils the following requirements:

- It ranges from 0 when no damage is present on any component up to 1 for complete damage.
- It considers the relative influence of each element over the whole damage index.
- It considers the importance of the capacity to carry gravity loads through the β factor, providing more participating weight to the lower storeys given its influence on the gravity load bearing system.

5.5. PROCEDURE

A basic procedure is proposed:

5.5.1. Initial steps

1. Collect the data of local damage at each element of each storey.
2. Obtain the mechanical and geometrical properties of the components: Young modulus *E*, cross section dimensions *b* and *h* and elements length *L*.
3. Estimate the gravity loads carried by each storey, W_k

5.5.2. α_b and α_c factors

4. Estimate the actual lateral stiffness of each storey by means of Equations (5.24) to (5.26), according to the storey being evaluated.
5. Compute the theoretical maximum lateral stiffness of each storey from Equation (5.20).
6. Compute the importance factors α_c and α_b by means of Equations (5.22) and (5.23).
7. According to the number of beams NB and columns NC, compute the individual factors $\alpha_{b,i}$ and $\alpha_{c,j}$.

5.5.3. β factor

8. From the information obtained on step 3, compute the β factor with Equation (5.27).

5.5.4. Storey damage and global damage

9. Estimate the damage at each storey by means of Equation (5.17), from the information of local damage obtained at step 1 and the $\alpha_{b,i}$ and $\alpha_{c,j}$ factors obtained at step 7.
10. Finally, compute the global damage with Equation (5.18), from the storey damage D_k and the β factor from step 8.

5.6. MECHANICAL APPROACH FOR VALIDATION

In order to verify the accuracy of the proposed probability-based approach, a mechanical approach will be used as the reference method. Thus, this study proposes to evaluate global damage from the change in the stiffness of the first-mode capacity spectrum obtained from a pushover analysis. Given the definition of the n*th*-mode capacity spectrum's components, the elastic stiffness of this curve coincides with the eigenvalue associated to the n*th*-mode, i.e. the square of the n*th* vibration frequency. Nielsen *et al*. [1992] have performed an extensive work for validating the use of such an approach: using the one dimensional maximum softening

damage indicator, which is in fact the time variation in the fundamental period of the building due to the structural damage. This indicator is reported to give an adequate measure of average damage of the structure.

5.6.1. Global damage index

The overall procedure applied in this work is illustrated in Figure 5.4. It consists in 3 stages. Firstly, it is required to perform a first-mode pushover analysis of the undamaged building, i.e. on a model which elements have been modelled with their original initial stiffness. Secondly, one should develop the "damaged building" pushover curve, by setting local damage indices (D_b and D_c for beams and columns) on the mechanical model of the building. Thereby, the behaviour of each element is affected by the damage index through the modification of its moment-curvature relationship, as explained later. Of course, local damage indices are supposed to be known. Finally, comparing both capacity curves the global damage index, D_G, may be obtained from an expression already stated (see §4.3.1.4), where K_d and K_0 represents the initial stiffness of the damaged and undamaged capacity spectra respectively.

$$D_G = 1 - \frac{K_d}{K_0} \tag{5.28}$$

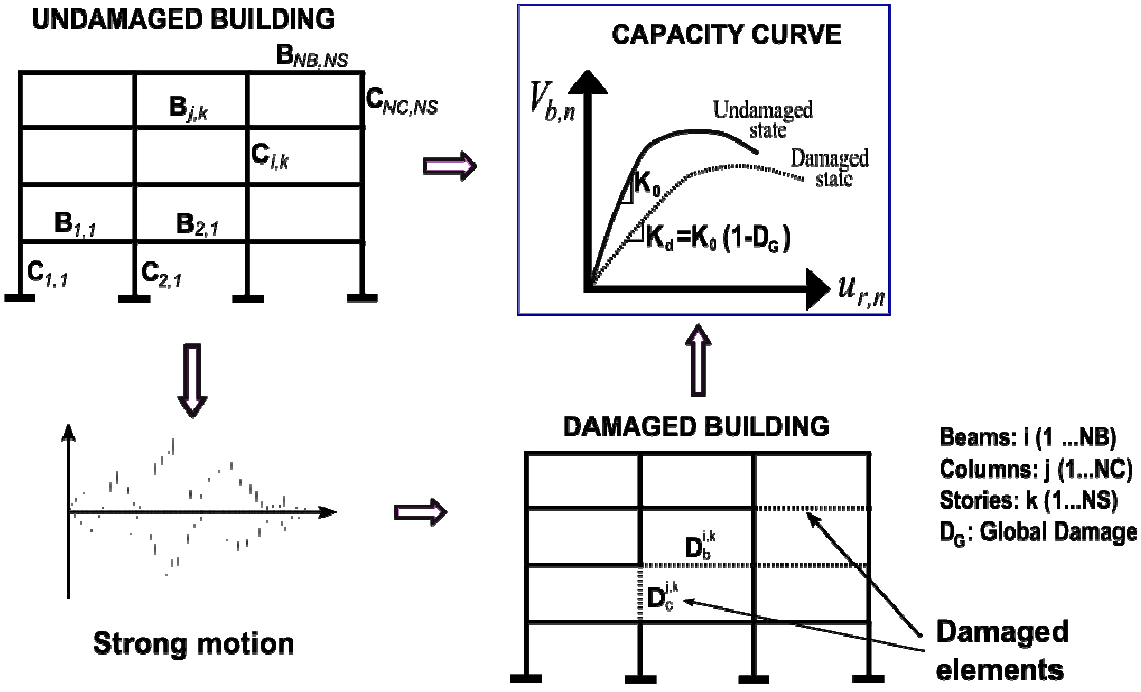

Figure 5.4 Evaluation of global damage through the changes in the capacity curve stiffness

5.6.2. Local damage indices

Concerning the building's model, the nonlinear behaviour of elements is modelled through a distributed plasticity model (for more details see §2.4.1 Modelling of nonlinear behaviour of components). The damage is modelled in the simplest way. It is considered as isotropic and set as a scalar internal variable D [Besson, *et al.*, 2001], so that the relationship between moment and curvature in the elastic domain may be written as:

$$M = K_0(1-D)\phi \tag{5.29}$$

Where: M represents the bending moment, K_0 the elastic stiffness of the element and ϕ the curvature of the section. The moment-curvature relationship is approximated by a bilinear curve, hence described by an elastic-plastic model with strain hardening. This proposal considers that there is only coupling between elasticity and damage and no coupling between damage and strain hardening [Besson, *et al.*, 2001]. Figure 5.5 displays the general behaviour obtained when working under these assumptions.

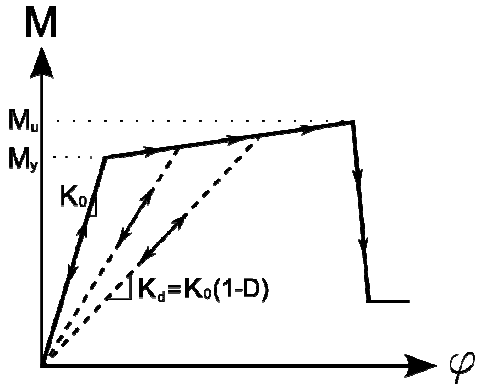

Figure 5.5 Nonlinear degrading model used to simulate damage on beams and columns

5.7. APPLICATION EXAMPLE

For illustration purposes, the complete procedure will be performed on a 4-storey gravity-load designed frame (GLD). It is a real, full-scale frame which was experimentally tested under seismic loads in the European Laboratory for Structural Assessment (ELSA) [Pinto, *et al.*, 2002]. This building has been already presented and analyzed in the precedent chapters in Part I; its elevation view (Figure 2.8) is repeated here for convenience in Figure 5.6:

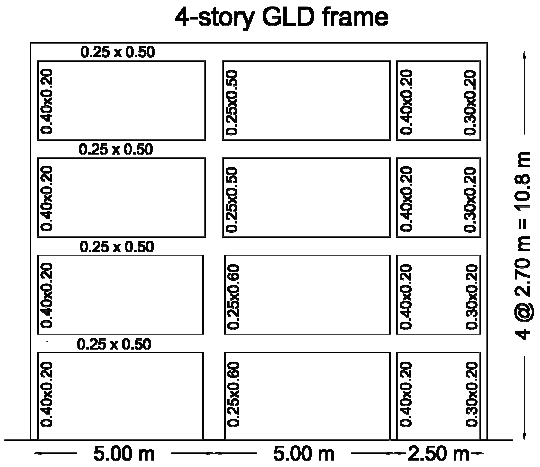

Figure 5.6 Elevation view of the 4-storey GLD frame (Repetition of Figure 2.8)

This strategy requires the knowledge of local damage indices of each component. Therefore, for this example, a specific pattern of damage is supposed to be known, see Figure 5.7.

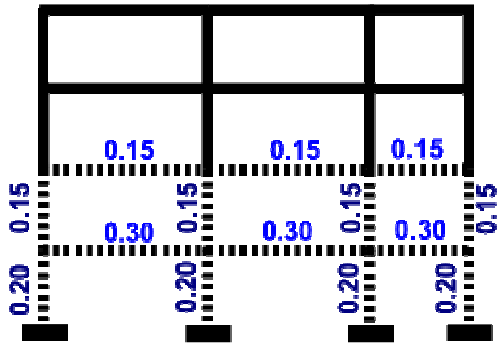

Figure 5.7 Assigned damage pattern for the 4-storey GLD frame

It consists in concentrating the damage in the first and second storeys: arbitrary values of damage of 30% to beams and 20% to columns at the first storey, and 15% to all elements of the second storey were assigned, see the first part of Table 5-3. Next from the geometrical and mechanical properties of the building (For beams and columns: E=27500000 kN/m^2) the current and the maximum lateral stiffness of each storey may be computed by means of Wilbur's expressions (Equations (5.24) to (5.26)), see Table 5-1. Subsequently the factors α_b and α_c are obtained by the Equations (5.20) to (5.23):

K_L (kN/m)	K_L^{max} (kN)	α_c	α_b
61 284	87 741	0,70	0,30
46 255	87 741	0,53	0,47
35 119	55 956	0,63	0,37
35 119	55 956	0,63	0,37

Table 5-1 Lateral stiffness (estimated and maximum) and α_b and α_c factors

Table 5-2 shows the gravity loads supported by each storey, W_i, computed from the cumulated gravity loads of each storey, w_i. Then the β factor is obtained.

w_i (kN)	W_i (kN)	β
255	974	0,41
254	719	0,30
253	465	0,20
211	211	0,09
974	**2370**	**1,00**

Table 5-2 Gravity loads at each storey and computation of β factor

Once the importance factors obtained, the storey damage D_k and the global damage D_G may be obtained, see the two last columns of Table 5-3.

Event	Damage												
	Story	Beam			Col				Factors				
		1	2	3	1	2	3	4	$\alpha_{b,i}$	$\alpha_{c,j}$	β_k	D_k	D_G
1	1	0,3	0,3	0,3	0,2	0,2	0,2	0,2	0,10	0,17	0,41	0,23	**0,146**
	2	0,15	0,15	0,15	0,15	0,15	0,15	0,15	0,16	0,13	0,30	0,15	
	3								0,12	0,16	0,20	0,00	
	4								0,12	0,16	0,09	0,00	

Table 5-3 Damage pattern and global damage estimation of the 4-storey GLD frame

The global damage estimated by the probability-based approach is then compared with that obtained by the "analytical method". The local damage index is implemented for each element following the degradation model of Figure 5.5. Subsequently, a pushover analysis is performed to obtain the capacity spectra for the undamaged and the damaged frame, see Figure 5.8.

Finally, the average damage is computed as a function of the elastic stiffness of these two

curves, by means of Equation (5.28):

$$D_G = 1 - \frac{K_d}{K_o} = 1 - \frac{53.2}{62.4} = 0.148 \tag{5.30}$$

A quite small difference is found for this particular case, of about 1.4%. General results in the following section aim to illustrate the efficiency of the proposed strategy for different arbitrarily chosen damage patterns, on different frame buildings.

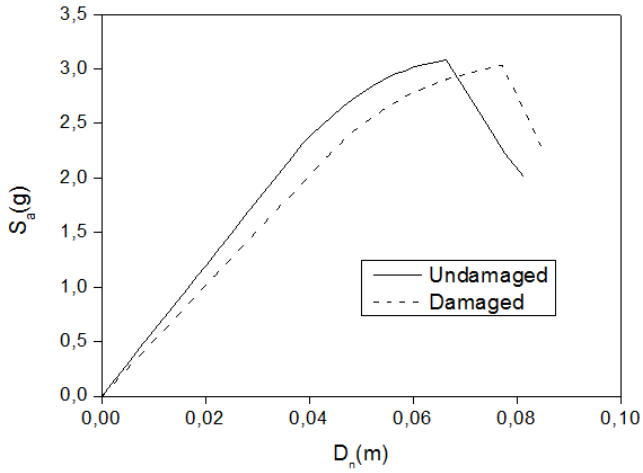

Figure 5.8 Capacity spectra of the damaged and undamaged model, for the 4-storey GLD frame

5.8. VALIDATION MODELS

For validation purposes three buildings (apart from the 4-storey GLD frame studied in the precedent section) have been tested under different patterns and distribution of local damage. They were already presented in section 3.2 but some of their features are repeated here for convenience. They are: a 4- and a 6-storey buildings designed for seismic loads typical of high seismic risk areas; and a 8-storey frame adapted from a study about seismic collapse safety in modern RC buildings [Haselton and Deierlein, 2007]. An elevation view of the three seismic designed frames is displayed in Figure 5.9. More detailed information about these models may be found in APPENDIX A.

The numerical models were simulated using OPENSEES platform [Mazzoni, *et al.*, 2007], under the same conditions as the precedent chapters: P-delta effects were considered; soil-structure interaction was not taken into account; hence the supports were modelled as

infinitely rigid. The nonlinear behaviour of elements was modelled through an available distributed plasticity model, the *nonlinear beamColumn* element. The moment-curvature relationships were obtained from a fibre element analysis over each element. They were then approximated as bilinear curves and modelled by an available *hysteretic* model.

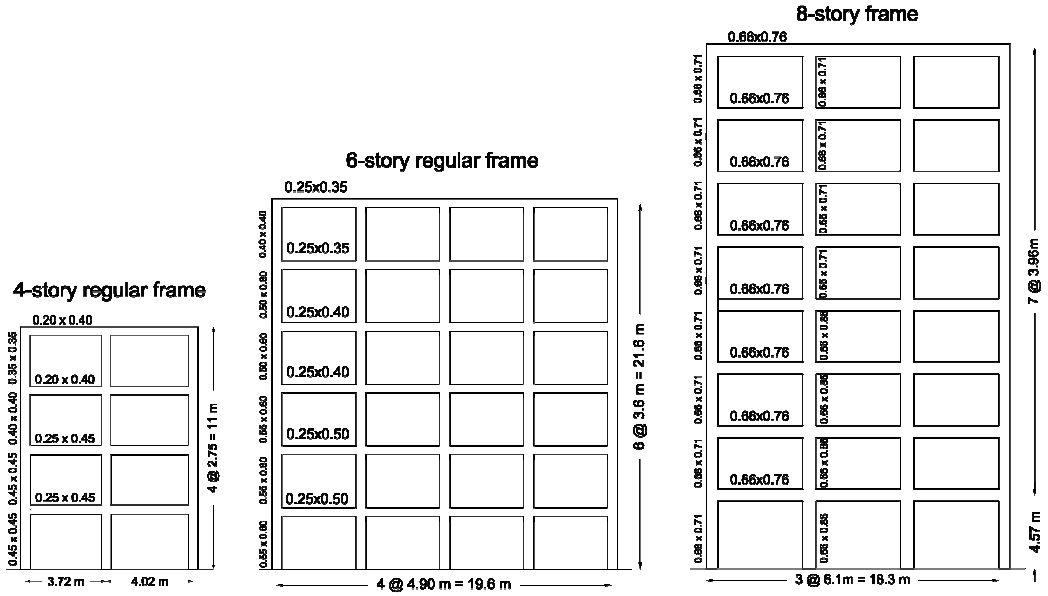

Figure 5.9 Elevation view of the four studied frames

5.9. IMPORTANCE FACTORS

Several analyses have been performed for evaluating the suitability and efficiency of α and β factors in the global damage estimation. Two levels of components damage have been studied: a low – medium level (LM), supposed to range between 0.10 and 0.40 and a medium-high level ranging between 0.4 and 0.8. Of course, damage levels of 0.8 are quite high so that in real situations they might be considered as complete damage. However, they have been used, herein, for evaluation purposes. Several patterns of damage have been investigated in order to have a significant insight on the accuracy and limits of the proposed approach. The most important results are presented in the followings sections.

5.9.1. Efficiency of β factor

For evaluating the β factor, which reflects the effect of damage at each storey on the global damage, uniform, concentrated damage patterns have been assigned separately to each storey (see Figure 5.10). Beams and columns have been assigned with equal levels of damage

for having only the effect of β factor: values of 30%, i.e. $D_c=D_b=0.30$ for low-medium level (LM) and $D_c=D_b=0.60$ for medium-high level (MH) of damage.

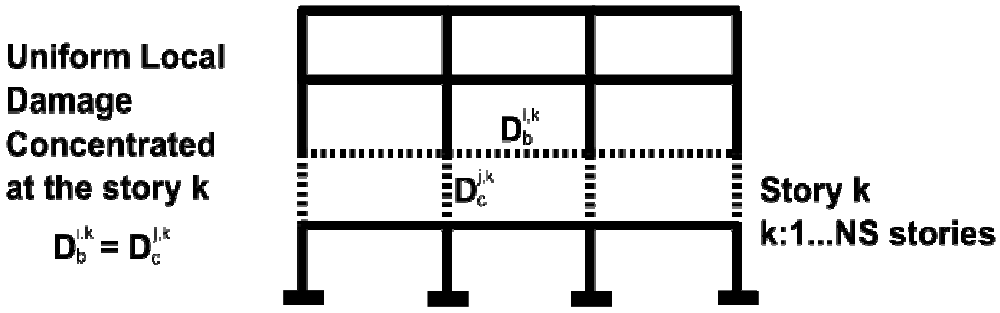

Figure 5.10 Overview of the damage distribution for studying the efficiency of b factor

Figure 5.11a shows the results for the 4-storey frame. Every single point on each graph represents an analysis, i.e. the calculated (D_{CALC} –by the mechanical approach) or the estimated (D_{EST} –by the proposed method) global damage when damage is concentrated at a given storey. This is illustrated by the upper graphics in Figure 5.11, where 60% of damage concentrated at the 3rd storey causes a global damage of 21%, obtained from the mechanical approach.

For low-medium level of damage, there is a good accordance with analytical results while for medium-high level it is observed that accuracy decreases as damage level increases. However, these results are acceptable, considering that damage is concentrated only in one storey, which may not be a common configuration in a real situation. In fact, as it is observed afterwards, better results are found when damage pattern is more uniform.

Moreover, when using global damage values to classify structures according to damage categories (e.g. slight, moderate, severe, complete damage), the associated damage ranges of those categories are normally wide enough, e.g. slight damage is considered when global damage value ranges between 0.0 up to 0.10. Therefore, considering the differences between calculated and estimated damage (ΔD_{GLOBAL}), one could observe that for most cases they do not exceed one category of damage, defining here a category as a range of 0.05 of damage value. These results are shown in Figure 5.11b, where all but two cases are in the first category, between 0 and 0.05 of damage value. It means that errors generated by using the probabilistic approach would not even produce a change of damage category.

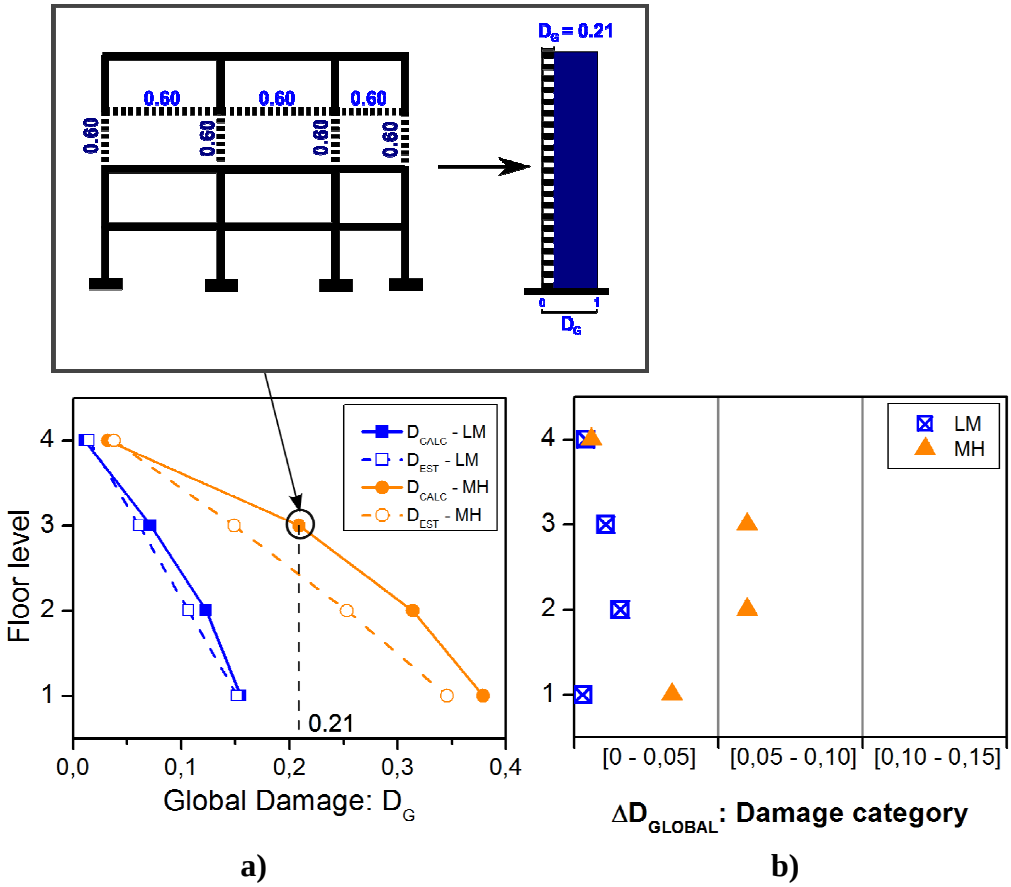

Figure 5.11 a) Calculated and estimated global damage for the 4-storey frame, b) Classification of ΔD_{GLOBAL} according to the damage category

The results of the same analyses for the 6- and the 8-storey frames are displayed in Figure 5.12 and Figure 5.13 respectively. According to these results, the tendencies observed from the 4-storey frame are confirmed in most cases: Errors usually increase with the damage level but they are in general low enough for staying in the first defined category (ΔD values between 0 and 0.05). As the effect of β factor is isolated from the other factors, its influence is evident in the results for the three buildings: global damage decreases as the damaged storey localization goes up. For MH damage level, the decreasing slope is higher than that of the LM level, both slopes being almost linear. In general, for MH level, the proposed method tends to under-estimate the effect of damage at medium storeys on the overall damage.

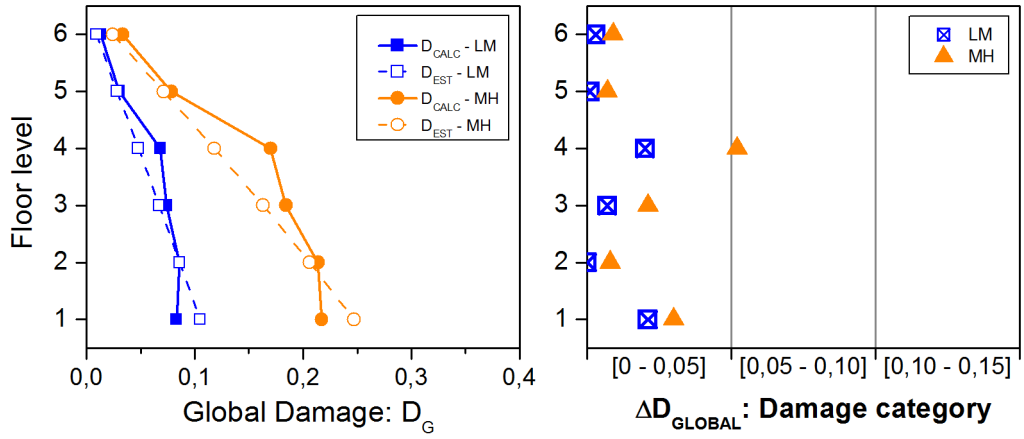

a) **b)**

Figure 5.12 a) Calculated and estimated global damage for the 6-storey frame, b) Classification of ΔD_{GLOBAL} according to the damage category

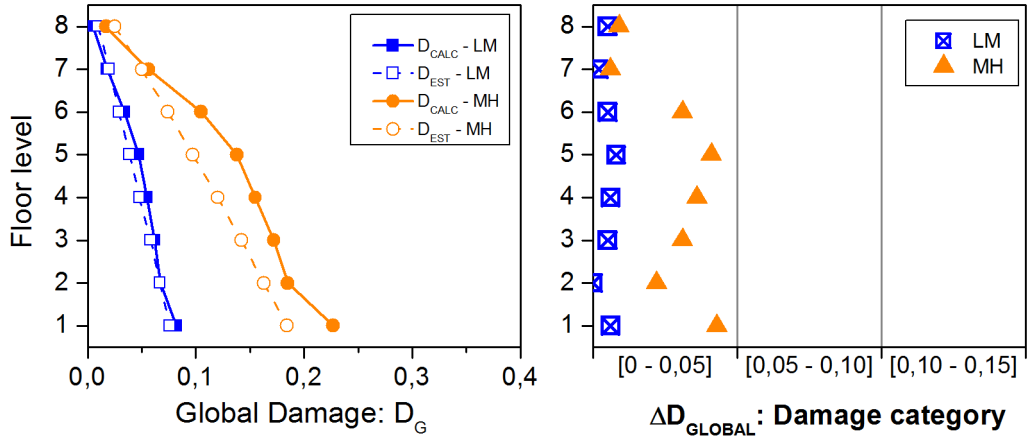

a) **b)**

Figure 5.13 a) Calculated and estimated global damage for the 8-storey frame, b) Classification of ΔD_{GLOBAL} according to the damage category

Some of these results must be taken carefully as they reflect a purely theoretical situation because of the concentrated patterns, as it was stated before. In fact, having a first storey with a damage level of 60% generates a global damage of 22%, according to the analytical method and 18.5% according to the proposed strategy, for the 8-storey frame as shown in Figure 5.13. This particular result may be hard to relate with a real situation since such an extent of damage at the lower storey would probably produce larger effects on the whole building. Repair costs may be too high or even repair works may be unfeasible so that the effective

consequence of damage would be more significant. Thereby, a damage index such this one proposed herein should be part of an extended strategy of damage assessment including also effects other than the strict mechanical damages.

Thus, on the basis of the obtained results, the β factor seems to be efficient in reflecting the significance of the localization of the damaged storey on the global damage. This conclusion is further investigated hereafter under different patterns.

5.9.2. Efficiency of α factors

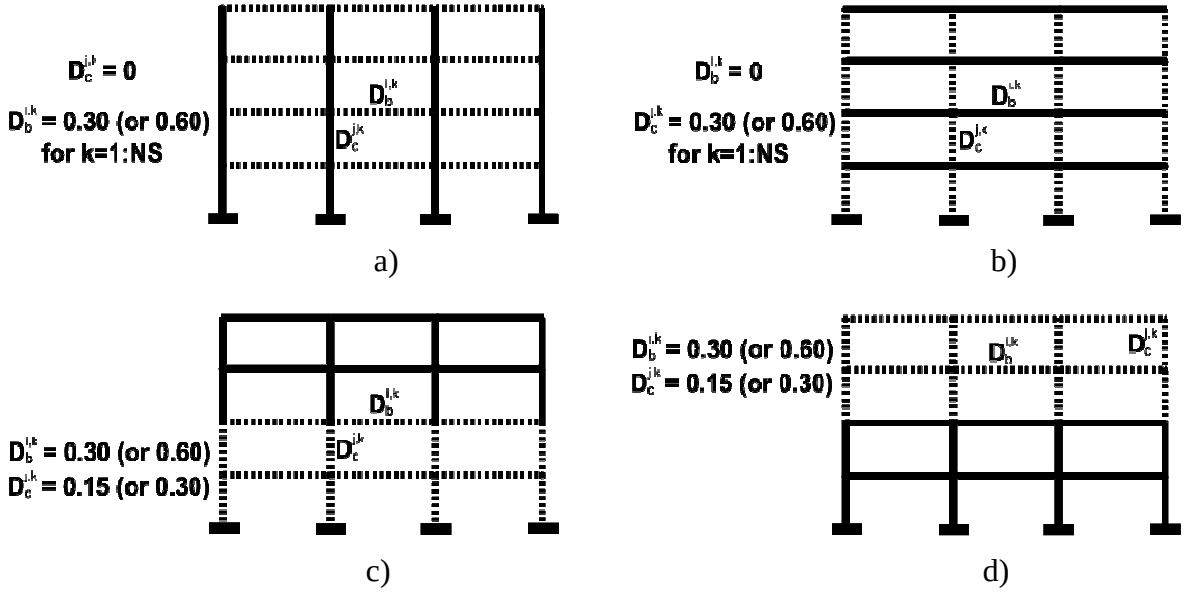

Figure 5.14 Concentrated local damage at a) beams, b) columns, c) lower storeys and d) higher storeys

Four cases are proposed for assessing α factors efficiency. In the first two cases, all the storeys of each building are supposed to be damaged: first it is concentrated on beams (case B in the results graphs), then on columns (case C); these patterns permit to isolate the effect of α factor for beams and columns, see Figure 5.14 a) and b). Next, in the other two cases, all the components of a storey are supposed to be damaged, but different indices are considered for beams and columns and the damage is supposed to be concentrated in the lower storeys (case LS), and in the higher storeys afterwards (case HS), see Figure 5.14 c) and d). These analyses are performed for each building and for low-medium (LM) and medium-high (MH) damage levels.

As for the case of β factors in the precedent section, results for the 4-storey frame are not always satisfactory. In this case, when damage is concentrated on columns, the differences between the proposed strategy and the reference method are important for both levels of damage, as it may be observed in Figure 5.15.

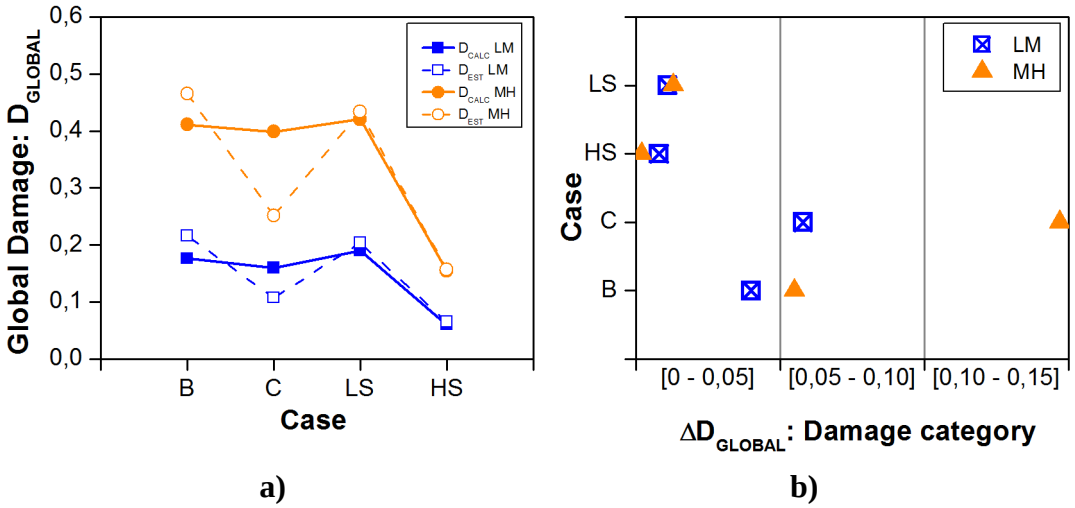

a) **b)**

Figure 5.15 Efficiency of α factors: a) Calculated and estimated damage of the 4-storey frame for the four analyzed cases, b) Classification of ΔD_{GLOBAL}

This may be due to particular features of the frame since results of the other buildings are satisfactory as confirmed later. Except for this particular case, the results of the proposed approach are very close to the analytical results for the two damage levels, according to Figure 5.15, Figure 5.16 and Figure 5.17. In addition, the differences range once again within acceptable limits. All of them are close to the first damage category with the exception of one case for the 4-storey frame, as observed before. All these results may suggest that α factors, proposed for considering the influence of beams and columns on the storey damage and on global damage, are successful in fulfilling their objective.

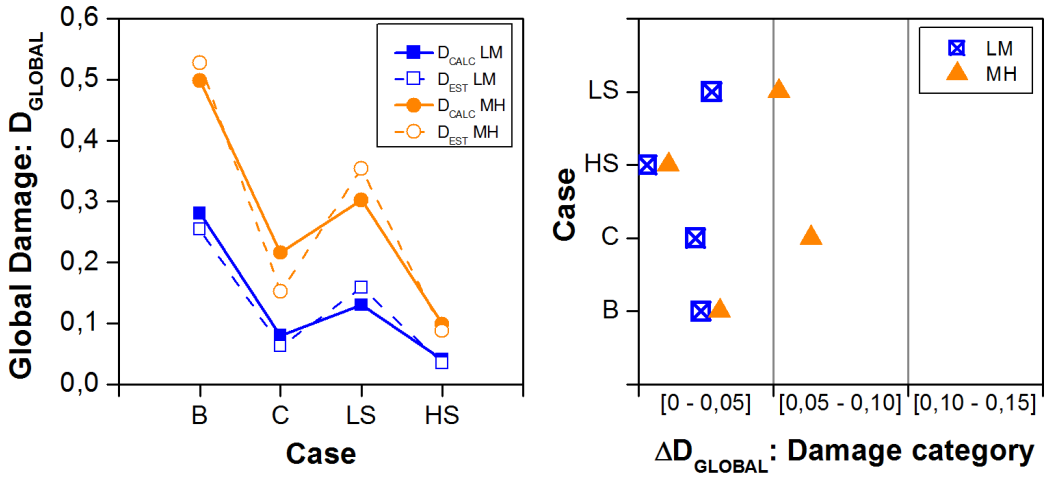

a) **b)**

Figure 5.16 Efficiency of α factors: a) Calculated and estimated damage of the 6-storey frame for the four analyzed cases, b) Classification of ΔD_{GLOBAL}

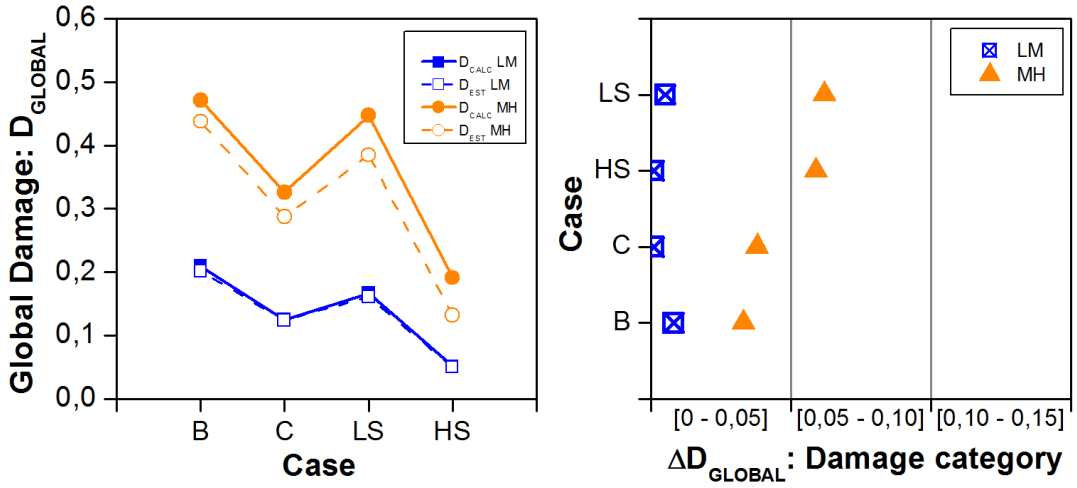

a) **b)**

Figure 5.17 Efficiency of α factors: a) Calculated and estimated damage of the 8-storey frame for the four analyzed cases, b) Classification of ΔD_{GLOBAL}

5.9.3. Global efficiency

For further validation of the proposed strategy, four different damage patterns have been also tested. The first two cases are symmetrical (denoted as S), variable patterns, with all the components being damaged, one gradually decreasing along the building height (denoted GV) and the other presenting sharper variations (denoted SV). These two cases, S_GV and S_SV, are displayed in Table 5-4, which illustrates the assigned damage patterns for the 6-storey

frame (Patterns used for the other two frames are included in APPENDIX C). Afterwards, unsymmetrical patterns of damage (denoted U) are investigated. Damage is first concentrated on lower storeys (LS) and then on higher storeys (HS), see also Table 5-4 cases U_LS and U_HS. As before, these configurations where applied for the two levels of damaged defined before, LM and MH.

Event	Damage										Event	Damage								
	Story	Beam				Columns						Story	Beam				Columns				
		1	2	3	4	1	2	3	4	5			1	2	3	4	1	2	3	4	5
S_GV	1	0,25	0,25	0,25	0,25	0,15	0,15	0,2	0,15	0,15	U_LS	1	0,4	0,2	0,15	0,35	0,3	0,35	0,25	0,2	0,3
	2	0,25	0,25	0,25	0,25	0,15	0,15	0,2	0,15	0,15		2	0,35	0,25	0,15	0,3	0,25	0,25	0,2	0,1	0,25
	3	0,2	0,2	0,2	0,2	0,15	0,15	0,2	0,15	0,15		3	0,15	0,1			0,2	0,2	0,15		
	4	0,2	0,2	0,2	0,2	0,1	0,1	0,15	0,1	0,1		4		0,1					0,1		
	5	0,1	0,1	0,1	0,1	0,1	0,1	0,15	0,1	0,1		5									
	6	0,1	0,1	0,1	0,1	0,1	0,1	0,15	0,1	0,1		6									
S_SV	1	0,4	0,4	0,4	0,4	0,2	0,2	0,2	0,2	0,2	U_HS	1									
	2	0,4	0,4	0,4	0,4	0,2	0,2	0,2	0,2	0,2		2									
	3	0,4	0,4	0,4	0,4	0,2	0,2	0,2	0,2	0,2		3		0,1							
	4	0,3	0,3	0,3	0,3	0,1	0,1	0,1	0,1	0,1		4	0,2	0,1	0,2	0,25	0,2	0,25	0,25		
	5	0,3	0,3	0,3	0,3	0,1	0,1	0,1	0,1	0,1		5	0,35	0,2	0,3	0,2	0,3	0,3	0,3	0,2	0,1
	6	0,3	0,3	0,3	0,3	0,1	0,1	0,1	0,1	0,1		6	0,15	0,15	0,2	0,15	0,15	0,25	0,2	0,15	

Table 5-4 Damage pattern of the 6-storey frame for low-medium (LM) level of damage

Results shown in Figure 5.18, Figure 5.19 and Figure 5.20 confirm the efficiency of the proposed approach since a very good accordance is found between analytical and estimated results. As it was suggested before, the results improve when damage patterns are more uniform instead of concentrated (in one single storey for example) as they are closer in the case of real situations. Both factors, α and β, seem to be adequate in getting the individual weight of components and storeys on the global damage.

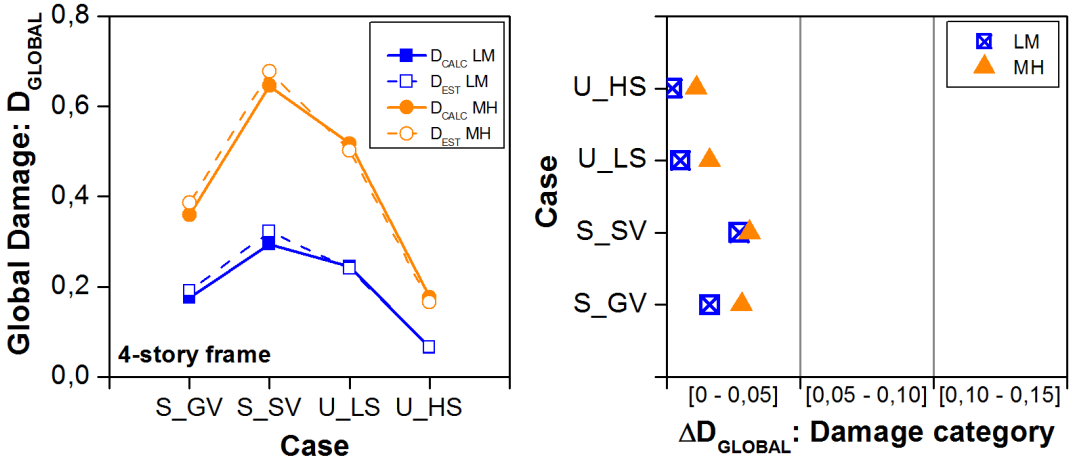

Figure 5.18 Global efficiency: a) Calculated and estimated damage of the 4-storey frame for the four analyzed cases, b) Classification of ΔD_{GLOBAL}

Concerning the differences ΔD, all but two cases for the 8-storey frame, remain in the first category between 0 and 0.05, for both levels of damage.

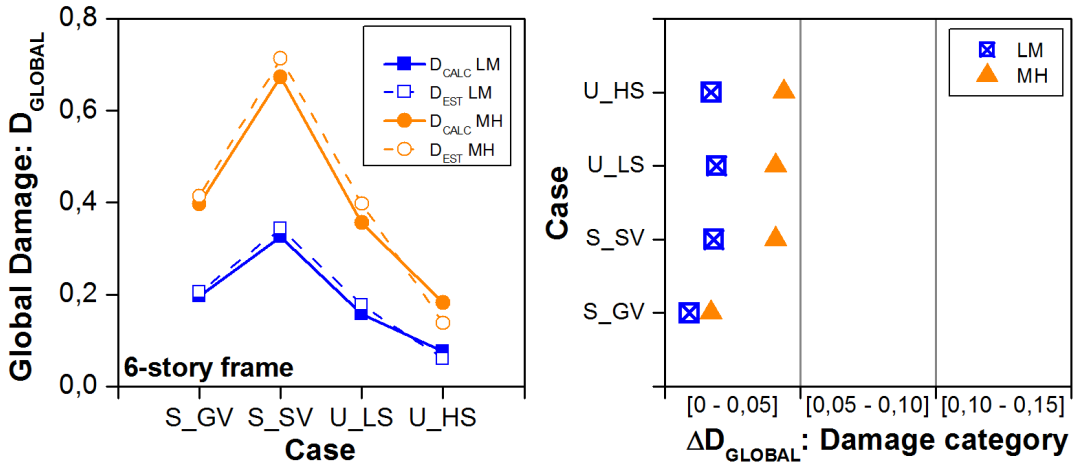

a) **b)**

Figure 5.19 Global efficiency: a) Calculated and estimated damage of the 6-storey frame for the four analyzed cases, b) Classification of ΔD_{GLOBAL}

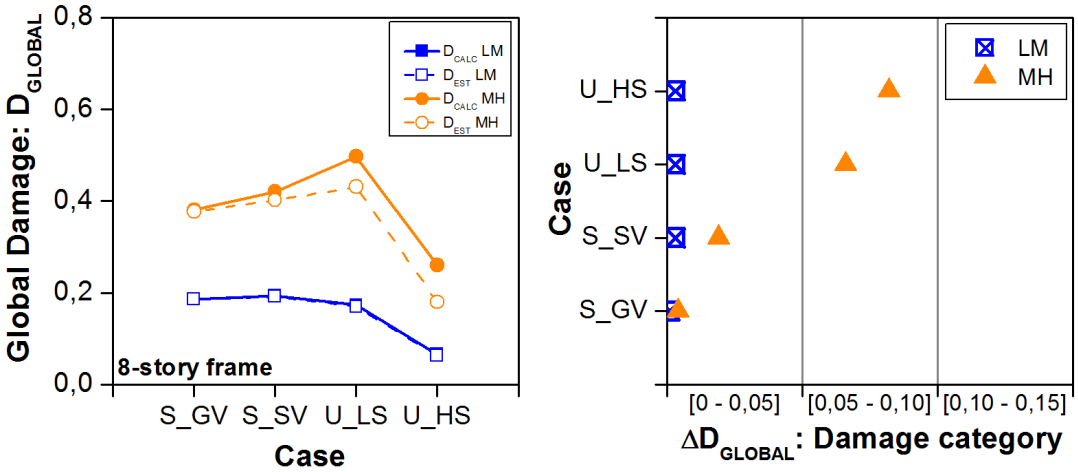

a) **b)**

Figure 5.20 Global efficiency: a) Calculated and estimated damage of the 8-storey frame for the four analyzed cases, b) Classification of ΔD_{GLOBAL}

5.9.4. Further validation: Damage patterns from NLTHA under real ground motions

With the aim of studying the proposed approach when compared to a real distribution of damage, the studied buildings have been subjected to a set of real ground motions (see Table 3-1 for further information) in order to obtain the theoretical patterns of damage. Some of

them have been scaled with the aim of producing a wide range of damage magnitudes.

Once the results obtained, local damage at each element was computed from peak values of the curvature, according to the model shown in Figure 5.5. In fact, it was supposed that the peak deformation reached during the earthquake would be the "yield" deformation of the damaged model. Therefore, the following expression has been derived in order to compute the local damage in each component:

$$D_{LOCAL} = \frac{(\phi_{peak} - \phi_y)(1-b)}{\phi_{peak}} \tag{5.31}$$

Where: ϕ_{peak} is the maximum curvature, reached during the earthquake; ϕ_y is the yielding curvature of the undamaged component; and b represents the post-yield slope. Thus, the obtained damage patterns were taken as given patterns and were investigated within the framework of the proposed method. The results are illustrated hereafter.

A wide range of damage arrangements has been observed according to the particular characteristics of both the ground motions and the buildings. In the case of the 4-storey building, the patterns are usually unsymmetrical and damage decreases along the building height, as shown in Table 5-5.

GM	Damage						GM	Damage					
	Story	Beam		Col				Story	Beam		Col		
		1	2	1	2	3			1	2	1	2	3
Erzincan	1	0,68	0,51	0	0,32	0	Loma Prieta	1	0,8	0,84	0,61	0,78	0,62
	2	0,59	0,18	0	0,48	0		2	0,85	0,82	0	0,86	0
	3	0	0	0	0,21	0		3	0,79	0,66	0,47	0,89	0,35
	4	0	0	0	0	0		4	0	0	0	0	0

Table 5-5 Examples of damage arrangements obtained for the 4-storey frame

In some other cases, damage is either concentrated on a section of the building or increasing along the building height. This behaviour is mostly due to a particular mechanical feature and the fact that some ground motions produce predominantly higher mode responses. It is the case of the 6-storey frame, which presents a change in stiffness between the 5th and the 6th storeys, in conjunction with Northridge record which excites higher modes. Hence the damage is concentrated in these zones as illustrated in Table 5-6. In any case, for this frame,

patterns are mainly symmetrical.

GM	Damage										GM	Damage								
	Story	Beam				Col						Story	Beam				Col				
		1	2	3	4	1	2	3	4	5			1	2	3	4	1	2	3	4	5
San Fernando	1	0	0	0	0	0	0	0	0	0	Northridge	1	0	0	0	0	0	0	0	0	0
	2	0	0	0	0	0	0	0	0	0		2	0,45	0,41	0,4	0,48	0	0	0	0	0
	3	0	0	0	0	0	0	0	0	0		3	0,5	0,51	0,51	0,52	0	0	0	0	0
	4	0	0	0	0	0	0	0	0	0		4	0,58	0,54	0,54	0,58	0	0	0	0	0
	5	0,87	0,87	0,87	0,87	0	0	0	0	0		5	0,91	0,91	0,91	0,91	0	0	0	0	0
	6	0,52	0,44	0,46	0,55	0	0	0	0	0		6	0,78	0,76	0,76	0,78	0	0	0	0	0

Table 5-6 Examples of damage arrangements obtained for the 6-storey frame

For the 8-storey frame, all kind of damage patterns have been observed, ranging from very uniform distributions under Imperial Valley record to concentrations of damage on higher storeys under Northridge record, as shown in Table 5-7.

GM	Damage								GM	Damage							
	Story	Beam			Col					Story	Beam			Col			
		1	2	3	1	2	3	4			1	2	3	1	2	3	4
Imperial Valley	1	0,78	0,78	0,77	0	0	0	0	Northridge	1	0	0	0	0	0	0	0
	2	0,72	0,73	0,7	0	0	0	0		2	0	0	0	0	0	0	0
	3	0,62	0,67	0,6	0	0	0	0		3	0	0	0	0	0	0	0
	4	0,74	0,75	0,7	0	0	0	0		4	0	0,09	0	0	0	0	0
	5	0,83	0,81	0,8	0	0	0	0		5	0	0,12	0,24	0	0	0	0
	6	0,85	0,84	0,82	0	0	0	0		6	0,29	0,25	0,21	0	0	0	0
	7	0,8	0,8	0,76	0	0	0	0		7	0,82	0,79	0,79	0	0	0	0
	8	0	0	0	0	0	0	0		8	0,55	0,45	0,57	0	0,71	0,64	0

Table 5-7 Examples of damage arrangements obtained for the 8-storey frame

When applying the proposed method for all these patterns taken as known patterns the results for the estimated global damage index are very close to the analytical results as shown in Figure 5.21, which confirms what had been found before concerning the suitability of the proposed α and β factors. Differences are very small regardless of the level of damage, which ranges from 0.1 to 0.8, of the building and of the damage pattern.

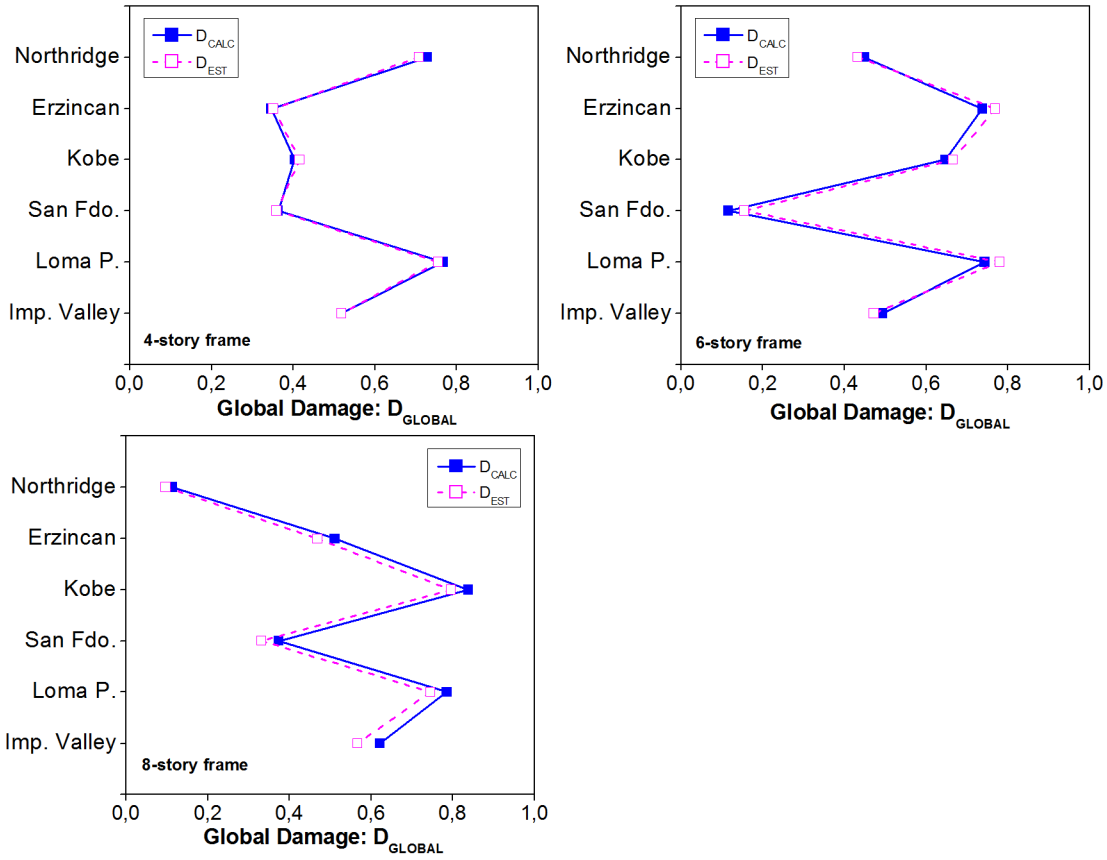

Figure 5.21 Calculated and estimated global damage for the three studied frames

5.10. CONCLUSIONS

A probability-based strategy has been developed with the aim of computing global damage indices on the basis of given component damage indices. It relies on an assumed relationship between structural damage and residual probability of failure, considering at the same time the significance of the damage of each component on the whole damage by means of importance factors. The results obtained by an analytical approach which considers the reduction in the capacity spectrum stiffness as an indicator of global damage are taken as reference results for calibration purposes.

The three proposed importance factors have proven to be suitable according to the obtained results for damage arrangements which allow identifying the individual influence of each factor. Differences between calculated and estimated global indices do not exceed, in most cases, one category of damage: very small differences between the two values of global damage are found. Concerning the general efficiency of the method, a number of damage

patterns have been tested. Some of them were arbitrarily chosen, others were typical of real situations since they were obtained from nonlinear time history analysis under real ground motion records. A good accordance between estimations and reference results was obtained, confirming the suitability of this approach.

Further validation with experimental or field results is required to this strategy in order to be of general application since analytical approaches are always subjected to uncertainties and usually do not account for all the phenomena inherent to this kind of task.

Finally, this strategy has the potential of being part of a decision-making tool which helps in performing fairly accurate assessments of global damage based on damage of components. Particularly, since only some geometrical and mechanical properties of the structure are required, its use for post-seismic evaluation of damage is also feasible by means of its implementation on PDA devices, for instance, at large scale as urban constructions after occurrence of an earthquake.

CONCLUSIONS AND FURTHER RESEARCH

Summary and general conclusions

The vulnerability of urban environments regarding natural hazards is an important scientific issue. Actually, when dealing with seismic hazard, the risk of structural failure is undeniably important and needs to be assessed correctly in order to mitigate and reduce the potential disaster. This scientific challenge includes at least three major tasks: i) developing code provisions to guarantee that new constructions are earthquake resistant, ii) reducing the risk of the existing buildings and facilities and iii) reducing the impact of a strong earthquake occurrence.

The main focus of the present dissertation is the development of methods dealing with tasks ii) and iii). Thus, it is divided into two main parts.

PART I: SEISMIC RESPONSE ASSESSMENT

Risk reduction requires vulnerability evaluation which in turn requires a reliable seismic response evaluation. Various existing methods with variable levels of difficulty have been proposed these last decades. Consensus exists regarding the most accurate method: a complete Nonlinear Time History Analysis, applied of course with good engineering judgment. However, it is highly time-consuming. Hence, the development of simplified but accurate methods is under continuous investigation. Some of the existing methods may provide good results but sometimes they are time-consuming or rely on quite complicated implementations not being suitable for current application.

Consequently, an approximate method for the assessment of seismic response is developed and proposed in Part I: The Pseudo-Adaptive Uncoupled Modal Response Analysis (PSA). PSA method is presented as an alternative to fully adaptive procedures. In fact, its pseudo-adaptive character gives, for given aspects, an advantage and a benefit in comparison to those methods. Actually, PSA does not require updating modal force vectors at each

increment since it assumes an invariant lateral load profile (it does not vary during the incremental steps). Nevertheless, it is able to reflect the effect of variations in modal shapes by approximating modal properties from the pushover analysis, on the basis of storey displacements. Therefore, the pushover analysis is completely performed with an invariant profile: $\mathbf{s}_n^* = \mathbf{m}\boldsymbol{\phi}_n$ so that updated modal shapes are computed afterwards and considered in the modal response calculation.

A second important feature of PSA is the development of the capacity curve by means of an energy-based approach. It accounts for the whole lateral deformational capacity of the building through an equivalent displacement instead of using the classic approach based on roof displacement. Actually, this is a more rational way of describing lateral performance as proven by the significant differences found between the classic and the energy-based curves, namely for higher modes. In fact, first-mode curves are essentially similar for both approaches while higher-mode energy-based curves are in general stiffer than the classic ones, for the cases considered in this study.

The validation of PSA is made on six reinforced concrete moment resisting frames, five of them being designed for seismic actions and the remaining being designed only for gravity loads. Responses of storey displacements, drifts, plastic hinge rotations, and shear forces are studied and compared to complete NLTHA, considered as reference method and also to MPA and UMRHA.

In comparison to complete nonlinear time history analysis, the proposed method provides an acceptable accuracy with a reduced computational demand. For instance, the time required for the analysis of an 8-storey building is reduced as much as 4 times or even more when applying PSA (21 sec) instead of NLTHA (95sec), with the contribution of three modes and two iterations. This reduction is an advantage when dealing with seismic reliability analyses (requiring Monte Carlo simulations for instance) and early post-quake damage evaluations at large scales (e.g. urban scale). Besides, results of multimodal procedures are improved when using superposition of modal responses instead of SRSS combination of peak responses, and the analysis duration time increases only by 3 sec (15% increase) in comparison to SRSS combination.

Some difficulties were encountered when working with Northridge record in most of the studied frames. In fact, it is a record with a particular frequency content which produces large

concentrations of inelastic deformations even for low levels of global deformation, according to the results of the 8-, 10- and 14- storey frames. Then, when such records are identified it is recommended to evaluate whether updating load profiles at some stages after yielding might improve the accuracy unless a complete NLTHA should remain the unique choice.

PART II: GLOBAL DAMAGE ASSESSMENT

Post-seismic damage assessment is among the multiple imperative tasks required to manage or mitigate the disastrous impact of a strong earthquake. Some of the existing methods rely on the assignation of damage states on the basis of observed damages. With the aim of improving the existing methods, a strategy based on a postulated relationship between residual probability of failure and damage is proposed. It is intended to provide global damage indices on the basis of given (observed) local indices. The strategy is implemented in order to be applied on frame buildings. Thereby, the first step consists in an evaluation at the storey level on the basis of beams and columns damage. In a second step, the overall damage is derived from the storey damage. Three importance factors are proposed to take into account the relative effect of components damage on global damage: α_b and α_c factors for beams and columns and β factor for storeys' influence.

Four RC frames are used for validation purposes. The obtained results are compared to those of an analytical approach, which evaluates global damage through the changes in the stiffness of the first-mode capacity spectrum. The calibration and efficiency of the three factors is studied first, by separating individually each factor effect. Global efficiency is then evaluated by means of several damage patterns as well as patterns obtained from NLTHA results. Except for a few exceptions, a very good accordance with the results of the analytical method is observed. The importance factors are found to be adequately calibrated. In fact, most differences between the predicted and the "observed" damages remain very small, since they almost range within the interval [0.00 – 0.05].

Since post-earthquake damage evaluation must be performed in the short term, the proposed method has the potential of being the basis of a decision-making tool, integrated with geo-referenced information systems (GIS) and implemented on PDA devices, for instance.

Significant contribution

The significant contributions of PSA method can be summarized as follows:

- It provides acceptable accuracy with reduced computational demands considering at the same time the whole record features, since the analyses are performed on SDOF systems. Hence it is a potential tool for large scale studies such as reliability analyses.
- It takes into account higher mode effects without using modal combination rules which are proven to be the source of additional uncertainties, since it is based on modal superposition. In addition, it eliminates at the same time the inaccuracy due to the use of roof displacement as indicator of lateral global behaviour through the use of an energy-based equivalent displacement.
- As neither eigenvalue analysis nor updating of load profiles are needed during pushover analysis, open source or special software platforms are not required for PSA to be applied. This is an important feature for current engineering practice.

The significant contributions of the probability-based strategy for global damage evaluation method are:

- The development of a simplified but accurate method for global structural damage assessment, which is based on observed damages and takes into account the available data about geometrical and mechanical properties of the components.
- The proposal of importance factors which express the relative influence of damage at each component on the global damage. Thus, this strategy is a potential post-seismic evaluation tool.

Further research

For further validation and development of both methods, additional studies are required:

PSA method:

- The extension and validation of the proposed PSA method to 3D structures and unsymmetrical buildings is required. Going from 2D to 3D implies considering torsion effects.
- Approximating the actual capacity curve as a bilinear curve may induce significant errors when early yielding is present, as is the case of some gravity load designed buildings. Thus, for these cases, it may be necessary to implement tri-linear or more precise capacity curves for improving accuracy.
- Given the objectives of this research, soil-structure interaction (SSI) has not been considered. However, it should be considered since SSI effects could be relevant in some cases.

Probability-based post seismic damage evaluation strategy:

- Damage of foundation components as well as non-structural components must be considered in the strategy for global damage evaluation in order to be applicable.
- Further validation needs to be done with experimental (forensic) results in order to confirm the suitability or the proposed factors. Also, it may be done with more detailed analytical methods based on cumulative damage models.
- Moreover, this strategy may be implemented and validated on infilled frames as they are a widely spread construction type everywhere.
- The proposed analytical procedure for global damage evaluation is based on the changes of the force-resisting properties of the whole building. However, despite the good results obtained by this approach, displacement-based techniques should be tested, following the recommendations of the well accepted performance-based engineering techniques.

BIBLIOGRAPHY

Agnanos, T., Rojahn, C. & Kiremidjian, A. S. (1995). *NCEER-ATC joint study on fragility of buildings*, Report:NCEER-95-0003, National Center for Earthquake Engineering Research., Buffalo, NY.

AIS (1998). *Normas colombianas de diseño y construcción sismorresistente, NSR-98*, Ley 400 de 1997, Decreto 33 de 1998, Asociación Colombiana de Ingeniería Sísmica.

Amziane, S. & Dubé, J. F. (2008). *Global RC Structural Damage Index Based on the Assessment of Local Material Damage*, Journal of Advanced Concrete Technology, **6**(3), 459-468.

Ang, A. H. S. (1988). *Seismic damage assessment and basis for damage-limiting design*, Probabilistic Engineering Mechanics, **3**(3), 146-150.

Antoniou, S. & Pinho, R. (2004). *Advantages and Limitations of Adaptive and Non-Adaptive Force Based Pushover Procedures*, Journal of Earthquake Engineering, **8**(4), 497-522.

ASCE (2000). *Prestandard and Commentary for the Seismic Rehabilitation of Buildings*, FEMA-356, Federal Emergency Management Agency, Washington D.C.

ATC (1985). *Earthquake damage evaluation data for California*, ATC-13, Applied Technology Council, Redwood City, California.

ATC (1995). *Addendum to the ATC-20 Postearthquake Building Safety Evaluation Procedures*, ATC-20, Applied Technology Council, Redwood City, California.

ATC (1996). *Seismic Evaluation and Retrofit of Concrete Buildings*, ATC - 40, Applied Technology Council, Redwood City, Calif.

ATC (1998a). *Evaluation of Earthquake Damaged Concrete and Masonry Wall Buildings. Basic Procedures Manual*, FEMA-306, Federal Emergency Management Agency, Redwood City, California.

ATC (1998b). *Repair of Earthquake Damaged Concrete and Masonry Wall Buildings*, FEMA-308, Federal Emergency Management Agency, Redwood City, California.

ATC (2005). *Improvement of Nonlinear Static Seismic Analysis Procedures*, FEMA - 440, Federal Emergency Management Agency, Redwood City, California.

Barbat, A. H., Pujades, L. G. & Lantada, N. (2008). *Seismic damage evaluation in urban areas using the capacity spectrum method: Application to Barcelona*, Soil Dynamics and Earthquake Engineering, **28**(10-11), 851-865.

Bazán, E. & Meli, R. (2002). *Diseño sísmico de edificios*, Editorial Limusa S.A. de C.V., Mexico.

Besson, J., Cailletaud, G., Chaboche, J. L. & Forest, S. (2001). *Mécanique non linéaire des matériaux*, Hermes Sciences Publications.

Bilham, R. (2009). *The seismic future of cities*, Bulletin of Earthquake Engineering, **7**(4), 839-887.

Bobadilla, H. & Chopra, A. K. (2007). *Modal Pushover Analysis for Seismic Evaluation of Reinforced Concrete Special Moment Resisting Frame Buildings*, Report:EERC 2007-01, Earthquake Engineering Research Center, Berkeley, CA.

Bonett, R. L. (2003). *Vulnerabilidad y riesgo sísmico de edificios. Aplicación a entornos urbanos en zonas de amenaza alta y moderada*, Universidad Politécnica de Cataluña, Barcelona, España, pp.474.

CEN (2003). *Eurocode 8: design of structures for earthquake resistance* - European Commitee For Standardisation (CEN).

Chai, Y. (1999). *Characterization of story-level seismic damage using an energy-based damage model*, Experimental Mechanics, **39**(1), 53-61.

Chintanapakdee, C. & Chopra, A. K. (2003). *Evaluation of modal pushover analysis using generic frames*, Earthquake Engineering & Structural Dynamics, **32**(3), 417-442.

Chopra, A. K. (2007). *Dynamics of Structures: Theory and Applications to Earthquake Engineering*, Pearson Prentice Hall, Upper Saddle River, NJ.

Chopra, A. K. & Goel, R. (2001). *A Modal Pushover Analysis Procedure to Estimate Seismic Demands on Buildings: Theory and Preliminary Evaluation*, Report:PEER 2001/03, Pacific Earthquake Engineering Research Center, Berkeley, CA.

Chopra, A. K. & Goel, R. K. (2002). *A modal pushover analysis procedure for estimating seismic demands for buildings*, Earthquake Engineering & Structural Dynamics, **31**(3), 561-582.

Chopra, A. K. & Goel, R. K. (2004). *A modal pushover analysis procedure to estimate seismic demands for unsymmetric-plan buildings*, Earthquake Engineering & Structural Dynamics, **33**(8), 903-927.

Clough, R. W. & Penzien, J. (1993). *Dynamics of Structures*, McGraw Hill, Singapore.

Colombo, A. & Negro, P. (2005). *A damage index of generalised applicability*, Engineering Structures, **27**(8), 1164-1174.

Computers and Structures Inc. (2003). *ETABS, V.*8.2.7,Berkeley, CA.

D'Ambrisi, A. & Filippou, F. C. (1999). *Modeling of Cyclic Shear Behavior in RC Members*, Journal of Structural Engineering, **125**(10), 1143-1150.

DiPasquale, E. & Cakmak, A. S. (1990). *Detection of seismic structural damage using parameter-based global damage indices*, Probabilistic Engineering Mechanics, **5**(2), 60-65.

Fajfar, P. (1999). *Capacity spectrum method based on inelastic demand spectra*, Earthquake Engineering & Structural Dynamics, **28**(9), 979-993.

Fajfar, P. (2007). *Seismic Assessment of Structures by a Practice-Oriented Method*, in Adnan Ibrahimbegovic & Ivica Kozar (eds.), *Extreme Man-Made and Natural Hazards in Dynamics of Structures*, Springer Netherlands, pp. 257-284.

Fajfar, P. & Gašperšič, P. (1996). *The N2 Method for the Seismic Damage Analysis of RC Buildings*, Earthquake Engineering & Structural Dynamics, **25**(1), 31-46.

FEMA440 (2005). *Improvement of Nonlinear Static Seismic Analysis Procedures*, FEMA - 440, Federal Emergency Management Agency, Redwood City, Calif.

Freeman, S. A., Nicoletti, J. P. & Tyrell, J. V. (1975). *Evaluations of Existing Buildings for Seismic Risk - A Case Study of Puget Sound Naval Shipyard, Bremerton, Washington*, in (ed.), U.S. National Conference on Earthquake Engineering, Berkeley, U.S.A., pp. 113-122.

Galasco, A., Lagomarsino, S. & Penna, A. (2006). *On the use of pushover analysis for existing masonry buildings*, in (ed.), First European Conference on Earthquake Engineering and Seismology (a joint event of the 13th. ECEE & 30th. General Assembly of the ESC). Geneva, Switzerland, pp. 1-10.

García, L. E. (1998). *Dinámica estructural aplicada al diseño sísmico*, Universidad de los Andes, Bogotá.

Goel, R. K. & Chopra, A. K. (2004). *Evaluation of Modal and FEMA Pushover Analyses: SAC Buildings*, Earthquake Spectra, **20**(1), 225-254.

Goel, R. K. & Chopra, A. K. (2005). *Extension of Modal Pushover Analysis to Compute Member Forces*, Earthquake Spectra, **21**(1), 125-139.

Gupta, B. & Kunnath, S. K. (2000). *Adaptive Spectra-Based Pushover Procedure for Seismic Evaluation of Structures*, Earthquake Spectra, **16**(2), 367-392.

Hamza, S., Bonnet, G. & Delmotte, P. (2005). *Deterministic and stochastic approach in estimating the reliability of civil-engineering structures submitted to earthquakes*, in C. Soize & G.I. Schueller (ed.), 6th. International Conference on Structural Dynamics, Paris, France, pp. 791-796.

Han, S. W. & Chopra, A. K. (2006). *Approximate incremental dynamic analysis using the modal pushover analysis procedure*, Earthquake Engineering & Structural Dynamics, **35**(15), 1853-1873.

Hanganu, A. D., Onate, E. & Barbat, A. H. (2002). *A finite element methodology for local/global damage evaluation in civil engineering structures*, Computers & Structures, **80**(20-21), 1667-1687.

Haselton, C. B. & Deierlein, G. G. (2007). *Assessing Seismic Collapse Safety of Modern Reinforced Concrete Moment-Frame Buildings*, Report:PEER 2007/08, Pacific Earthquake Engineering Research Center, Berkeley, CA.

Hernández-Montes, E., Kwon, O.-S. & Aschheim, M. A. (2004). *An Energy-Based Formulation for First- and Multiple-Mode Nonlinear Static (Pushover) Analyses*, Journal of Earthquake Engineering, **8**(1), 69-88.

Ibarra, L. F., Medina, R. A. & Krawinkler, H. (2005). *Hysteretic models that incorporate strength and stiffness deterioration*, Earthquake Engineering & Structural Dynamics, **34**(12), 1489-1511.

J.M.Bracci, A.M.Reinhorn, J.B.Mander & S.K.Kunnath (1989). *Deterministic Model for Seismic Damage Evaluation of Reinforced Concrete Structures*, Report:NCEER-89-0033, National Center for Earthquake Engineering Research.,

Jeong, S.-H. & Elnashai, A. S. (2006). *New Three-Dimensional Damage Index for RC Buildings with Planar Irregularities*, Journal of Structural Engineering, **132**(9), 1482-1490.

Jerez, S. & Mebarki, A. (2009). *Seismic Assessment of Buildings: Proposal of a New Modified Uncoupled Modal Response History Analysis*, in American Institute of Physics (ed.), 2nd. International Symposium on Computational Mechanics (ISCMII) in conjunction with the 12th. International Conference on the Enhancement and Promotion of Computational Methods in Engineering and Science (EPMESC XII), Hong Kong - Macau, pp. 1642 - 1647.

Jerez, S. & Mebarki, A. (2010). *A Pseudo-Adaptive uncoupled modal response analysis for seismic assessment of framed buildings*, in (ed.), Colloque international Seisme d'El Asnam du 10 Octobre 1980. Trente ans après., Alger, Algeria., pp. In Press.

Jerez, S. & Mebarki, A. (In press). *Seismic Assessment of Framed Buildings: A Pseudo-Adaptive Uncoupled Modal Response Analysis*, Journal of Earthquake Engineering, In press.

Kalkan, E. & Kunnath, S. K. (2006). *Adaptive Modal Combination Procedure for Nonlinear Static Analysis of Building Structures*, Journal of Structural Engineering, **132**(11), 1721-1731.

Kappos, A. J., Stylianidis, K. C. & Pitilakis, K. (1998). *Development of Seismic Risk Scenarios Based on a Hybrid Method of Vulnerability Assessment*, Natural Hazards, **17**(2), 177-192.

Kent, D. C. & Park, R. (1971). *Flexural members with confined concrete*, Journal of the Structural Division, ASCE, **97**(ST7), 1969-1989.

Kirçil, M. S. & Polat, Z. (2006). *Fragility analysis of mid-rise R/C frame buildings*, Engineering Structures, **28**, 1335-1345.

Krawinkler, H. & Zohrei, M. (1983). *Cumulative damage in steel structures subjected to earthquake ground motions*, Computers & Structures, **16**(1-4), 531-541.

Kwon, O.-S. & Elnashai, A. (2006). *The effect of material and ground motion uncertainty on the seismic vulnerability curves of RC structure*, Engineering Structures, **28**, 289-303.

Lagomarsino, S. & Giovinazzi, S. (2006). *Macroseismic and mechanical models for the vulnerability and damage assessment of current buildings*, Bulletin of Earthquake Engineering, **4**, 415-443.

Lee, T.-H. & Mosalam, K. M. (2006). *Probabilistic Seismic Evaluation of Reinforced Concrete Structural Components and Systems*, Report:PEER 2006/04, Pacific Earthquake Engineering Research Center, Berkeley, CA.

Lemaitre, J. (1985). *Coupled Elasto-Plasticity and Damage Constitutive-Equations*, Computer Methods in Applied Mechanics and Engineering, **51**(1-3), 31-49.

Li, Q. (2006). *Mathematical Formulation of Tools for Assessment of Fragility and Vulnerability of Damaged Buildings*, Ph.D. Thesis, Georgia Institute of Technology, Georgia, pp.191.

Li, Q. & Ellingwood, B. R. (2005). *Structural Response and Damage Assessment by Enhanced Uncoupled Modal Response History Analysis*, Journal of Earthquake Engineering, **9**(5), 719-737.

Li, Q. & Ellingwood, B. R. (2007). *Performance evaluation and damage assessment of steel frame buildings under main shock-aftershock earthquake sequences*, Earthquake Engineering & Structural Dynamics, **36**(3), 405-427.

Mazzoni, S., McKenna, F., Scott, M. H. & Fenves, G. L. (2007). *Open System for Earthquake Engineering Simulation (OpenSees) User Command-Language Manual*, in Pacific Earthquake Engineering Research Center. (ed.), University of California, Berkeley.

Mebarki, A. (2006). *Post-seismic structural damage evaluation: an integrated probabilistic proposal*, in BHV Topping (ed.), Intern. Conf. ECT 2006, Las Palmas de Gran Canaria, pp.

Mebarki, A. & Laribi, A. (2008). *Evaluation post-sismique des dommages structuraux: méthodologie probabiliste*, in Ahmed Mebarki, Carlos Genatios & Marianela Lafuente (eds.), *Risques Naturels et technologiques*, Presses de l'Ecole Nationale des Ponts et Chaussées, Paris, pp. 155-172.

Mebarki, A., Laribi, A. & Jerez, S. (2010). *Evaluation post-sismique des dommages structuraux. Une finalisation probabiliste intégrée*, in (ed.), Colloque international Seisme d'El Asnam du 10 Octobre 1980. Trente ans après., Alger, Algeria., pp.

Mebarki, A., Laribi, A. & Kharchi, F. (Pending). *Post-earthquake overall damage evaluation: a probabilistic framework for buildings - Part I: The theoretical methodology*, European Journal of Environmental and Civil Engineering, **Pending.**

Mebarki, A. & Valencia, N. (2008). *Vulnerabilité et fiabilité des constructions en maçonnerie.*, in Ahmed Mebarki, Carlos Genatios & Marianela Lafuente (eds.), *Risques Naturels et technologiques*, Presses de l'Ecole Nationale des Ponts et Chaussées, Paris, pp. 105-129.

Mergos, P. & Kappos, A. (2010). *Seismic damage analysis including inelastic shear–flexure interaction*, Bulletin of Earthquake Engineering, **8**(1), 27-46.

Molinari, M., Savadkoohi, A. T., Bursi, O. S., Friswell, M. I. & Zonta, D. (2009). *Damage identification of a 3D full scale steel-concrete composite structure with partial-strength joints at different pseudo-dynamic load levels*, Earthquake Engineering & Structural Dynamics, **38**(10), 1219-1236.

Nielsen, S. R. K., Köylüog, lu, H. U. & Çalmak, A. S. (1992). *One and two-dimensional maximum softening damage indicators for reinforced concrete structures under seismic excitation*, Soil Dynamics and Earthquake Engineering, **11**(8), 435-443.

Norris, C. H., Wilbur, J. B. & Utku, S. (1991). *Elementary Structural Analysis*, Mc. Graw Hill.

Paret, T. F., Sasaki, K. K., Eilbeck, D. H. & Freeman, S. A. (1996). *Approximate inelastic procedures to identify failure mechanisms from higher mode effects*, in Elsevier Science (ed.), 11 World Conference on Earthquake Engineering, Acapulco, Mexico, Paper No. 966., pp.

Park, Y.-J., Ang, A. H. S. & Wen, Y. K. (1985). *Seismic Damage Analysis of Reinforced Concrete Buildings*, Journal of Structural Engineering, **111**(4), 740-757.

Park, Y. J. & Ang, A. H. S. (1985). *Mechanistic seismic damage model for reinforced-concrete*, Journal of Structural Engineering, **111**(4), 722-739.

Park, Y. J., Ang, A. H. S. & Wen, Y. K. (1987). *Damage-Limiting Aseismic Design of Buildings*, Earthquake Spectra, **3**(1), 1-26.

Paulay, T. & Priestley, M. N. J. (1992). *Seismic Design of Reinforced Concrete and Masonry Buildings*, John Wiley & Sons, New York.

PEER (2005). *Pacific Earthquake Engineering Research Center: NGA Database*, University of California, Berkeley. http://peer.berkeley.edu/nga/

Pinto, A., Verzeletti, G., Molina, J., Varum, H., Pinho, R. & Coelho, E. (2002). *Pseudo-dynamic tests on non-seismic resisting RC frames (bare and selective retrofit frames)*, Report:EUR20244, European Laboratory for Structural Assessment, Ispra, Italy.

Porter, K. A. (2003). *An Overview of PEER's Performance-Based Earthquake Engineering Methodology*, in (ed.), Ninth International Conference on Applications of Statistics and Probability in Civil Engineering (ICASP), San Francisco, California, pp.

Pujol, S., Ramírez, J. & Sarria, A. (1999). *Coffee Zone, Colombia, January 25 Earthquake. Observations on the behaviour of low-rise reinforced concrete buildings*, The Earthquake Engineering Online Archive, http://nisee.berkeley.edu/lessons/colombia.pdf.

Reinhorn, A. M., Kunnath, S. K. & Mander, J. B. (1992). *Seismic Design of Structures for Damage Control*, in P. Fajfar & Helmut Krawinkler (eds.), *Nonlinear Seismic Analysis and Design of Reinforced Concrete Buildings*, Routledge, UK., London, pp. 63-76.

Scott, B. D., Park, R. & Priestley, M. N. J. (1982). *Stress-Strain Behavior of Concrete Confined by Overlapping Hoops at Low and High Strain Rates*, ACI Journal, **79**(1), 13-27.

Scotta, R., Tesser, L., Vitaliani, R. & Saetta, A. (2009). *Global damage indexes for the seismic performance assessement of RC structures*, Earthquake Engineering & Structural Dynamics, **38**(8), 1027-1049.

SeismoSoft Ltd. (2008). *SeismoSignal, V.*4.0.0,Pavia, Italy.

Simoen, E., Lombaert, G., Reynders, E. & De Roeck, G. (2010). *Uncertainty quantification in the vibration-based damage assessment of a reinforced concrete beam*, in (ed.), ISMA 2010, pp.

Spacone, E., Filippou, F. C. & Taucer, F. F. (1996). *Fibre beam-column model for non-linear analysis of R/C frames: Part I. Formulation*, Earthquake Engineering & Structural Dynamics, **25**(7), 711–725.

Sucuoğlu, H. & Günay, M. S. (2010). *Generalized force vectors for multi-mode pushover analysis*, Earthquake Engineering & Structural Dynamics, DOI: 10.1002/eqe.1020.

Takeda, T., Nielsen, N. N. & Sozen, M. A. (1970). *Reinforced Concrete Response to Simulated Earthquakes*, Journal of the Structural Division, ASCE, **96**(12), 2557-2573.

Taucer, F. F., Spacone, E. & Filippou, F. C. (1991). *A Fiber Beam-Column Element for Seismic Response Analysis of Reinforced Concrete Structures*, Report:EERC-91/17, Earthquake Engineering Research Center, Berkeley, CA.

The MathWorks (2007). *Matlab, V.*2007a,Natick, MA.

Tjhin, T., Aschheim, M. & Hernández-Montes, E. (2005). *Estimates of Peak Roof Displacement Using "Equivalent" Single Degree of Freedom Systems*, Journal of Structural Engineering, **131**(3), 517-522.

Tjhin, T., Aschheim, M. & Hernández-Montes, E. (2006). *Observations on the Reliability of Alternative Multiple-Mode Pushover Analysis Methods*, Journal of Structural Engineering, **132**(3), 471-477.

Uriostegui, J. L. (2005). *Seguridad y costo estructural de edificios de concreto reforzado con diseño normal y diseño dúctil en la ciudad de Chilpancingo, Guerrero*, Universidad Autónoma de Guerrrero, Chilpancingo, Gro., pp.140.

Valencia, N. (2006). *Risques naturels, aléa, vulnerabilité mécanique: cas de constructions en maçonnerie vis-a-vis des seismes et inondations.*, Ph.D. Thesis, Université de Marne la Vallée, Marne la Vallée, France., pp.188.

Vamvatsikos, D. & Cornell, C. A. (2002). *Incremental dynamic analysis*, Earthquake Engineering & Structural Dynamics, **31**(3), 491-514.

Vamvatsikos, D. & Cornell, C. A. (2005). *Direct Estimation of Seismic Demand and Capacity of Multidegree-of-Freedom Systems through Incremental Dynamic Analysis of Single Degree of Freedom Approximation*, Journal of Structural Engineering, **131**(4), 589-599.

Voyiadjis, G. Z. (2005). *Continuum Damage Mechanics*, *Handbook of Materials Modeling*, pp. 1183-1192.

Williams, M. S. & Sexsmith, R. G. (1995). *Seismic Damage Indices for Concrete Structures: A State-of-the-Art Review*, Earthquake Spectra, **11**(2), 319-349.

APPENDIX A
DESIGN INFORMATION OF THE VALIDATION MODELS

For validation purposes of the methods proposed within this thesis, five reinforced concrete frames have been studied. This appendix chapter aims to provide the relevant information about these frames. The graphic format used by Haselton *et al*. [Haselton and Deierlein, 2007] is used here.

4-storey GLD building (from [Pinto, *et al.*, 2002])

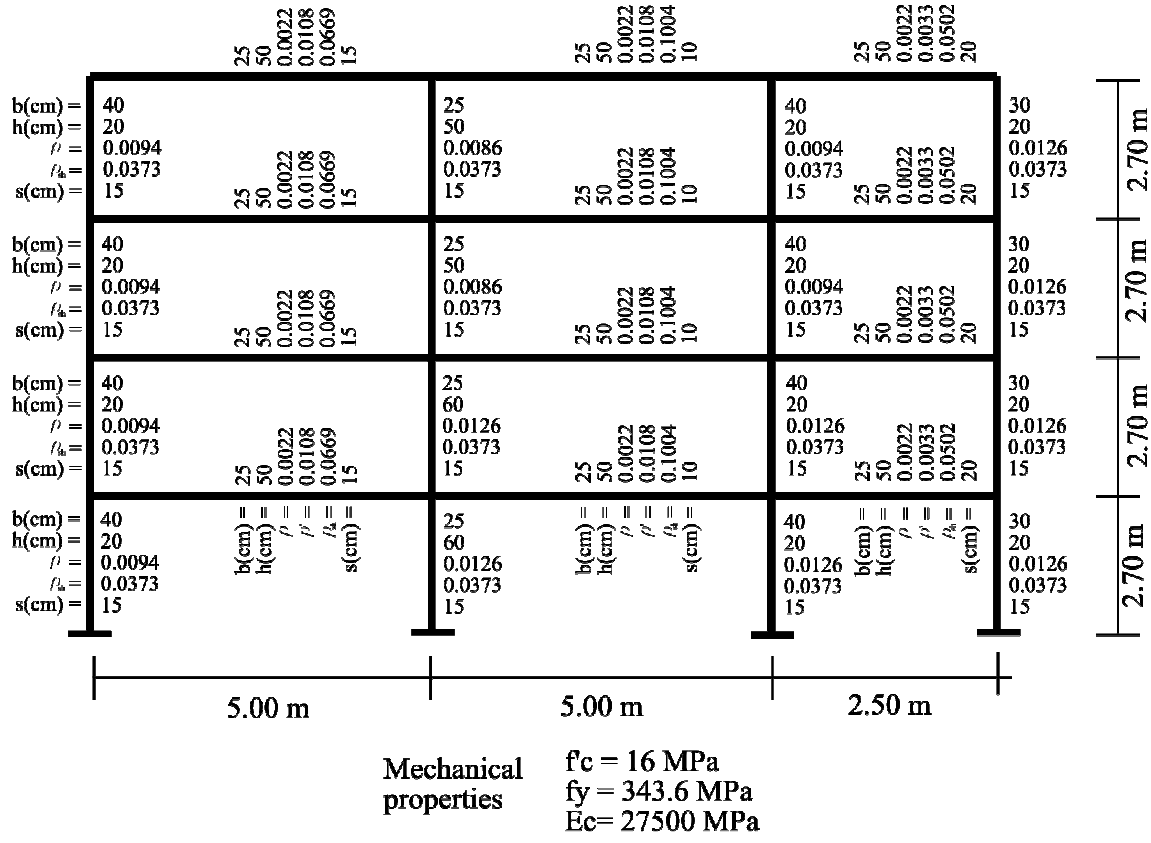

4-storey building

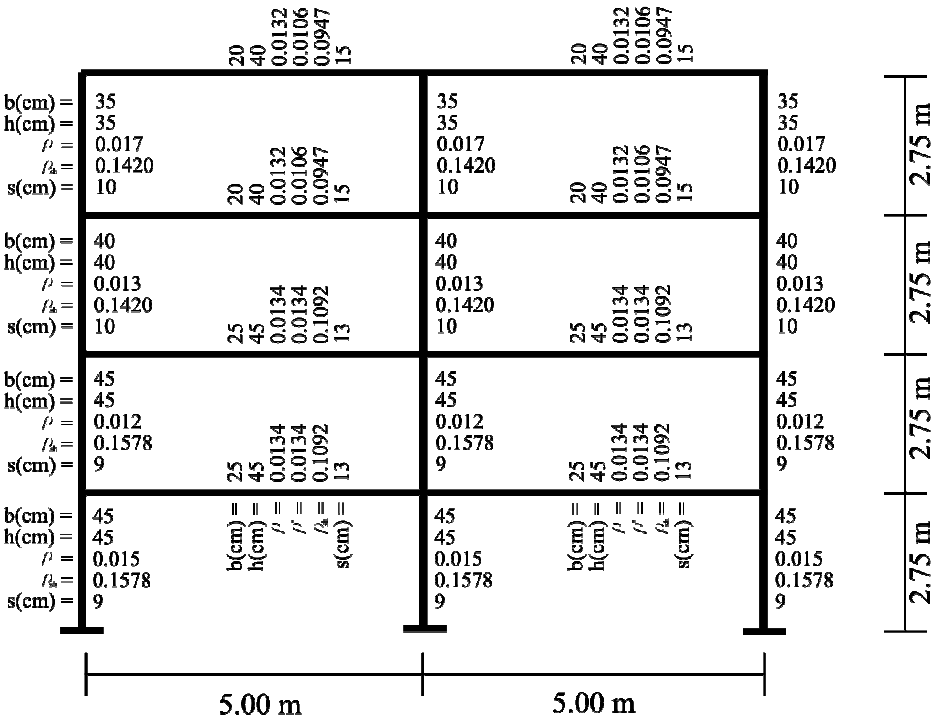

Mechanical properties

f'c = 25 MPa
fy = 420 MPa
Ec= 19500 MPa

6-storey building

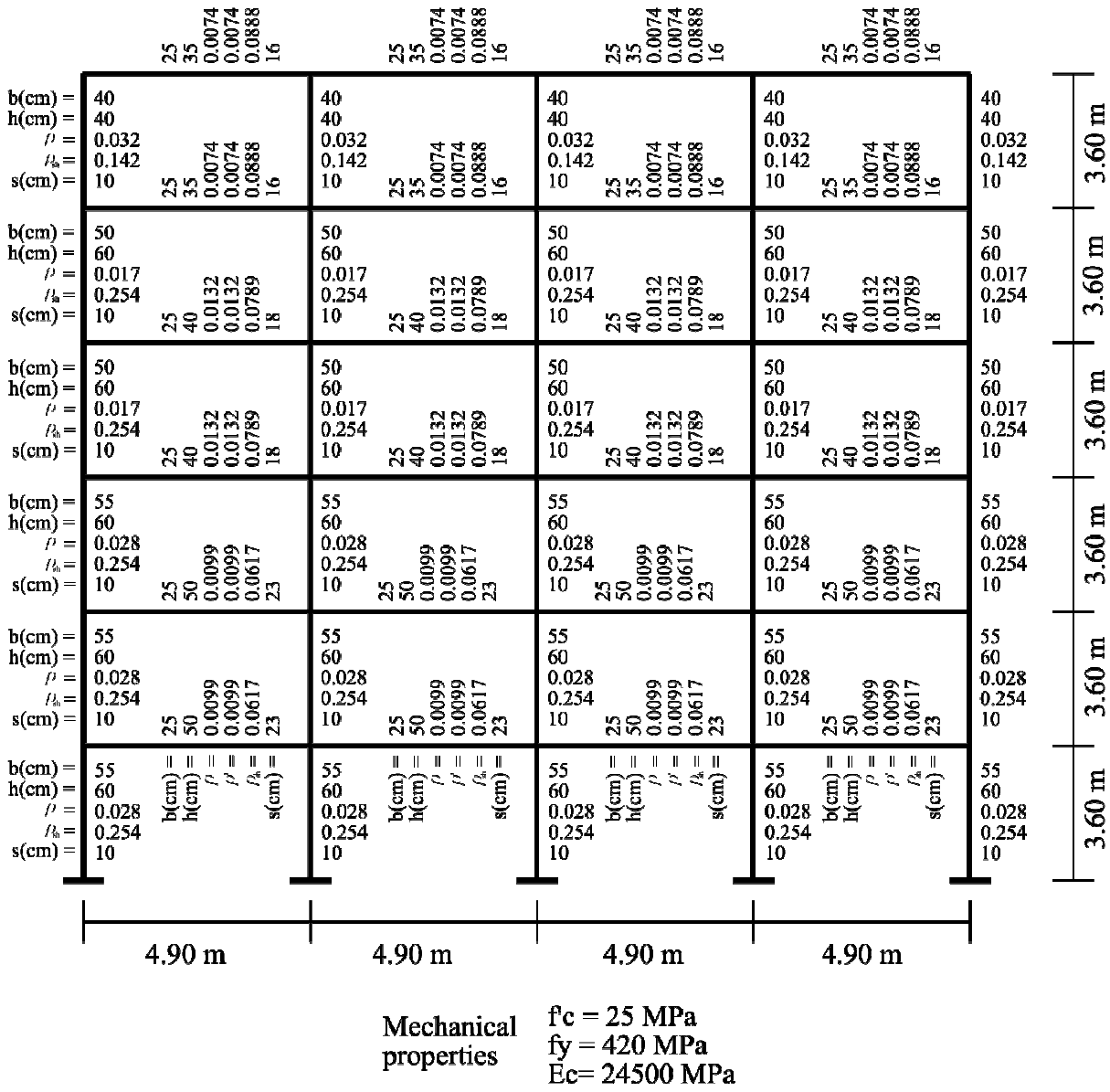

8-storey building [Haselton and Deierlein, 2007]

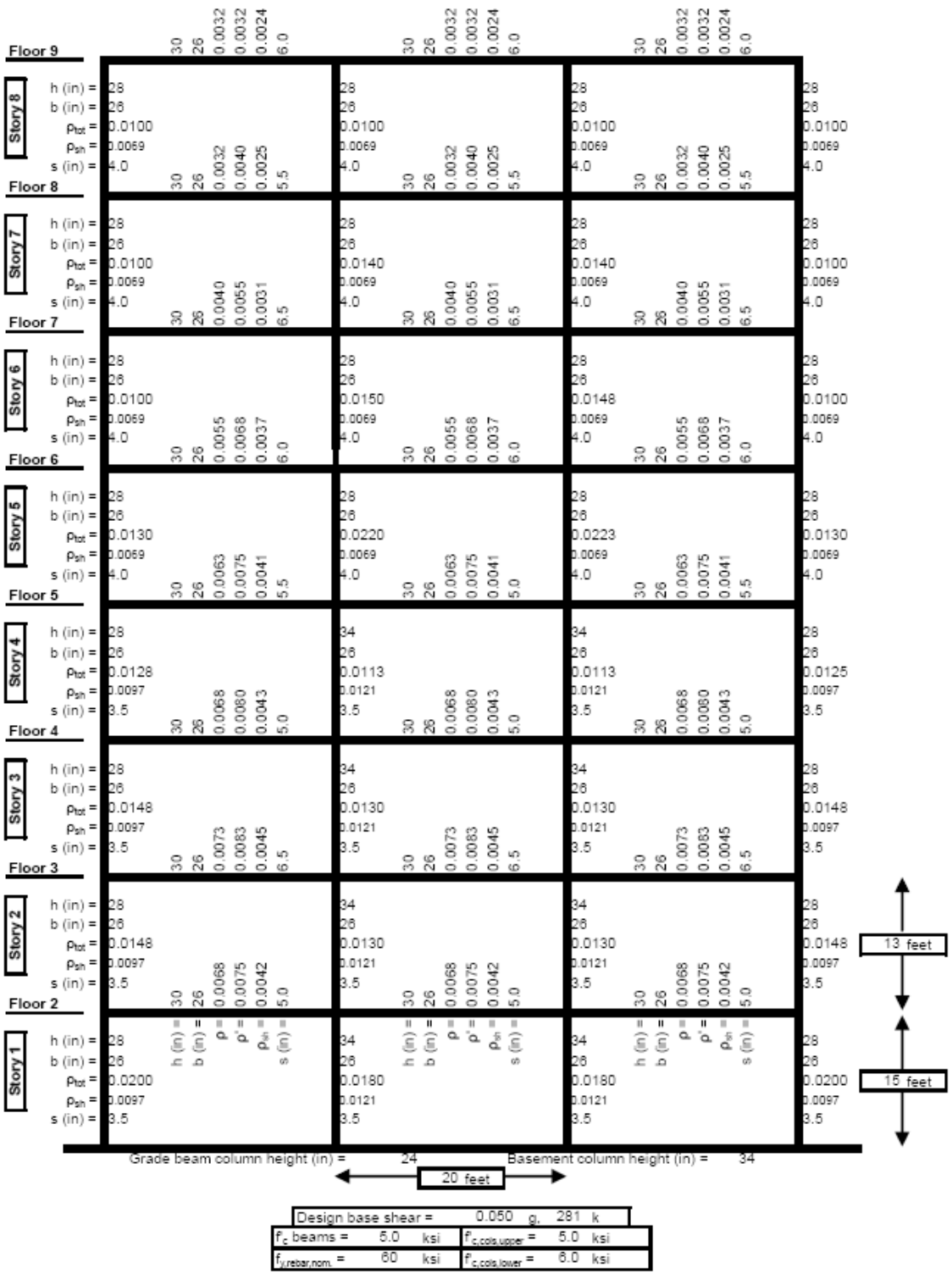

10-storey building

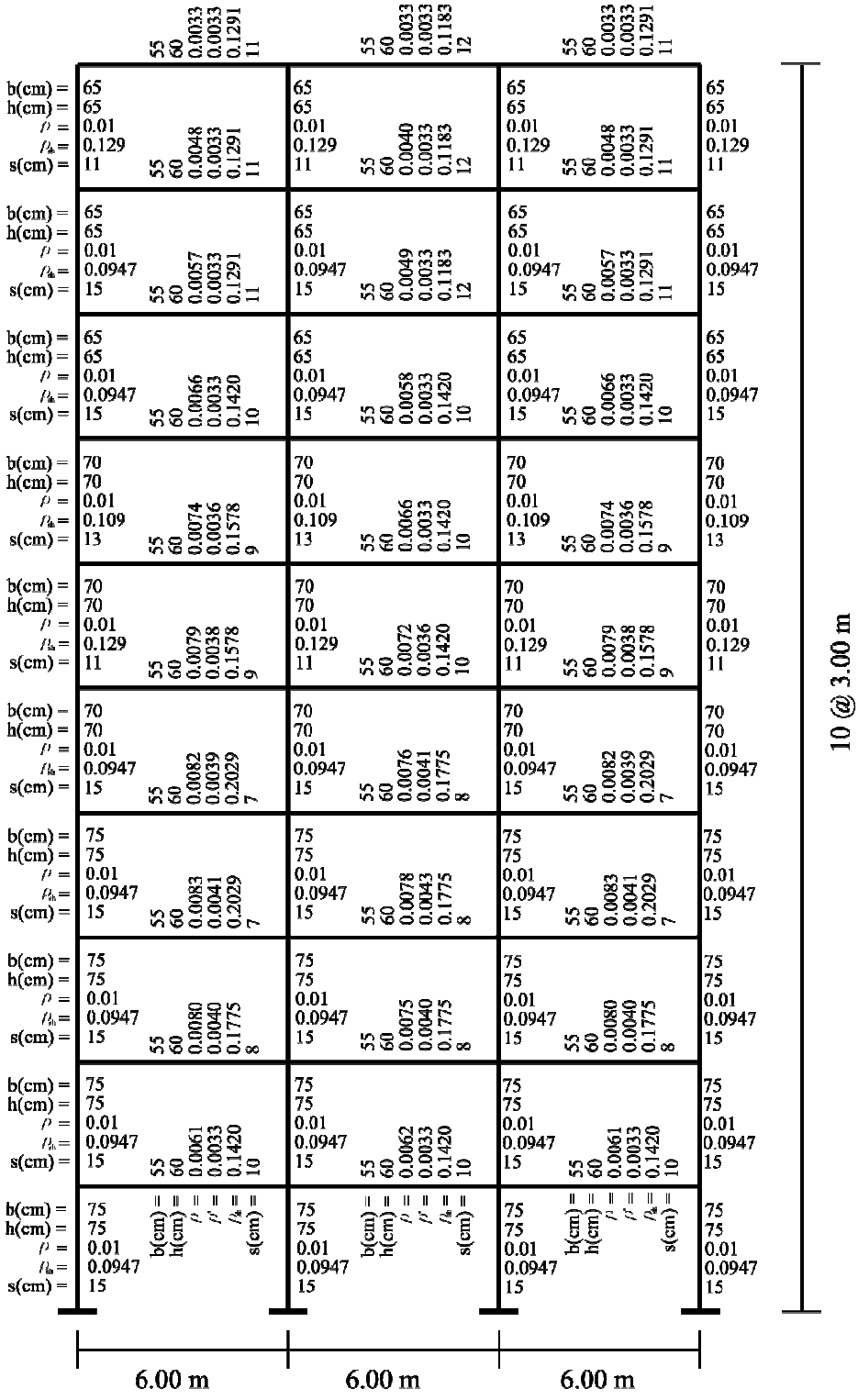

Mechanical properties
f'c beams = 28 MPa
f'c cols = 35 MPa
Eb = 20600 MPa
Ec = 23000 MPa
fy = 420 MPa

14-storey building

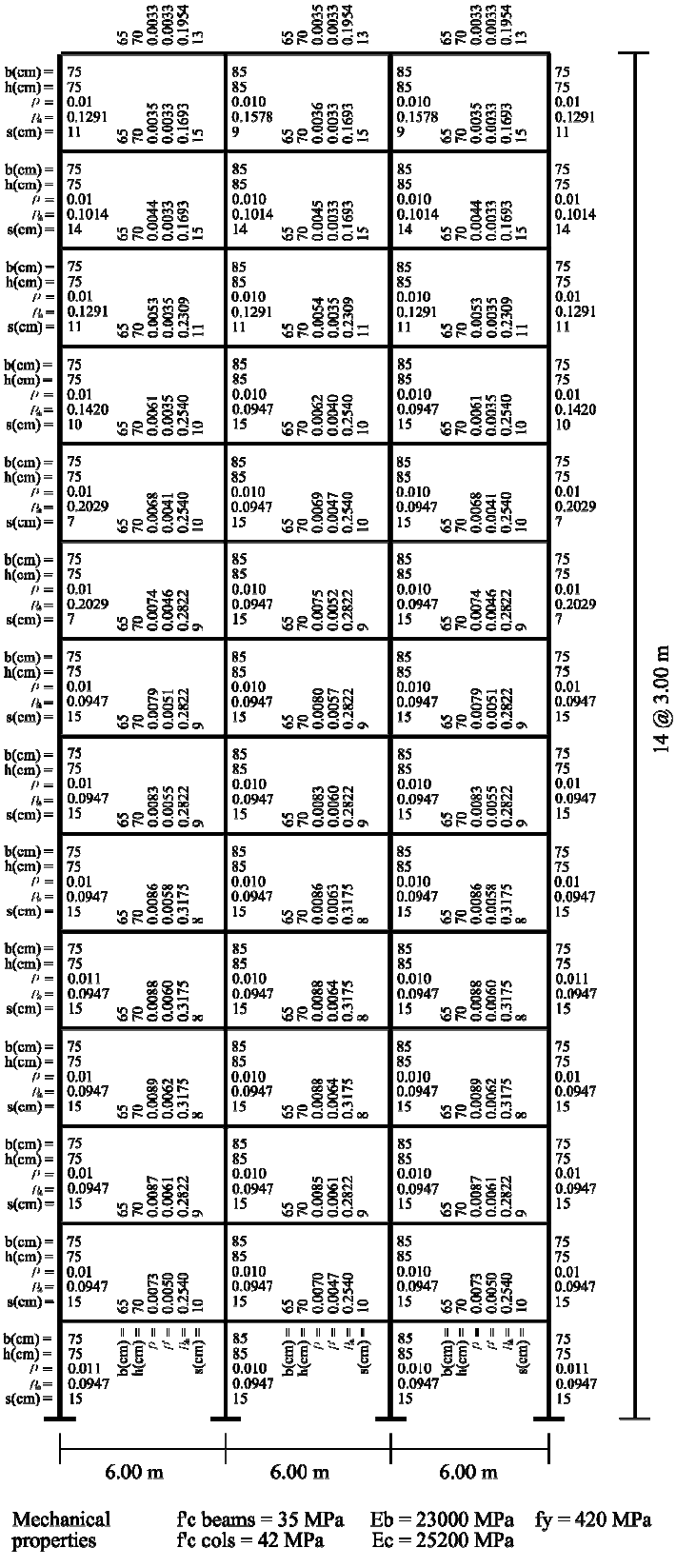

Mechanical properties	f'c beams = 35 MPa	Eb = 23000 MPa	fy = 420 MPa
	f'c cols = 42 MPa	Ec = 25200 MPa	

APPENDIX B
EVALUATION FORMS FOR POST-SEISMIC ASSESSMENT OF DAMAGE

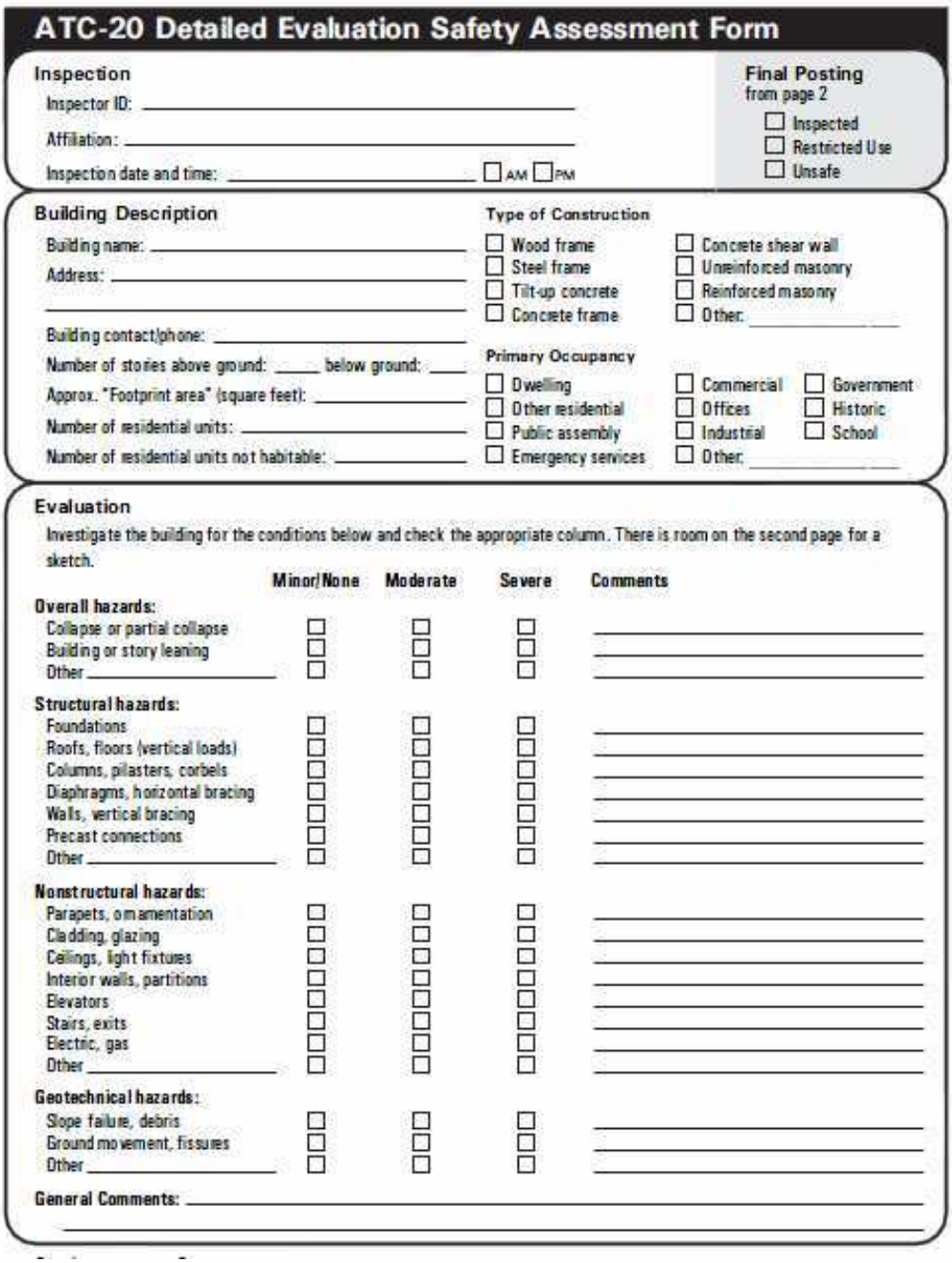

ATC-20 Detailed Evaluation Safety Assessment Form

Inspection

Inspector ID: _____

Affiliation: _____

Inspection date and time: _____ ☐ AM ☐ PM

Final Posting from page 2

☐ Inspected
☐ Restricted Use
☐ Unsafe

Building Description

Building name: _____

Address: _____

_____

Building contact/phone: _____

Number of stories above ground: _____ below ground: _____

Approx. "Footprint area" (square feet): _____

Number of residential units: _____

Number of residential units not habitable: _____

Type of Construction

☐ Wood frame
☐ Steel frame
☐ Tilt-up concrete
☐ Concrete frame
☐ Concrete shear wall
☐ Unreinforced masonry
☐ Reinforced masonry
☐ Other: _____

Primary Occupancy

☐ Dwelling
☐ Other residential
☐ Public assembly
☐ Emergency services
☐ Commercial
☐ Offices
☐ Industrial
☐ Other: _____
☐ Government
☐ Historic
☐ School

Evaluation

Investigate the building for the conditions below and check the appropriate column. There is room on the second page for a sketch.

	Minor/None	Moderate	Severe	Comments
Overall hazards:				
Collapse or partial collapse	☐	☐	☐	_____
Building or story leaning	☐	☐	☐	_____
Other _____	☐	☐	☐	_____
Structural hazards:				
Foundations	☐	☐	☐	_____
Roofs, floors (vertical loads)	☐	☐	☐	_____
Columns, pilasters, corbels	☐	☐	☐	_____
Diaphragms, horizontal bracing	☐	☐	☐	_____
Walls, vertical bracing	☐	☐	☐	_____
Precast connections	☐	☐	☐	_____
Other _____	☐	☐	☐	_____
Nonstructural hazards:				
Parapets, ornamentation	☐	☐	☐	_____
Cladding, glazing	☐	☐	☐	_____
Ceilings, light fixtures	☐	☐	☐	_____
Interior walls, partitions	☐	☐	☐	_____
Elevators	☐	☐	☐	_____
Stairs, exits	☐	☐	☐	_____
Electric, gas	☐	☐	☐	_____
Other _____	☐	☐	☐	_____
Geotechnical hazards:				
Slope failure, debris	☐	☐	☐	_____
Ground movement, fissures	☐	☐	☐	_____
Other _____	☐	☐	☐	_____

General Comments: _____

Evaluation form for post-seismic screening of buildings, according to the ATC 20 guidelines, page 1 [ATC, 1995]

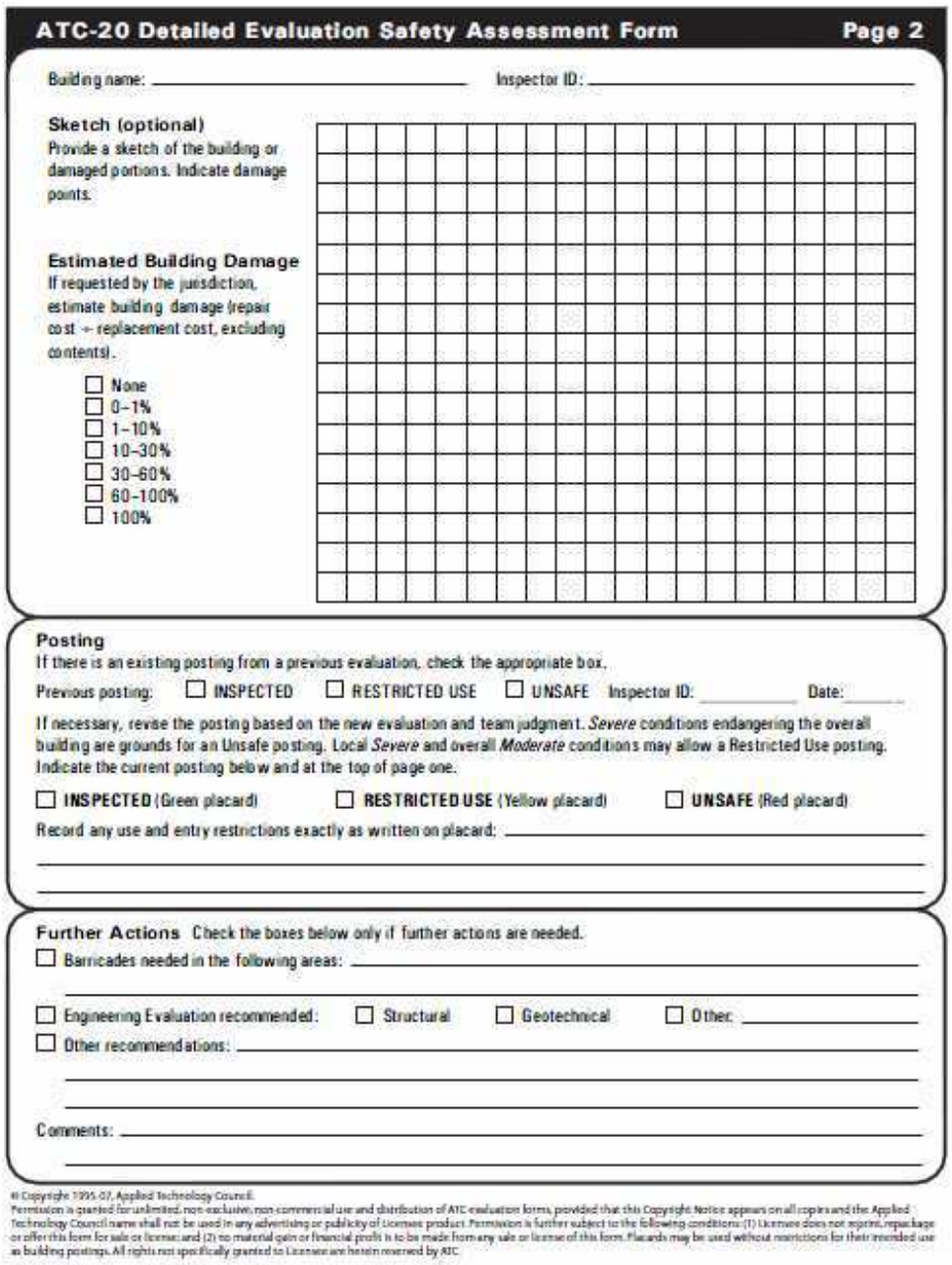

ATC-20 Detailed Evaluation Safety Assessment Form **Page 2**

Building name: _____ Inspector ID: _____

Sketch (optional)
Provide a sketch of the building or damaged portions. Indicate damage points.

Estimated Building Damage
If requested by the jurisdiction, estimate building damage (repair cost ÷ replacement cost, excluding contents).

- ☐ None
- ☐ 0–1%
- ☐ 1–10%
- ☐ 10–30%
- ☐ 30–60%
- ☐ 60–100%
- ☐ 100%

Posting
If there is an existing posting from a previous evaluation, check the appropriate box.

Previous posting: ☐ INSPECTED ☐ RESTRICTED USE ☐ UNSAFE Inspector ID: _____ Date: _____

If necessary, revise the posting based on the new evaluation and team judgment. *Severe* conditions endangering the overall building are grounds for an Unsafe posting. Local *Severe* and overall *Moderate* conditions may allow a Restricted Use posting. Indicate the current posting below and at the top of page one.

☐ **INSPECTED** (Green placard) ☐ **RESTRICTED USE** (Yellow placard) ☐ **UNSAFE** (Red placard)

Record any use and entry restrictions exactly as written on placard: _____

Further Actions Check the boxes below only if further actions are needed.

☐ Barricades needed in the following areas: _____

☐ Engineering Evaluation recommended: ☐ Structural ☐ Geotechnical ☐ Other: _____

☐ Other recommendations: _____

Comments: _____

Evaluation form for post-seismic screening of buildings, according to the ATC 20 guidelines, page 2 [ATC, 1995]

APPENDIX C
DAMAGE PATTERNS FOR VALIDATION

The main goal of this appendix chapter is to provide for illustration purposes the damage arrangements used for the validation of the probability-based approach proposed in Chapter 5. Some of the used patterns are really simple and clear, as those used to evaluate the efficiency of the importance factors since damage was concentrated in well defined elements or sections, with a defined value according to the damage level: 0.30 for LM and 0.60 for MH; therefore those cases are not illustrated here. The following tables illustrate configurations of damage used to evaluate the global efficiency in the 4-, 6- and 8-storey frames. They are a complement to the example tables shown in Chapter 5.

4-storey frame

Level: LM

Event	Damage						Event	Damage					
	Story	Beam		Columns				Story	Beam		Columns		
		1	2	1	2	3			1	2	1	2	3
S_GV	1	0,25	0,25	0,15	0,1	0,15	U_LS	1	0,3	0,25	0,3	0,35	0,3
	2	0,2	0,2	0,15	0,1	0,15		2	0,3	0,25		0,25	
	3	0,2	0,2	0,15	0,1	0,15		3	0,3			0,25	
	4	0,1	0,1	0,1	0,1	0,1		4					
S_SV	1	0,4	0,4	0,2	0,2	0,2	U_HS	1					
	2	0,4	0,4	0,2	0,2	0,2		2					
	3	0,3	0,3	0,1	0,1	0,1		3	0,3	0,35	0,2	0,2	0,2
	4	0,3	0,3	0,1	0,1	0,1		4		0,3		0,2	

Level: MH

Event	Damage						Event	Damage					
	Story	Beam		Columns				Story	Beam		Columns		
		1	2	1	2	3			1	2	1	2	3
S_GV	1	0,5	0,5	0,3	0,2	0,3	U_LS	1	0,6	0,5	0,6	0,7	0,6
	2	0,4	0,4	0,3	0,2	0,3		2	0,6	0,5		0,5	
	3	0,4	0,4	0,3	0,2	0,3		3	0,6			0,5	
	4	0,2	0,2	0,2	0,2	0,2		4					
S_SV	1	0,8	0,8	0,4	0,4	0,4	U_HS	1					
	2	0,8	0,8	0,4	0,4	0,4		2					
	3	0,6	0,6	0,2	0,2	0,2		3	0,6	0,7	0,4	0,4	0,4
	4	0,6	0,6	0,2	0,2	0,2		4		0,6		0,4	

Damage patterns after subjected to a ground motion record:

GM	Damage						GM	Damage					
	Story	Beam		Col				Story	Beam		Col		
		1	2	1	2	3			1	2	1	2	3
Centro	1	0,77	0,71	0	0,58	0	San Fernando	1	0,61	0,37	0	0	0
	2	0,59	0,63	0	0,71	0		2	0,63	0,43	0	0,58	0
	3	0,19	0,28	0	0,47	0		3	0,19	0,25	0	0,46	0
	4	0	0	0	0	0		4	0	0	0	0	0
Kobe	1	0,68	0,69	0	0,34	0	Northridge	1	0,84	0,68	0,68	0,81	0,67
	2	0,44	0,59	0	0,52	0		2	0,8	0,7	0	0,86	0
	3	0	0	0	0	0		3	0,75	0,62	0	0,82	0
	4	0	0	0	0	0		4	0	0	0	0	0

6-storey frame

Level: MH

Event	Damage										Event	Damage									
	Story	Beam				Columns						Story	Beam				Columns				
		1	2	3	4	1	2	3	4	5			1	2	3	4	1	2	3	4	5
S_GV	1	0,5	0,5	0,5	0,5	0,3	0,3	0,4	0,3	0,3	U_LS	1	0,8	0,4	0,3	0,7	0,6	0,7	0,5	0,4	0,6
	2	0,5	0,5	0,5	0,5	0,3	0,3	0,4	0,3	0,3		2	0,7	0,5	0,3	0,6	0,5	0,5	0,4	0,2	0,5
	3	0,4	0,4	0,4	0,4	0,3	0,3	0,4	0,3	0,3		3	0,3	0,2			0,4	0,4	0,3		
	4	0,4	0,4	0,4	0,4	0,2	0,2	0,3	0,2	0,2		4		0,2					0,2		
	5	0,2	0,2	0,2	0,2	0,2	0,2	0,3	0,2	0,2		5									
	6	0,2	0,2	0,2	0,2	0,2	0,2	0,3	0,2	0,2		6									
S_SV	1	0,8	0,8	0,8	0,8	0,4	0,4	0,4	0,4	0,4	U_HS	1									
	2	0,8	0,8	0,8	0,8	0,4	0,4	0,4	0,4	0,4		2									
	3	0,8	0,8	0,8	0,8	0,4	0,4	0,4	0,4	0,4		3		0,2							
	4	0,6	0,6	0,6	0,6	0,2	0,2	0,2	0,2	0,2		4	0,4	0,2	0,4	0,5	0,4	0,5	0,5		
	5	0,6	0,6	0,6	0,6	0,2	0,2	0,2	0,2	0,2		5	0,7	0,4	0,6	0,4	0,6	0,6	0,6	0,4	0,2
	6	0,6	0,6	0,6	0,6	0,2	0,2	0,2	0,2	0,2		6	0,3	0,3	0,4	0,3	0,3	0,5	0,4	0,3	0

Damage patterns after subjected to a ground motion record:

GM	Damage									GM	Damage								
	Story	Beam				Columns					Story	Beam				Columns				
		1	2	3	4	1	2	3	4	5		1	2	3	4	1	2	3	4	5
Centro	1	0	0	0	0	0	0	0	0	0	Loma Prieta	1	0,76	0,75	0,75	0,76	0	0	0	0	0
	2	0,49	0,45	0,45	0,52	0	0	0	0	0		2	0,83	0,83	0,83	0,84	0	0	0	0	0
	3	0,42	0,42	0,42	0,44	0	0	0	0	0		3	0,8	0,8	0,8	0,8	0	0	0	0	0
	4	0,75	0,73	0,73	0,73	0	0	0	0	0		4	0,85	0,85	0,85	0,86	0	0	0	0	0
	5	0,94	0,94	0,94	0,94	0	0	0	0	0		5	0,97	0,97	0,97	0,97	0	0	0	0	0
	6	0,75	0,71	0,71	0,75	0	0	0	0	0		6	0,93	0,93	0,93	0,94	0	0	0	0	0
Kobe	1	0,4	0,31	0,32	0,39	0	0	0	0	0	Erzincan	1	0,71	0,69	0,69	0,72	0	0	0	0	0
	2	0,78	0,76	0,76	0,78	0	0	0	0	0		2	0,83	0,83	0,84	0,84	0	0	0	0	0
	3	0,77	0,77	0,77	0,77	0	0	0	0	0		3	0,84	0,84	0,84	0,84	0	0	0	0	0
	4	0,78	0,76	0,76	0,78	0	0	0	0	0		4	0,87	0,86	0,86	0,87	0	0	0	0	0
	5	0,95	0,95	0,95	0,95	0	0	0	0	0		5	0,94	0,95	0,95	0,94	0	0	0	0	0
	6	0,73	0,7	0,7	0,72	0	0	0	0	0		6	0,84	0,82	0,82	0,83	0	0	0	0	0

8-storey frame

Level: LM

Event	Damage								Event	Damage							
	Story	Beam			Col					Story	Beam			Col			
		1	2	3	1	2	3	4			1	2	3	1	2	3	4
S_GV	1	0,25	0,25	0,25	0,2	0,2	0,2	0,2	U_LS	1	0,4	0,2	0,15	0,3	0,35	0,25	0,2
	2	0,25	0,25	0,25	0,2	0,2	0,2	0,2		2	0,35	0,25	0,3	0,25	0,2	0,3	0,2
	3	0,2	0,2	0,2	0,15	0,15	0,15	0,15		3	0,15	0,15	0,25	0,2	0,15	0,2	0,2
	4	0,2	0,2	0,2	0,15	0,15	0,15	0,15		4	0,1	0,2			0,1	0,15	
	5	0,15	0,15	0,15	0,1	0,1	0,1	0,1		5		0,1				0,15	
	6	0,15	0,15	0,15	0,1	0,1	0,1	0,1		6							
	7	0,1	0,1	0,1	0,05	0,05	0,05	0,05		7							
	8	0,1	0,1	0,1	0,05	0,05	0,05	0,05		8							
S_SV	1	0,3	0,3	0,3	0,15	0,15	0,15	0,15	U_HS	1							
	2	0,3	0,3	0,3	0,15	0,15	0,15	0,15		2							
	3	0,3	0,3	0,3	0,15	0,15	0,15	0,15		3							
	4	0,15	0,15	0,15	0,05	0,05	0,05	0,05		4		0,15					
	5	0,15	0,15	0,15	0,05	0,05	0,05	0,05		5	0,1	0,2			0,1	0,15	
	6	0,15	0,15	0,15	0,2	0,05	0,05	0,05		6	0,4	0,2	0,15	0,3	0,35	0,25	0,2
	7	0,05	0,05	0,05	0,2	0,05	0,05	0,05		7	0,35	0,25	0,3	0,25	0,2	0,3	0,2
	8	0,05	0,05	0,05	0,2	0,05	0,05	0,05		8	0,15	0,15	0,25	0,2	0,15	0,2	0,2

Level: MH

Event	Damage								Event	Damage							
	Story	Beam			Col					Story	Beam			Col			
		1	2	3	1	2	3	4			1	2	3	1	2	3	4
S_GV	1	0,5	0,5	0,5	0,4	0,4	0,4	0,4	U_LS	1	0,8	0,4	0,3	0,6	0,7	0,5	0,4
	2	0,5	0,5	0,5	0,4	0,4	0,4	0,4		2	0,7	0,5	0,6	0,5	0,4	0,6	0,4
	3	0,4	0,4	0,4	0,3	0,3	0,3	0,3		3	0,3	0,3	0,5	0,4	0,3	0,4	0,4
	4	0,4	0,4	0,4	0,3	0,3	0,3	0,3		4	0,2	0,4			0,2	0,3	
	5	0,3	0,3	0,3	0,2	0,2	0,2	0,2		5		0,2				0,3	
	6	0,3	0,3	0,3	0,2	0,2	0,2	0,2		6							
	7	0,2	0,2	0,2	0,1	0,1	0,1	0,1		7							
	8	0,2	0,2	0,2	0,1	0,1	0,1	0,1		8							
S_SV	1	0,6	0,6	0,6	0,3	0,3	0,3	0,3	U_HS	1							
	2	0,6	0,6	0,6	0,3	0,3	0,3	0,3		2							
	3	0,6	0,6	0,6	0,3	0,3	0,3	0,3		3							
	4	0,3	0,3	0,3	0,1	0,1	0,1	0,1		4		0,3					
	5	0,3	0,3	0,3	0,1	0,1	0,1	0,1		5	0,2	0,4			0,2	0,3	
	6	0,3	0,3	0,3	0,4	0,1	0,1	0,1		6	0,8	0,4	0,3	0,6	0,7	0,5	0,4
	7	0,1	0,1	0,1	0,4	0,1	0,1	0,1		7	0,7	0,5	0,6	0,5	0,4	0,6	0,4
	8	0,1	0,1	0,1	0,4	0,1	0,1	0,1		8	0,3	0,3	0,5	0,4	0,3	0,4	0,4

Damage patterns after subjected to a ground motion record:

GM	Damage								GM	Damage							
	Story	Beam			Col					Story	Beam			Col			
		1	2	3	1	2	3	4			1	2	3	1	2	3	4
Loma Prieta	1	0,88	0,88	0,88	0,72	0,85	0,85	0,73	**San Fernando**	1	0,66	0,67	0,66	0	0	0	0
	2	0,86	0,86	0,86	0	0	0	0		2	0,32	0,36	0,33	0	0	0	0
	3	0,82	0,83	0,82	0	0	0	0		3	0,23	0,32	0,27	0	0	0	0
	4	0,73	0,75	0,76	0	0	0	0		4	0	0	0	0	0	0	0
	5	0,76	0,71	0,72	0	0	0	0		5	0,44	0,33	0,2	0	0	0	0
	6	0,89	0,88	0,88	0	0,43	0,42	0		6	0,81	0,78	0,77	0	0	0	0
	7	0,91	0,91	0,92	0	0,6	0,61	0		7	0,83	0,83	0,85	0	0	0	0
	8	0,87	0,85	0,91	0	0,8	0,81	0		8	0,79	0,76	0,81	0	0	0	0
Kobe	1	0,89	0,89	0,89	0,82	0,89	0,89	0,83	**Erzincan**	1	0,71	0,72	0,71	0	0	0	0
	2	0,86	0,86	0,86	0	0	0	0		2	0,67	0,7	0,69	0	0	0	0
	3	0,86	0,87	0,86	0	0	0	0		3	0,68	0,73	0,7	0	0	0	0
	4	0,87	0,87	0,87	0	0	0	0		4	0,58	0,66	0,62	0	0	0	0
	5	0,88	0,88	0,87	0	0	0	0		5	0,38	0,5	0,54	0	0	0	0
	6	0,9	0,91	0,91	0,08	0,71	0,71	0,31		6	0,55	0,57	0,58	0	0	0	0
	7	0,91	0,92	0,92	0	0	0	0		7	0,5	0,47	0,26	0	0	0	0
	8	0,84	0,83	0,87	0	0	0	0		8	0	0	0	0	0	0	0